THE ROLE OF QKI-5 IN CG4 OLIGODENDROCYTE DIFFERENTIATION

A Thesis Submitted to the

College of Graduate Studies and Research

In Partial Fulfillment of the Requirements

for the Degree of Master of Science

In the College of Pharmacy and Nutrition

University of Saskatchewan

Saskatoon

By

Jotham Gan

PERMISSION TO USE

In presenting this thesis in partial fulfillment of the requirements for a Master of Science degree from the University of Saskatchewan, I agree that the Libraries of this University may make it freely available for inspection. I further agree that permission for copying this thesis in any manner, in whole or in part, for scholarly purposes may be granted by the professor or professors who supervised my thesis work or, in their absence, by the Dean of the College in which my thesis work was done. It is understood that any copying or publication or use of this thesis or parts thereof for financial gain shall not be allowed without my written permission. It is also understood that due recognition shall be given to me and to the University of Saskatchewan in any scholarly use which may be made of any material in my thesis.

Requests for permission to copy or to make use of material in this thesis in whole or in part should be addressed to:

Dean of the College of Pharmacy and Nutrition

University of Saskatchewan

110 Science Place, Rm 116 Thorvaldson Building

Saskatoon, Saskatchewan, S7N 5C9

ABSTRACT

The Quaking (*qk*) gene has been implicated in the development of oligodendroglial cells which are the primary source of myelin in the mammalian central nervous system (CNS). *Qk* encodes three alternatively spliced variants, QKI-5, QKI-6 and QKI-7, all of which are RNA binding proteins. Loss of QKI-6 and QKI-7 results in a dysmyelination phenotype that is present shortly after birth while loss of QKI-5 results in embryonic lethality. CG4 oligodendroglial cells were transfected with either pIRES2-QKI5 to up regulate QKI-5 expression or a QKI-5 specific siRNA to down regulate QKI-5. Cells were cultured for 6d in differentiation medium (DM) following which total RNA and protein was collected from the cell cultures, and coverslips with attached cells were processed for immunofluorescence. Increased QKI-5 expression following transfection with pIRES2-QKI5 resulted in increased *Sirt2* and *Plp* mRNA expression, but did not affect SIRT2 and PLP protein expression. Down regulation of QKI-5 expression had no significant effect on mRNA or protein levels for QKI-6, QKI-7, *Plp* or *Sirt2*. Immunocytochemistry revealed that up regulation of QKI-5 resulted in significantly higher percentage of A2B5$^+$ cells and a lower percentage of GalC$^+$ cells, whereas siRNA treatment resulted in an increase in the percentage of GalC$^+$ cells. Our results suggest QKI-5 regulates CG4 oligodendroglial differentiation and modulates the transcription and availability of target mRNAs, such as *Sirt2* and *Plp*, for translation. In order to gain a more complete understanding of the relationship between *qk* and both *Sirt2* and *Plp,* future studies would include RNA coimmunoprecipitation, miRNA studies, and expanding the list of target genes to include various cell cycle components.

ACKNOWLEDGEMENTS

TABLE OF CONTENTS

LIST OF FIGURES

LIST OF APPENDICES

LIST OF ABBREVIATIONS

ANOVA	analysis of variance
APC	adenomatous polyposis coli
bp	base pair
BRK	breast tumor kinase
cAMP	cyclic adenosine monophosphate
CC1	anti-APC clone
cDNA	complementary DNA
CGT	ceramide galactosyltransferase
CNS	central nervous system
CREB	cAMP response element binding protein
DM	differentiation media
DM20	alternative splice variant of *Plp*
DMEM	Dulbecco's modified eagle medium
DNA	deoxyribonucleic acid
DTT	dithiothreitol
E. coli	*Escherichia coli*
EGF	epidermal growth factor
eIF4F	eukaryotic initiation factor complex
ENU	*N*-ethyl-*N*-nitrosourea
FGF-2	fibroblast growth factor 2
FYN	a member of the Src family of tyrosine protein kinases
GalC	galactocerebroside
GFP	green fluorescent protein
GLD-1	defective in germline development 1

GM	growth media
HDAC	histone deacetylase
hnRNPA1	heterogeneous nuclear ribonucleoprotein A1
HOW	held out wings mutation
HRP	horse radish peroxidase
kDa	kilodalton
KEP1	KH encompassing protein 1
KH	Protein K homology
IPTG	isopropyl β-D-1-thiogalactopyranoside
MAG	myelin associated glycoprotein
Map1B	microtubule-associated protein 1B
MAPK	mitogen-activated protein kinase
MAPKK	MAPK kinase
Maxi KH	an enlarged K homology domain RNA-binding domain
MBP	myelin basic protein
MOG	myelin oligodendrocyte glycoprotein
mRNA	messenger ribonucleic acid
NAD	nicotinamide adenine dinucleotide
NG2	chondroitin sulphate proteoglycan
OL	oligodendrocyte
OPC(s)	oligodendrocyte progenitor cell(s)
O-2A	oligodendrocyte-type-2 astrocyte progenitor cell
p27^{KIP1}	cyclin-dependent kinase inhibitory protein 1
PBS	phosphate buffer saline
PCR	polymerase chain reaction

PDGF	platelet-derived growth factor
PDGFαR	platelet-derived growth factor receptor α
Pfx	*Pyrococcus* sp. strain KOD1
PKA	Protein kinase A
Plp	Proteolipid protein
PLP-ISEdel	Proteolipid protein – intron splicing enhancer deletion
PNS	peripheral nervous system
qk	quaking gene
QUA	quaking homology
QKI	quaking protein
QRE	quaking response element
Qk^v	quaking viable mutant mouse
RIPA	radioimmunoprecipitation assay buffer
RNA	ribonucleic acid
RT-PCR	reverse-transcription polymerase chain reaction
SAM68	Src-associated in mitosis 68 kDa
SDS	sodium dodecyl sulfate
SDS-PAGE	sodium dodecyl sulfate-polyacrylamide gel electrophoresis
SEM	standard error of the mean
SH3	Src homology 3 domain
siRNA	small interfering RNA
Src	a family of non-receptor tyrosine kinases
SIRT	sirtuin
STAR	signal transduction and activation of RNA
Taq	*Thermus aquaticus*

UDP	uridine diphosphate
UTR	untranslated region
VEGFA	vascular endothelial growth factor A

I   INTRODUCTION

The Quaking (*Qk*) gene has been implicated in the development of a number of different tissues. The use of several *N*-ethyl-*N*-nitrosourea (ENU)-induced or knockout alleles of *Qk*, have resulted in defects in vascular development (Noveroske et al., 2002), heart defects, cranial defects, disorganization along the anterior-posterior axis (Justice and Bode 1988), with many of the defects resulting in embryonic lethality. Along with the various developmental defects, there are also numerous nervous system defects. These include hypomyelination in both the central and peripheral nervous system (Noveroske et al., 2005), early onset seizures, severe ataxia and Purkinje cell axonal swellings (Sidman et al., 1964).

The homozygous *quaking viable (Qk^v/Qk^v)* mutant contains a recessive mutation that results in the loss of a large portion of the promoter and enhancer sequences for the *Qk* gene. *Qk^v/Qk^v* mutants thus exhibit a hypomyelination phenotype due to diminished QKI mRNA and subsequent decrease in QKI protein expression, specifically in oligodendrocytes (OL) (Hardy et al., 1996; Bockbrader and Feng 2008). Any myelin that is present is thin and malformed. *Qk* encodes three alternatively spliced variants, QKI-5, QKI-6, and QKI-7. All three variants contain the same K homology KH RNA binding domain, with the main difference being the presence of a nuclear localization signal in the C-terminal region of QKI-5. As a result, QKI-5 is mainly localized to the nucleus while QKI-6 and QKI-7 mainly localize to the cytoplasm. QKI-5 is not only highly expressed in OLs, but can also be found in the heart, smooth muscle, and testis (Ebersole et al., 1996; Matsumoto et al., 1999; Li et al., 2003).

QKI is a member of the signal transduction and activation of RNA (STAR) family of proteins. STAR proteins are involved in pre-mRNA splicing, mRNA localization, mRNA transport, mRNA stability, and translation efficiency (Galarneau and Richard

1

2009). An increase in QKI-5 causes partial nuclear retention of myelin basic protein (MBP) mRNA in the nucleus (Larocque et al., 2002), which results in a reduction in MBP protein leading to myelination defects. In contrast, QKI-6 is able to enhance MBP protein expression and rescue the hypomyelination phenotype seen in the Qk^V/Qk^V mutant (Zhao et al., 2006b). QKI-5 has been implicated in the control of alternative splicing of a number of different mRNA targets. QKI-5 has been shown to bind an intronic sequence element in myelin associated glycoprotein (MAG) *in vitro* and regulate alternative exon inclusion from a modified MAG minigene reporter (Wu et al., 2002). Induced expression of the cytoplasmic isoform, QKI-6, was sufficient to rescue the dysregulation of alternative splicing of MAG pre-mRNA in the Qk^V/Qk^V mutant. As well, QKI-6 specifically suppressed translation of the splicing factor heterogeneous nuclear ribonucleoprotein A1 (hnRNPA1) (Zhao et al., 2010). Since hnRNPA1 regulates MAG alternative splicing (Zhao et al., 2010) it is possible that QKI proteins may both directly and indirectly regulate target RNA metabolism.

Two target genes that have been shown to be regulated by QKI in OLs is proteolipid protein 1 (*Plp*) and sirtuin 2 (*Sirt2*). *Plp* accounts for approximately 50% of the myelin protein in CNS and is necessary for OL differentiation and proper compaction of the myelin sheath (Griffiths et al., 1998; Le Bras et al., 2005; Werner et al., 2007; Karim et al., 2010). In the CNS, *Sirt2* is expressed predominantly in OLs and is up-regulated during myelination (Li et al., 2007; Southwood et al., 2007). The over expression of *Sirt2* in primary cell cultures resulted in a reduction in α-tubulin acetylation, MBP expression, and cell process arborization (Li et al., 2007), suggesting the ability of *Sirt2* to impede OL differentiation. However, a more recent study has shown that an increase in *Sirt2* expression resulted in enhanced MBP expression along with facilitating CG4 OL differentiation by generating more cellular processes (Ji et al., 2011). In the *Plp*-ISEdel mutant mouse, the deletion of a critical splicing enhancer results

2

in a severe reduction in *Plp* but not in DM20, an alternatively spliced isoform of *Plp* (Wang et al., 2008). In this model, SIRT2 protein but not its mRNA is severely reduced, suggesting that *Plp* but not DM20 is required for SIRT2 protein expression (Zhu et al., 2012). *Sirt2* also co-localizes with *Plp* to the compact myelin and is absent from the myelin proteome in the Plp1 knockout mouse (Li et al., 2007; Werner et al., 2007). In the *Qk^V* mutant, re-expression of the QKI-6 isoform is sufficient to rescue most of the QKI targets, including *Plp* and *Sirt2*, and is also able to correct the hypomyelination phenotype (Zhao et al., 2006b). In the *Qk^V* mutant, SIRT2 protein levels are reduced but mRNA levels are unaffected. This can be corrected by re-expression of QKI-6, through an increase in *Plp* expression (Zhu et al., 2012).

The majority of research regarding QKI and its role in myelin formation has focused on QKI-6. Since QKI-5 and QKI-6 have been proposed to play differential roles on the same mRNA targets, such as MBP, we decided to examine the function of QKI-5 with respect to regulating OL differentiation. The identification of a QKI-6-*Plp* pathway to regulate *Sirt2* expression provides a firm basis to work from. While it is unlikely that QKI-5 can completely inhibit differentiation, it is possible that QKI-5 may slow down the differentiation of OLs. While the differentiation of OLs is crucial to the proper formation of myelin in adequate quantities, the ability to hold OLs in an earlier progenitor state would allow the nervous system to tightly control the timing of myelinogenesis as well as the proper targeting and induction of remyelination.

1.1 HYPOTHESIS

1. The up regulation of QKI-5 will inhibit *Sirt2* and *Plp* expression, resulting in a delay in CG4 OL differentiation

2. The down regulation of QKI-5 will enhance *Sirt2* and *Plp* expression, driving the differentiation of CG4 OLs.

1.2 OBJECTIVES

1. Changes in the *Plp* and *Sirt2* mRNA and protein levels will be determined in CG4 OLs following overexpression or knockdown of QKI-5 over a six day period of differentiation.

2. Cell differentiation using two cell markers, A2B5 for early stage oligodendrocyte progenitors (OPCs) and GalC for mature, myelinating OLs will be determined in CG4 OLs following overexpression or knockdown of QKI-5 over a six day period of differentiation.

II   LITERATURE REVIEW

2.1   MYELINOGENESIS

In vertebrates, the neural tube gives rise to the central nervous system (CNS), including all CNS glia cells such as oligodendrocytes and astrocytes (Doetsch et al., 1997). The main function of glial cells is to provide support and protection for neurons. Astrocytes are important for regulation of synaptic transmissions, although they carry out a variety of active functions in the CNS. The OLs are a specialized glial cell type whose main function is the production and maintenance of the myelin sheath. In humans, myelination production begins in the fourteenth week of fetal development, although total myelin levels remain low until birth. Myelination is predominantly a post-natal process, with the vast majority of myelination occurring in infancy and continuing until adolescence. OL myelination continues *de novo* in white matter of prefrontal, parietal, and temporal areas of the human brain well into the fifth decade of life (Bartzokis 2004a; Bartzokis 2004b; Bartzokis et al., 2004).

Myelin is an electrically insulating membrane that forms around the axon of neurons. The presence of myelin decreases the capacitance of the axonal membrane, resulting in the ability to both efficiently propagate electrical signals as well as give them directionality. The plasma membrane of OLs extends outward and wraps multiple times around the axon, forming a multilayered myelin sheath that both protects and insulates the axon. The myelin sheath forms alternating regions of covered regions along the axon. Voltage-gated sodium channels cluster in uncovered gaps in the myelin sheath, termed the nodes of Ranvier, where saltatory nerve conduction (Latin *saltare*, 'to jump') takes place. This insulation, along with the proper spacing of nodes of Ranvier, is necessary for the proper propagation of action potentials which leap from one node to the next, allowing for rapid intercellular communication. Without myelin, electrical

impulses would move in waves along the axon membrane. This is both slow and inefficient. The resistance provided by the myelin sheath forces the electrical impulses to leap from one node to the next, allowing for much greater rates of conduction. The impulse speed of myelinated axons increases linearly along with axon diameter compared to unmyelinated axons where speed increases with the square root of the axon diameter. Thus, the presence of the myelin sheath maintains a small axonal diameter while still allowing electrical signals to travel at sufficient speeds. The formation and maintenance of myelin is crucial for proper development of the nervous system. The myriad of demyelinating conditions highlights the large number of ways that myelin degeneration can affect neuron structure and survival. As well, dysmyelinating diseases where the myelin sheath structure is defective rather than deteriorated emphasize the importance of myelin sheath formation to development as most dysmyelinating diseases are fatal with treatment generally being therapeutic rather than curative.

Myelin is a multilayered structure consisting of OL plasma membrane which wraps multiple times around the axon. When viewed in cross-section, myelin sheath appears as alternating thin, dark lines and thick, pale lines. The darker, thinner, major period line is the phospholipid bilayer fused on the cytoplasmic surface. The paler, thicker, interperiod line is the apposed outer layer of the cell membrane (Figure 1A). Internodes are the myelinated segments of an axon, and their length varies according to axon diameter. Each internode is separated by a node of Ranvier (Figure 1B), which are unmyelinated segments of the axon. The portion of myelin bordering each node is termed the paranodal region. Here, the cytoplasmic surfaces of myelin are not compacted and OL cell cytoplasm is included within the myelin sheath. In the paranodal region, the myelin sheath forms a loop-shaped structure called *lateral loops*,

which are the open major dense lines at the edge of the sheath and are filled with cell cytoplasm (Figure 1B)

Formation of the myelin membrane requires significant alteration of the plasma membrane. OLs must produce myelin specific proteins and coordinate their delivery to the myelin sheath. Following specific targeting of myelin proteins to the membrane, they must then be assembled into an organized structure of multilayered membrane stacks. For example, MBP mRNA is targeted to the myelin membrane during compaction of the myelin sheath. MBP mRNA is transported to the growing myelin membrane in granules and upon reaching its target destination it is then locally translated following integrin activation (White et al., 2008; Laursen et al., 2011). Following translation, the highly positively-charged MBP protein immediately binds to the negatively-charged myelin membrane, which brings the cytoplasmic faces of the myelin membrane together resulting in compaction of the myelin sheath. Similarly, *Plp* inserts into the membrane and by binding to other copies of itself in adjacent membranes helps compact the extracellular surfaces of the myelin membrane, forming the intraperiod line (Siegel et al., 2011).

A

Extracellular

PLP

SIRT2

Cytoplasmic

MBP

} major dense line

Extracellular

} intraperiod line

B

Lateral Loops

Axon

Node of Ranvier

Paranode Region

Paranode Region
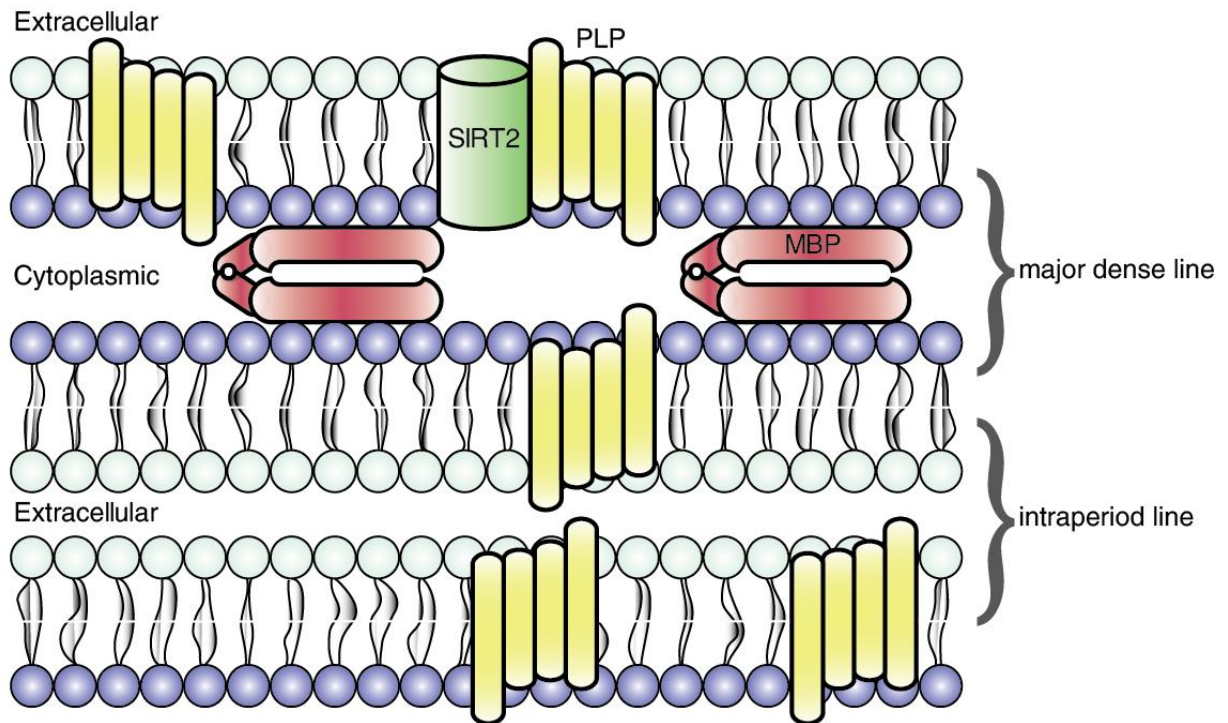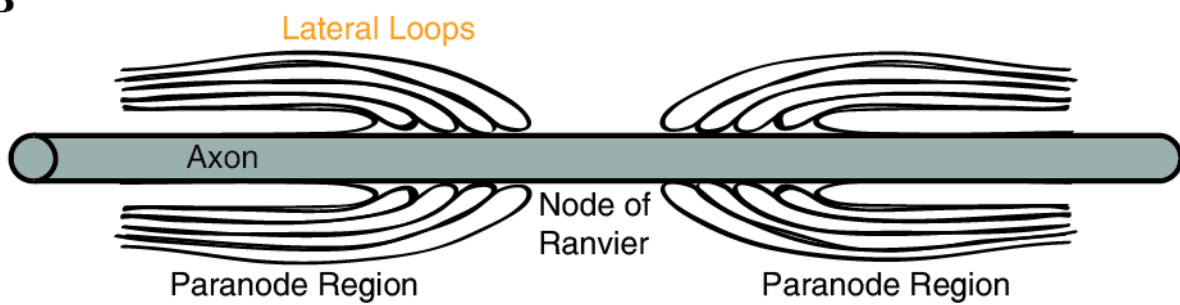
Figure 1. *The structure of the myelin sheath.* **A.** Schematic representation of the major myelin components. Myelin is compacted by removal of the cytoplasm and subsequent layering of the cytoplasmic plasma membrane surfaces (intraperiod line) and the extracellular plasma membrane surfaces (major dense line). Various proteins such as MBP are able to tightly fasten the cytoplasmic layers together while other proteins such as PLP and SIRT2 insert into the plasma membrane and help to secure the extracellular surfaces to one another. **B.** The compact myelin sheath expands the closer it is to the Node of Ranvier. This region, termed the paranodal region, consists of non-compacted myelin sheath. The myelin sheath forms a loop shaped structure, termed lateral loops, which is filled with cytoplasm. These lateral loops have been found to form organized channels which allow for the distribution of nutrients and metabolites throughout the compact myelin sheath. (Adopted from (Aggarwal et al., 2011)

Within the vertebrate nervous system, the propagation of electrical signaling relies on myelin. Myelin is a specialized structure that is formed by specialized glial cells; OLs in the CNS and Schwann cells in the peripheral nervous system (PNS). OLs arise from subventricular cells found within the brain and spinal cord and are the last cell type generated in the developing CNS (Thomas et al., 2000). These eventually differentiate into committed oligodendrocyte progenitor cells (OPCs) that migrate in waves throughout the CNS. The main function of OLs is to support neurons and insulate axons. OLs are distinguishable from other glial cells by their distinct morphology. They extend many processes, each of which contacts and envelopes a specific segment of an axon. The subsequent compaction of the membrane forms the myelin sheath around each segment of axon. In contrast, Schwann cells only extend a single process and thus each Schwann cell is only able to myelinate a single axon.

A2B5 is a monoclonal antibody developed by Raff et al. (Raff et al., 1983), that recognizes an epitope on a cell surface ganglioside expressed by OPCs as well as by thymic epithelial cells and neuroendocrine cells (Raff et al., 1983). The expression of this ganglioside in OPCs allows for *in vitro* identification by the A2B5 monoclonal antibody. OPCs that are A2B5$^+$ have the potential to differentiate into both OLs and type 2 astrocytes, depending on growth media conditions (Raff et al., 1983). A2B5 is a useful *in vitro* marker for OPCs but *in vivo* identification is generally accomplished using platelet-derived growth factor-α receptor (PDGFαR) and the sulfated proteoglycan (NG2) (Nishiyama et al., 1996; Levine et al., 2001). However, both NG2$^+$ and A2B5$^+$ cells arise from overlapping cell populations, with NG2$^+$ cells occurring earlier than A2B5$^+$ cells. NG2$^+$ cells can eventually give rise to A2B5$^+$ cells, suggesting that NG2$^+$/A2B5$^-$ cells are potentially O2A progenitors or pre-OPCs (Baracskay et al., 2007).

Galactosylceramide (GalC) is a glycosphingolipid that is highly enriched in the myelin membrane. GalC along with sulfatide, the sulfated version of GalC, comprises almost a third of the total lipid mass in myelin (Marcus and Popko 2002). GalC is expressed later than A2B5, mainly in differentiating OLs (Ranscht et al., 1982; Schaeren-Wiemers et al., 1995). Blocking GalC function through the use of anti-GalC antibodies has been shown to disrupt myelination, both *in vitro* and *in vivo* (Ranscht et al., 1987; Owens and Bunge 1990; Rosenbluth et al., 1994). Interestingly, mutant mice which lack uridine diphosphate (UDP)-galactose:ceramide galactosyltransferase (CGT) the synthase responsible for GalC formation (Coetzee et al., 1996b), were able to myelinate axons but the myelin sheaths were thinner, displayed an immature morphology, altered myelin lipid composition and improper targeting of contact proteins to the paranodal region (Bosio et al., 1996; Coetzee et al., 1996a; Dupree et al., 1999; Poliak et al., 2001). GalC appears to be essential for the proper maintenance of axo-glial interactions as well as compaction of the myelin sheath (Boggs et al., 2010). However, the absence of GalC does not impact the formation of myelin. This suggests a dysmyelination phenotype with defects in the myelin sheath structure as myelin still developed and is able to myelinate axons. Indeed, CGT-null mutant mice develop severe clinical symptoms with tremors starting around 2 weeks after birth as well as paralysis and eventually early death (Marcus and Popko 2002).

An additional function of GalC is as a signal transmitter, able to regulate OL differentiation by influencing cytoplasmic microtubule polymerization (Boggs and Wang 2001), membrane organization and myelin protein expression (Bansal and Pfeiffer 1989; Bansal and Pfeiffer 1994). The location of GalC along with the effects of anti-GalC antibodies suggests that GalC may function in transmitting signals across the myelin membrane. The ability of GalC to interact with both homo- and hetero-carbohydrate polymers has the ability to drive clustering of GalC on the extracellular

side of the membrane, as well as aggregation of MBP, *Plp* and myelin/oligodendrocyte glycoprotein (MOG) on the cytoplasmic side of the membrane (Boggs and Wang 2004; Boggs et al., 2004; Boggs et al., 2008). This suggests a role for GalC in guidance and organization of membrane rafts. Several proteins involved in signal transduction, such as mitogen activated protein kinase (MAPK) and some phosphotyrosine-containing proteins also clustered with GalC and MBP. The 'activation' of these membrane rafts, using GalC-containing liposomes, was able to cause depolymerization of microtubules and actin filaments within the myelin membrane sheets, suggesting that extracellular surface GalC may facilitate trans membrane signal transduction and possibly influence morphological changes (Boggs and Wang 2004).

2.1.1.1 *Intracellular Kinase Cascades in Developing OL*

Mitogen-activated protein kinases (MAPKs) are serine/threonine-specific kinases which are activated in response to a myriad of extracellular signals. MAP kinases, such as p38MAPK, are activated via phosphorylation by upstream MAPK kinases (MAPKK). p38MAPK is a stress response mediator in neural cells (Stariha and Kim 2001) and regulates several cellular processes including cell growth and survival (Zetser et al., 1999; Zhang et al., 2006; Ventura et al., 2007). Specifically, p38MAPK has been shown to affect both cell proliferation and differentiation in the presence of platelet-derived growth factor (PDGF) and fibroblast growth factor 2 (FGF-2) (Baron et al., 2000). A role for p38MAPK in OL maturation and initiation of myelination has also been discovered, both in Schwann cells (Fragoso et al., 2003) and in OLs (Fragoso et al., 2007). As well, inhibition of p38MAPK resulted in a reduction in OL-specific antigen expression (i.e., GalC) and protein expression (i.e., MBP, MAG) (Bhat et al., 2007). It is involved in both myelin-specific lipid synthesis as well as myelin-specific protein expression, making p38 essential for early stage OL differentiation.

Forskolin is an agent that increases intracellular cyclic adenosine monophosphate (cAMP) and induces cAMP response element-binding (CREB) protein phosphorylation by activating protein kinase A (PKA), ultimately leading to OL differentiation (Bhat et al., 2007). However, inhibition of p38MAPK can block forskolin-induced CREB phosphorylation as well as suppress MBP expression at both the translational and transcriptional level (Bhat et al., 2007). This suggests a potential link between PKA and p38 pathways in the differentiation of OLs. p38MAPK is important during OPC transition to the preoligodendrocyte stage, as inhibition of p38MAPK during this time point reduced myelin gene expression (Fragoso et al., 2007). The phosphorylation of p38MAPK coincides temporally with MBP protein expression in CNS white matter, and its detection at P11 in CC1+ OLs (Chew et al., 2010), supports a role in promoting OL differentiation. It was also shown that p38MAPK activity stimulates Sox enhancer and MBP promoter activity, as well as promoting Sox10 function (Chew et al., 2010). While the study only examined the role of p38MAPK and Sox10 on MBP promoter binding, it is also possible that since Sox10 has been linked with both MBP and *Plp* gene expression (Stolt et al., 2002) that QKI regulates *Plp* gene expression via the p38MAPK pathway. Further to this, inhibition of p38MAPK resulted in a reduction in Sox10 mRNA as well as decreasing $p27^{KIP1}$ protein accumulation (Fragoso et al., 2007). The ability of QKI to bind $p27^{KIP1}$ mRNA leading to enhanced MBP promoter activity specifically in OLs (Miskimins et al., 2002) combined with requirement of Sox10 expression for MBP promoter activation through $p27^{KIP1}$ (Wei et al., 2004) provides another pathway through which QKI can affect myelin-specific gene expression.

2.1.2 *Proteolipid protein 1*

Proteolipid protein 1 (*Plp*) is the most abundant myelin protein found within the CNS. It constitutes approximately 50% of the total myelin protein (Dubois-Dalcq et al.,

1986). *Plp* is a 4 transmembrane domain protein that inserts into the plasma membrane and is a structural constituent of the myelin sheath. By binding to other copies of itself it facilitates the compaction of the myelin layers (Figure 1). The *Plp* gene is located on the X chromosome in man, mouse and rat and consists of 7 exons spanning ~17kb (Campagnoni and Skoff 2001). The *Plp1* gene encodes for two slice variants, *Plp* and DM20. Both arise from the same primary transcript but through alternative splicing, the final DM20 protein differs from *Plp* by an internal deletion of 35 amino acids (Nave et al., 1987). However, *Plp* is the more abundant protein isoform in the mammalian post-natal brain and its expression is unique to myelin. The exclusion of exon 3B by DM20 results in loss of axo-glial interaction signaling (Stecca et al., 2000; Gudz et al., 2002). The ratio of *Plp*/DM20 has been shown to be important in many processes including myelin-axon integrity, stabilization of the myelin sheath, and axonal transport (Griffiths et al., 1998; Yin et al., 2006; Werner et al., 2007; Regis et al., 2009). The abundance of *Plp* to DM20 coupled with the unique ability of *Plp* to interact with axons and glial cells points to the importance of *Plp* rather than DM20 in myelinogenesis. In the quaking viable mutant mouse brain, *Plp* mRNA but not DM20 mRNA is severely reduced. Up regulation of QKI-6 is able to rescue the shortage of *Plp* mRNA in the Qk^v/Qk^v mutant (Zhu et al., 2012). While the main function of *Plp* is generally based around structural integrity of myelin, there exists a role for *Plp* as a signal transduction molecule. The selective regulation of *Sirt2* by *Plp* suggests that the two proteins are able to interact with each other (Zhu et al., 2012). However, the exact nature of this interaction has yet to be determined. However, since QKI has been demonstrated to regulate *Plp* expression, it is possible that QKI, via *Plp*, can ultimately regulate *Sirt2* expression.

2.1.3   NAD-dependent deacetylase sirtuin-2

Sirtuins (Sirt) are nicotinamide adenine-dinucleotide (NAD)-dependent deacetylases that regulate cellular function via protein deacetylation (Michan and Sinclair 2007). There are 7 sirtuins, with *Sirt2* being predominantly expressed in OLs (Tang and Chua 2008). Sirtuins belong to a larger group of proteins called histone deacetylases (HDACs), which have been shown to be involved in neuron and glial cell development (Gray and Ekstrom 2001). SIRT1 has been shown to regulate energy metabolism and extension of lifespan in both yeast and *Drosophila* (Denu 2005; Donmez and Guarente 2010). Excess of SIRT2 protein may be harmful for neurons (Suzuki and Koike 2007; Pfister et al., 2008). Indeed, pharmological inhibition of *Sirt2* has been demonstrated to have neuroprotective effects in varying models of neurodegenerative disease, including Parkinson's disease (Outeiro et al., 2007; Luthi-Carter et al., 2010) and Huntington's disease (Luthi-Carter et al., 2010). *Sirt2* has been shown to function as an α-tubulin deacetylase and is involved in both cell division and differentiation (Dryden et al., 2003; North et al., 2003; Li et al., 2007). The majority of studies on neuronal microtubule acetylation have focused on HDAC6 activity (Hubbert et al., 2002; Matsuyama et al., 2002; Zhang et al., 2003a), however *Sirt2* has the highest RNA levels in postnatal brain tissue of all the 18 characterized HDACs and sirtuins (Pandithage et al., 2008). One of the protein isoforms of *Sirt2*, SIRT2.2, is preferentially expressed in the brain and spinal cord (Maxwell et al., 2011). As well, there is an age-dependent accumulation of SIRT2 in the CNS of wild-type mice (Maxwell et al., 2011). The larger SIRT2.1 isoform is generally expressed in non-neuronal cell types and immortalized cells in culture (Maxwell et al., 2011) rather than in neurons. Strong *Sirt2* immunoreactivity is associated with focal areas of decreased acetylated α-tubulin staining in neurons, along with the preferential expression of *Sirt2* in the CNS, suggests a role for SIRT2.2 in regulating microtubule acetylation in mature neurons (Maxwell et

al., 2011). The functions of *Sirt2* combined with the presence of a QKI binding site in *Sirt2* mRNA (our laboratory data) make *Sirt2* a prime candidate to be regulated by QKI protein in the developing CNS.

Sirt2 is upregulated during myelinogenesis and is now considered an essential component of the myelin proteome (Southwood et al., 2007; Werner et al., 2007). The alternatively spliced variant *Sirt2* variant 2 (v2) localizes to the paranodal and compact myelin in close proximity of *Plp* (Li et al., 2007; Southwood et al., 2007; Werner et al., 2007). In the *Plp1* gene knockout mouse brain in which both PLP and DM20 are absent, SIRT2v2 protein, but not mRNA, is severely reduced. Its absence from the myelin proteome as well suggests that PLP/DM20 is required both for the correct transport of SIRT2 to the myelin membrane, as well as the stabilization of SIRT2. SIRT2 protein has also been shown to control process arborization in differentiating OLs *in vitro*, by regulating α–tubulin acetylation. Although most researchers, including work done in our lab (Ji et al., 2011) have shown that *Sirt2* enhances OL differentiation, one group has shown that by deacetylating α–tubulin, *Sirt2* was able to delay OL differentiation (Li et al., 2007). Since process arborization in OLs is crucial *in vivo* for the proper myelination of axons, it suggests an important role for *Sirt2* in regulating the development of OLs.

In the quaking viable mutant mouse brain, SIRT2v2 protein, but not mRNA, is severely reduced but can be rescued by up regulation of QKI-6 (Zhu et al., 2012). It was also shown that SIRT2 abundance in myelin is dependent on PLP dosage, but not DM20 (Zhu et al., 2012), providing further evidence that PLP regulates the transport and/or stability of SIRT2 in the myelin membrane. The same group also demonstrated that hypomyelination is not sufficient to cause a reduction in SIRT2, but rather that the specific reduction of PLP due to QKI-6 deficiency affects SIRT2 regulation (Zhu et al., 2012). Furthermore, when PLP, but not DM20 was selectively reduced, SIRT2 accumulated in OL cell bodies instead of transporting to the membrane periphery (Zhu

et al., 2012). The end result is an abundance of SIRT2 in the OL cell bodies due to defective transport of SIRT2 to the myelin membrane via PLP. This defective targeting of SIRT2 suggests a crucial role for PLP in regulating OL development.

2.2   STAR PROTEINS

The signal transduction and activation of RNA (STAR) family is a class of evolutionarily conserved proteins that link signal transduction with RNA metabolism. Members of the STAR family include the *Drosophila melanogaster* gene *held out wings* (HOW) and KH encompassing protein 1 (KEP1) proteins, the *Caenorhabditis elegans* germline development defective 1 (GLD-1) protein, and the mammalian Src-associated in mitosis (SAM68) and *quaking* (QKI) proteins (Lukong and Richard 2003). The common feature among all STAR proteins is the presence of a triple domain structure, referred to as the STAR domain (Vernet and Artzt 1997). The STAR domain consists of an uncommon single expanded KH RNA binding domain (Maxi-KH), flanked by two conserved domains: QUA1 (amino terminal) and QUA2 (carboxyl terminal). The KH domain is present in a variety of nucleic acid-binding proteins and is able to bind either RNA or single stranded DNA (Garcia-Mayoral et al., 2007). The QUA1 domain is both necessary and sufficient for dimerization and that dimerization is crucial for proper function. The QUA1 domain is necessary for homo/heterodimerization and aids in stabilizing RNA binding (Chen and Richard 1998; Wu et al., 1999). Dimerization is necessary for successful RNA binding as most other RNA binding proteins contain multiple KH domains, which stabilize binding, while STAR proteins contain only a single KH domain. The KH and QUA2 domain form an extended RNA-binding interface, able to bind to short penta- or hexanucleotide consensus sequences (Ryder et al., 2004; Galarneau and Richard 2005). KH and QUA2 domains are sufficient for RNA-binding activity, with the QUA2 domain facilitating high affinity binding (Ryder et al., 2004). Dimerization improves affinity, likely mediated by direct interactions with RNA

from both subunits of the dimer, although exactly how this influences binding is unresolved. One other aspect that is shared among the STAR proteins is the presence of a various signal transduction elements including proline-rich regions or Src homology 3 domain (SH3) and WW-binding sites (Lukong and Richard 2003; Rajan et al., 2008a).

Functionally, all of the STAR proteins are involved in regulating developmental differentiation. In *D. melanogaster*, HOW is involved in the development of the heart, somatic muscles, and tendons (Volk et al., 2008). In *C. elegans*, GLD-1 is required for the advancement of germ line cells through the prophase of meiosis (Hansen and Schedl 2006). The mammalian SAM68 and QKI protein are the most well characterized of the STAR family proteins. The mouse SAM68 was the first characterized STAR protein and is a phosphoprotein that is found downstream of SRC (Fumagalli et al., 1994) and FYN (Fusaki et al., 1997). It is involved developmentally in bone metabolism, male fertility, and locomotion (reviewed in Sette et al., (2010)). Tyrosine phosphorylation by Src during mitosis suggests that SAM68 additionally plays a role in cell cycle regulation and signaling. The other major mammalian STAR protein, QKI, has a well described role in myelinogenesis during CNS development.

One other similarity among STAR proteins is the presence of alternative splice sites within their mRNA transcripts and the generation of multiple isoforms. Both the mammalian *Qk* and the *Drosophila* homologue *how* generate multiple splice forms (Ebersole et al., 1996; Nabel-Rosen et al., 2002). Two opposing isoforms of the RNA-binding protein HOW regulate Stripe, a key protein in the differentiation of tendon cells. The isoform How(L) is a negative regulator while How(S) elevates Stripe levels through binding of the 3′-UTR of *stripe* mRNA. How(S) is able to neutralize the repression of Stripe by How(L) when both isoforms are coexpressed. Binding of How(L) to *stripe* mRNA leads to increased degradation while binding of How(S) stabilizes the target mRNA (Nabel-Rosen et al., 2002). The interesting thing about How(L) activity is

that the nuclear retention signal present in the 3′-UTR of How(L) is necessary for its ability to repress Stripe expression (Nabel-Rosen et al., 2002). This is quite similar to the role of QKI-5, which also contains a nuclear localization signal in its 3′-UTR, which has been implicated in the regulation of alternative splicing of MAG. While a role for QKI-5 in the degradation of mRNA targets has not yet been described, the ability of QKI-6 to stabilize mRNA targets through 3′-UTR binding (Larocque et al., 2005; Zhao et al., 2006a) is strikingly similar to the function of How(S). Below I provide a review of the various functions of STAR proteins as well as the *quaking* mutation and the role of the *quaking* gene in regulating RNA metabolism and oligodendrocyte differentiation.

2.2.1 Post-Transcriptional Regulation by STAR Proteins

STAR proteins are involved with pre-mRNA splicing, mRNA localization, transport, and mRNA stability and translation efficiency (Galarneau and Richard 2005). QKI regulates nuclear retention of MBP mRNA and transport to the myelinating membranes (Li et al., 2000; Larocque et al., 2002). *C. elegans* GLD-1 protein controls gene expression by acting through a hexanucleotide sequence (NACUCA) called TGE in the target 3′ UTR to repress translation of Tra-1 protein (Jan et al., 1999). QKI-6 acts in a similar manner through the *Gli1* mRNA to repress translation (Saccomanno et al., 1999; Lakiza et al., 2005). Another level of regulation in Qk is through its very long and conserved 3′-UTR that theoretically contains a large variety of miRNA binding sites (57% of the 677 defined human miRNAs). QKI belongs to a small group of genes (<40 cDNAs that contain more than 350 different miRNA sites) that have the highest predicted number of miRNA binding sites in the human genome (Artzt and Wu 2010). This provides great flexibility in the regulation of QKI in many different tissues, resulting in the ability of cells to exercise precise spatial and temporal control. There is also the possibility of transcriptional control with possibly several alternate tissue-

specific promoters (Hardy et al., 1996). This high number of potential miRNA binding sites is actually unique to QKI as its 3′-UTR has 3 times as many potential binding partners as the next STAR protein, splicing factor 1 (Artzt and Wu 2010).

By studying several ENU-induced or knockout alleles of Qk, a number of mutant phenotypes were created. These include mice with abnormal somites, heart defects, cranial defects, and a disorganized anterior-posterior axis (Justice and Bode 1988), lack of vascular development (Lorenzetti et al., 2004a), mis-regulation of visceral endoderm function (Bohnsack et al., 2006), smooth muscle cell differentiation, kinky and open neural tubes (Li et al., 2003). The presence of viable alleles point out important functions in the nervous system, mainly the lack of myelination in both CNS and PNS (Sidman et al., 1964), but also include, early-onset seizures, severe ataxia, dramatically reduced lifespan and Purkinje cell axonal swellings indicative of neurodegeneration (Noveroske et al., 2005).

2.2.2   *RNA Recognition by STAR Domain Proteins*

In situ crosslinking studies in cell culture demonstrate that QKI self-associates (Chen and Richard 1998). Self-association requires the QUA1 region, shown through mutagenesis. A single point mutation within the QUA1 region of QKI eliminates dimerization both *in vitro* and in cell culture and causes an embryonic lethal phenotype in mice (Chen and Richard 1998). ENU-induced point mutations within the KH and QUA2 domains of QKI yield an embryonic lethal phenotype, thus, both regions are required for proper function (Justice and Bode 1988). QKI is homologous to GLD-1 and is capable of binding to TGE RNA *in vitro* and QKI-6 can functionally substitute for GLD-1 in a reporter assay in worms (Saccomanno et al., 1999; Ryder and Williamson 2004). A consensus sequence, termed the STAR-binding element (SBE) is 5′ - NA(A/C)UAA – 3′, is found within the KH domain, which has also been identified in

QKI (Ryder and Williamson 2004). In an independent study, binding specificity of QKI was determined using an *in vitro* SELEX protocol (Galarneau and Richard 2005). This led to the identification of a number of aptamer sequences, many of which contained separate "core" 5′ - NACUAAY – 3′ and "halfsite" 5′ - YAAY – 3′ motifs with variable spacing (Galarneau and Richard 2005). The discovery that the QKI consensus sequence contained a bipartite RNA motif lead to the discovery that SLM-2, SAM68, and GLD-1 protein also bind bipartite RNA direct repeats (Galarneau and Richard 2009)

2.2.3   *Post-Translational Regulation of STAR Proteins*

Sam68 is the most well characterized STAR protein when it comes to post-translational modification. Sam68 enhances export and cytoplasmic utilization of viral RNAs (Li et al., 2002a; Coyle et al., 2003) modulates transcription of target genes (Hong et al., 2002), and alternative splicing (Rajan et al., 2008b). It has been shown to regulate the choice of alternatively spliced exons in CD44, Bul-x and a subset of transcripts required for neurogenesis (Matter et al., 2002; Paronetto et al., 2007; Chawla et al., 2009). It is detected in primary neurons (Ben Fredj et al., 2004; Grange et al., 2009), germ cells (Paronetto et al., 2011; Messina et al., 2012), where it associated with the translation initiation complex eIF4F and polyribosomes, thereby enhancing translation. Many varied tasks in different cell types (activity and localization) needs to be fine-tuned according to the specific requirements of the cell. Human breast tumor kinase (BRK) associates with and phosphorylates Sam68 tyrosine residues (Derry et al., 2000). BRK localized to the nucleus and accumulates in the same nuclear bodies as Sam68. Tyrosine phosphorylation of Sam68 leads to decreased affinity for RNA (Wang et al., 1995; Derry et al., 2000). BRK-mediated tyrosine phosphorylation of Sam68 promotes its nuclear translocation in breast cancer cells under stimulation with epidermal growth factor (EGF) (Lukong et al., 2005). BRK is aberrantly regulated in prostate cancer (Derry et al.,

2003), a tumor type in which Sam68 is upregulated (Busa et al., 2007) and hyperphosphorylated (Paronetto et al., 2004) and its expression supports growth and survival of the neoplastic cells (Busa et al., 2007). Serine phosphorylation of Sam68 by ERK1/2 (extracellular regulated kinases 1 and 2, a member of the MAPK family) affected the splicing activity, enhancing inclusion of the variable exon 5 (v5) in the CD44 mRNA (Matter et al., 2002). ERK1/2 mediated phosphorylation was the main regulator of the association of Sam68 with the translational machinery (Paronetto et al., 2006). Translocation of Sam68 to the cytoplasm and its association with polyribosomes was required for translational activation of a subset of mRNAs that are a target in germ cells (Paronetto et al., 2009; Paronetto et al., 2011). Thus, serine/threonine mainly affects its RNA-binding activity.

Similar to Sam68, phosphorylation of the C-terminal tyrosine residues in QKI proteins by Src or Fyn decreased their affinity for target RNA *in vivo* and *in vitro* (Zhang et al., 2003b). Tyrosine phosphorylation of QKI proteins was maximal at 7d postnatal and rapidly declined from 7d to 20d, concomitantly with the strong induction in MBP mRNA and protein levels and with myelinogenesis (Zhang et al., 2003b). Expression of Fyn was elevated in OPCs, whereas the activity of this Src family kinase declined later on during myelin accumulation (Lu et al., 2005). Fyn and QKI activity also seemed to antagonistically regulate alternative splicing of MBP mRNA isoforms (Lu et al., 2005).

2.3 QK GENE

The *Qk* gene codes for a STAR family, RNA-binding protein that is responsible for post-transcriptional regulation of RNA targets. It was first discovered following the characterization of a viable mutant strain in mice that resulted in a homozygous recessive deletion. Mice with this deletion exhibited a 'quaking' phenotype (Sidman et al., 1964), whole body tremors that presented shortly after birth. This ~1Mbp deletion

resulted in a reduction in expression of myelin proteins as well as severe

hypomyelination in the CNS (Hardy 1998), and it was eventually found that a gene

directly downstream of the deletion was responsible for the dysmyelination phenotype.

The recessive mutation first reported by Sidman et al., (1964) results in the loss of a

promoter/enhancer region for a gene immediately downstream of the deletion, which

was termed the *quaking* gene.

The mouse Qk gene was cloned in 1996 by Artzt's group (Ebersole et al., 1996).

The coding sequence and genomic organization are highly conserved in mammals

(Matsumoto et al., 1999; Li et al., 2002b). There are 3 major isoforms which arise from

alternative splicing (Ebersole et al., 1996), named according to the length of the mRNA

sequence, QKI-5, QKI-6, and QKI-7. All 3 isoforms share the same N-terminus, which

contains an extended hnRNP K homology (KH) domain which is responsible for RNA-

binding. Each isoform has a distinct C-terminus that determines their subcellular

localization. QKI-5 contains a nuclear localization signal (Wu et al., 1999) while QKI-6

and QKI-7 are mainly found within the cytoplasm. QKI isoforms have similar

selectivity and affinity to similar mRNA ligands *in vitro* (Zhang et al., 2003b; Galarneau

and Richard 2005) and their separate cellular localization is thought to result in

differential and perhaps even opposing influences. QKI plays an essential role in

controlling proliferation and differentiation of myelinating glial cells (Larocque et al.,

2005; Chen et al., 2007), as well as in the actual ensheathment of axons by the

specialized myelin membrane (Li et al., 2000; Wu et al., 2001; Zhao et al., 2006b). A lack

of QKI in the white matter also may contribute to impairment in cognitive diseases such

as schizophrenia and depression (Aberg et al., 2006a; Aberg et al., 2006b; Haroutunian

et al., 2006; Klempan et al., 2009).

The *quaking* gene consists of nine exons which are distributed over ~65kb (Matsumoto et

al., 1999). The first 5 exons are shared by all the transcripts and it is the last 4 exons

along with the 3'-UTRs that give rise to the splice variants. Exons 2-5 encode the conserved QUA1, KH, and QUA2 domains. All 3 isoforms, QKI-5, QKI-6, and QKI-7, contain the same N-terminal region, as well as a QUA1, KH, and QUA2 domains. Exon 9 provides the 3'-UTR for QKI-5, the 3'-UTR of QKI-6 is formed from part of exon 7 and the whole of exons 8 and 9, while the majority of exon 7 forms the 3'-UTR of QKI-7 (Figure 2). However, exon 7, contains an internal stop codon that is normally spliced out of the QKI-5 message, can sometimes be partially included in a 5-kb message. This results in a protein produced by this 5-kb message that is identical to QKI-6 but its mRNA contains a 3'-UTR that is the same as QKI-5. Interestingly, because of the stop codons found within exon 7, QKI-5 actually contains the largest coding sequence and shortest 3'-UTR, while QKI-7 contains the shortest coding sequence and the largest 3'-UTR.

Since the RNA binding domain is shared by all 3 transcripts, theoretically all 3 isoforms are able to bind the same mRNA targets. However, the presence of a nuclear localization signal in the C-terminal region of QKI-5 (Wu et al., 1999) results in it being predominantly found in the nucleus while QKI-6 and QKI-7 are predominantly found within the cytoplasm. As previously mentioned there are transcripts that code for the QKI-6 but contain the 3'-UTR from QKI-5 and thus are able to be shuttled into the nucleus. QKI mainly functions in pre-mRNA splicing, mRNA localization, transport, mRNA stability, and translation efficiency (Galarneau and Richard 2009). The expression of *quaking* is abundant in myelinating glial cells in both the CNS and PNS. As well, QKI proteins have been found in Bergmann glia and astrocytes, but their expression is absent from CNS neurons (Hardy et al., 1996). The expression profile of QKI also follows a developmental profile. QKI mRNA transcripts can be detected early in embryonic development and their expression continues on until well past birth. In mouse development, the QKI-5 isoform is expressed earliest, with expression
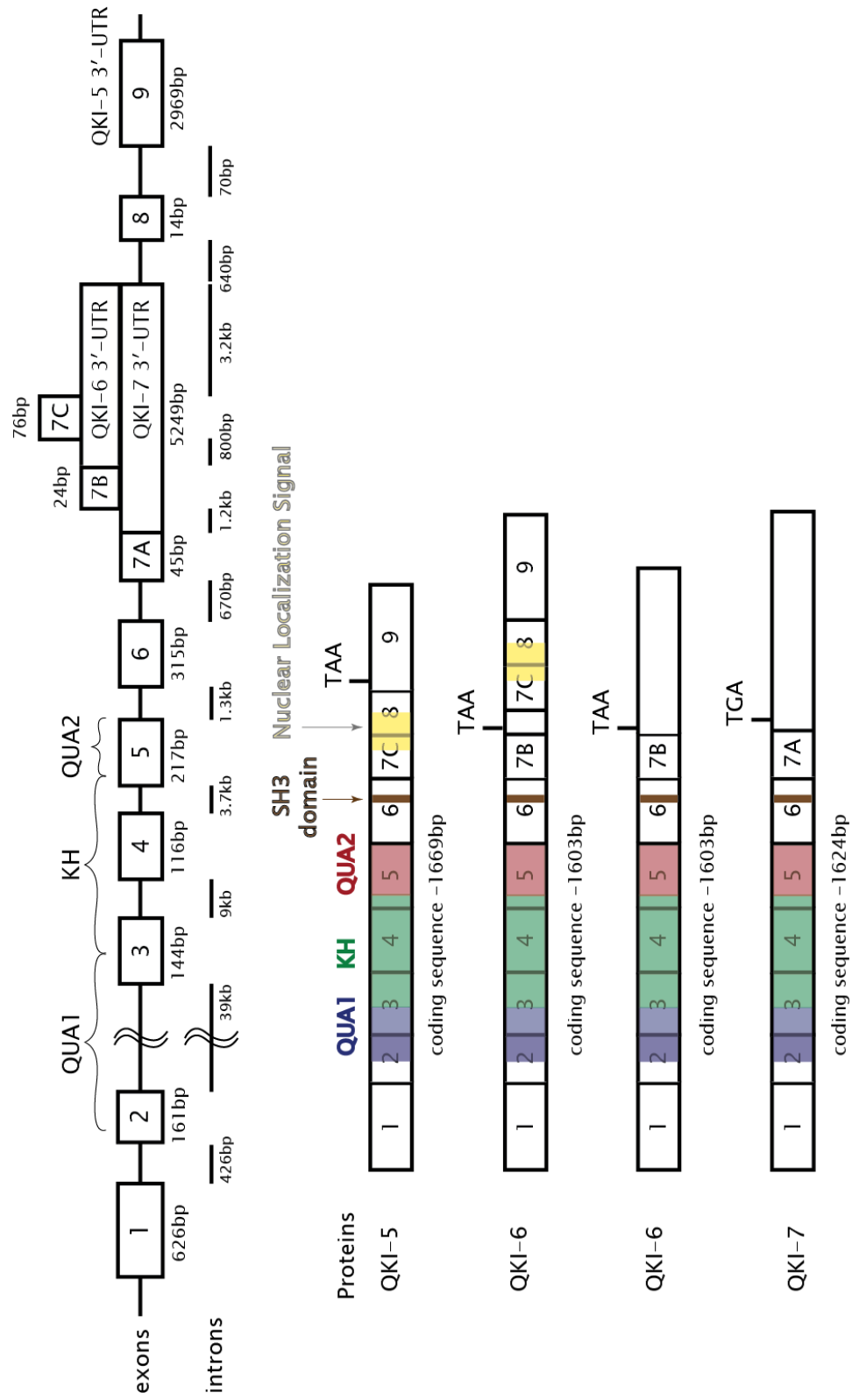
Figure 2. *Organization of the QKI gene.* Schematic representation of the QKI gene. Shown up top are the 9 exons that make up the entire QKI gene along with the sizes for each exon. The regions that code for the QUA1, KH, and QUA2 domains are also marked. There are four isoforms generated through alternative splicing. All four isoforms contain the same RNA binding domains with the main difference being the coding sequence of their 3′-UTR. There is also the possibility of an isoform being generated that contains the coding sequence for QKI-6 but with the 3′-UTR of QKI-5.

expression decreasing by P14 (Ebersole et al., 1996). On the other hand, QKI-6 and QKI-7 are not expressed until closer to birth, reaching the peak of expression at P14 in mice, which correlates with the peak of myelination (Ebersole et al., 1996). Specifically, mRNA transcripts for all three isoforms can be detected from total embryonic RNA at E5.5, but by E7.5 expression is limited to the extraembryonic visceral endoderm and is absent from the mesoderm (Bohnsack et al., 2006). The expression of QKI-5 in particular is limited to the visceral endodermal layer and is absent from both mesodermal-derived endothelial and mesenchymal cells (Noveroske et al., 2002). In mutant mice that do not express QKI-5, a reduction in QKI-6 and QKI-7 transcript and protein levels was also observed, suggesting that QKI-5 may regulate QKI-6 and QKI-7 expression during early development (Bohnsack et al., 2006).

QKI has been proposed to regulate myelin formation by three different mechanisms. The first is that QKI stabilizes various mRNAs required for proper myelinogenesis. These include MBP, *Plp*, microtubule associated protein 1B (Map1B), and p27^{Kip1} (Li et al., 2000; Larocque et al., 2005; Zhao et al., 2006a). The second is that QKI controls the cellular localization of target mRNAs. The discovery of a QRE in the 3′-UTR of *Mbp* mRNA combined with EMSA and UV-crosslinking assays showed that all three QKI isoforms can directly bind *Mbp* mRNA (Larocque et al., 2002). The overexpression of QKI-5 in primary mouse OL cultures resulted in both mislocalization of *Mbp* mRNA and lowered protein expression. The majority of *Mbp* mRNA was found to be retained in the nucleus, with little mRNA being present in OL processes (Larocque et al., 2002). This is evident when *Mbp* mRNA is retained within the nucleus following up regulation of the nuclear isoform, QKI-5 (Larocque et al., 2002). The third mechanism is the regulation of alternative splicing. QKI has been demonstrated to regulate alternative splicing of *Mbp*, *Plp1*, and *Mag* (Wu et al., 2002). There is an imbalance in the ratio of alternative splice variants for *Mbp*, *Plp1*, and *Mag* in the

homozygous *Qk^V/Qk^V* mutant. It appears that the location of the QRE and subsequently the location at which QKI binds the target mRNA is a main determinant of the mechanism by which QKI regulates the target mRNA. When the QRE exists in the 3'-UTR, we see stabilization of these targets as well possible mislocalization of the target transcripts. However, when the QRE is present in the coding region, usually at a splice site, then we see the effect of QKI as regulating alternative splicing. In *Mag* RNA, the QRE is present at the 5' splice site of exon 12 and inclusion of *Mag* exon 12 is repressed in a substrate specific manner by QKI-5 (Wu et al., 2002). Since the only difference between the three QKI isoforms is their 3'-UTR sequences, the distinctive functional differences between the three isoforms is largely attributed to the location of the QRE in the target mRNA sequence, combined with the differences both spatially and temporally in the expression of the three isoforms.

More recently, QKI has been increasingly linked with other RNA binding proteins such as hnRNPA1. By binding to the 3'-UTR of hnRNPA1, QKI is able to enhance hnRNPA1 mRNA stability (Zearfoss et al., 2011). Additionally, hnRNPA1 and QKI both regulate a subset of myelin-related mRNAs (Zearfoss et al., 2011). Thus, QKI is able to indirectly regulate the expression of a larger variety of myelin related genes by modulating the expression of hnRNPA1. QKI is able to have two opposing effects on *Mbp* and *Hnrnpa1*, chiefly by increasing mRNA abundance and inhibiting translational efficiency (Zearfoss et al., 2011). This suggests a mode of action whereby QKI targets are transcribed but then kept in a translationally inactive but stable state. This would enable the cell to respond rapidly to a signal, perhaps by allowing the translation of sequestered target mRNAs.

2.3.1 The Quaking viable mutant

The homozygous *quaking* viable *(Qk^V/Qk^V)* mutant mice carry a recessive mutation which affects three different genes; deletion of the entire *parkin* coregulated gene (Lockhart et al., 2004; Lorenzetti et al., 2004b), deletion of part of the *parkin* gene (Lockhart et al., 2004; Lorenzetti et al., 2004a), and deletion of the promoter and enhancer region of the *qk* gene (Ebersole et al., 1996; Matsumoto et al., 1999). Mice with this deletion exhibited a 'quaking' phenotype, typically whole body tremors that presented shortly after birth. It was eventually found that this deletion resulted in a reduction in expression of myelin proteins as well as severe hypomyelination in the CNS (Hardy 1998). The *Qk^V* mutation leads to development of whole body tremors or 'quaking', which manifests itself around 10 days after birth (Sidman et al., 1964). The resulting dysmyelination phenotype is as a result of a reduced number of mature OLs in the CNS, defects in Schwann cell maturation, the reduced number of myelin lamellae produced and the failure of the resulting myelin to compact (Hardy 1998; Chenard and Richard 2008). The severity of the dysmyelination phenotype exhibited by *Qk^V* mutant mice is not globally distributed. Tracts in the forebrain, such as the corpus callosum, are more severely dysmyelinated while tracts in the caudal region of the brain, such as the medulla and optic nerve, are less severely affected (Friedrich 1975). This rostral-caudal gradient is unusual among dysmyelinating mutants and it is not entirely clear what is the root cause. However, there is a correlation with QKI-5 expression in the *Qk^V* mutant. Expression of QKI-5 is present in almost all OLs in the medulla and optic nerve, while QKI-5 is virtually nonexistent in the corpus callosum or anterior commissure (Hardy et al., 1996). The expression of QKI-6 and QKI-7 do not follow the dysmyelination gradient, as almost all OLs do not express either protein. These changes in QKI protein expression are unique to the *Qk^V* mutant, as examination of other dysmyelinating mutants such as *shiverer* and *jimpy* reveal normal QKI protein expression in OLs (Hardy

et al., 1996). While expression of QKI-6 and QKI-7 are severely reduced in myelinating cells, their expression appears to be unaffected in astrocytes and Bergmann glia.

It is interesting to note that the Qk^V deletion results in specific down regulation of QKI proteins in OLs, but not in other cell types. When QKI proteins, specifically QKI-5, is absent during development, the mice are embryonically lethal (Cox et al., 1999). This suggests a broader role for Qk beyond myelination. Combined with the fact that Qk mRNAs have been found in tissues outside of the CNS, including the heart, lung, and testes (Ebersole et al., 1996) and it is becoming increasingly clear that Qk is important for proper embryonic development.

The embryonic defects associated with down regulation of QKI-5 are absent in the Qk^V mutant mice. The Qk^V mutant mice are viable, able to survive past birth and even produce offspring. As well, the only mutant phenotypes expressed in Qk^V mutant mice are a dysmyelination phenotype and male sterility. Due to the close proximity of Qk to the mutation site and the down regulation in QKI protein expression in OLs, it has been speculated that the mutation results in the loss of a promoter/enhancer sequence for Qk. However, only QKI-6 and QKI-7 are greatly affected in Qk^V mutants with QKI-5 expression still present in OLs. The exact mechanism by which QKI-5 expression is unaffected by the Qk^V mutation is largely unknown, but most likely has a basis in misregulation of alternative splicing resulting in the sole production of QKI-5.

Expression of Qk is still regulated in a time and tissue-specific manner in Qk^V homozygotes (Ebersole et al., 1996), indicating that qk is still being expressed but is unable to reach the same levels as seen in wild-type mice. In the Qk^V mutant part of the enhancer/promoter region of qk is deleted (Ebersole et al., 1992) which results in a reduction in QKI-6 and QKI-7 protein expression in OLs and myelinating Schwann cells (Hardy et al., 1996). However, expression of QKI-6 is comparable in astrocytes to wild-

type levels. This down regulation does not affect QKI-5, the main isoform found within the nucleus. However, QKI-5 abundance did correlate with the severity of dysmyelination, with the OLs in the most severely affected CNS regions completely lacking QKI-5 protein (Hardy et al., 1996). Expression of only QKI-6 specifically in OLs *in vivo* was sufficient to rescue the hypomyelination phenotype arising from the Qk^V mutation (Zhao et al., 2006b). This implicated QKI-6 as the main isoform involved in myelinogenesis, and suggested a possible role for QKI-5 in embryogenesis but its overall function is less well characterized than QKI-6. While QKI expression is vastly reduced in OLs, astrocytes in the Qk^V mutant still exhibit wildtype levels of QKI protein expression (Hardy et al., 1996). The OL-specific down regulation of QKI-6 in the quaking mutant is likely the cause of the dysmyelination phenotype. However, QKI-5 may still play a role both in oligodendrogenesis as well as myelinogenesis.

Various myelin gene transcripts are also drastically reduced in Qk^V mutants, including MBP mRNA, MAG mRNA, and *Plp* mRNA (Roth et al., 1985; Sorg et al., 1986; Sorg et al., 1987; Li et al., 2000). This reduction has been attributed to destabilization and metabolism of the target transcript, as transcription of MBP and *Plp* mRNA was not affected (Li et al., 2000). The OLs in the Qk^V mutation are defective in their export of MBP mRNA from the nucleus, with the majority of the MBP mRNA being localized to the nuclei and perinuclear region. However, the cause of nuclear accumulation of MBP mRNA in Qk^V mutants has been attributed to maturation defects rather than an imbalance in QKI-5 to QKI-6 ratio (Larocque et al., 2002). Expression of MBP in the corpus callosum is down regulated *in vivo* following overexpression of QKI-5 protein (Larocque et al., 2002). This suggests that the loss of MBP expression in the Qk^V mutation is not a result of nuclear retention of MBP mRNA but rather is likely dependent on other post-transcriptional defects, which may result indirectly from an inability of OLs in Qk^V mutants from maturing in a timely manner.

31

2.3.2 QKI and *Cell Signaling*

There is also evidence to suggest QKI has a role in tumorigenesis and in human glioma (Ichimura et al., 2006; Mulholland et al., 2006; Yin et al., 2009) and colon cancer (Yang et al., 2010). RNA-binding activity of QKI is regulated by Src-PTK-dependent tyrosine phosphorylation (Kirla et al., 2003). Several proline-rich SH3-binding motifs exist in all vertebrate QKI isoforms, leading to the hypothesis that QKI is a target of Src-PTKs (Vernet and Artzt 1997) and that RNA-binding activity may be governed by Src-PTK-dependent phosphorylation similar to SAM68 (Paronetto et al., 2007). A cluster of 5 tyrosine residues is located immediately downstream of the SH3-binding motifs in QKI. The C-terminal tyrosine cluster, but not tyrosines in the KH domain or at the N-terminus mediate phosphorylation of QKI by Src-PTKs *in vitro*, in transfected cells and in isolated myelin during brain development (Zhang et al., 2003b). The predicated SH3-binding motifs are important for Src-dependent QKI phosphorylation (Zhang et al., 2003b), but does not form a stable complex with Src-PTKs, suggesting a transient interaction. QKI phosphorylation negatively affects binding to MBP mRNA (Zhang et al., 2003b; Zhao et al., 2006b). QKI deficiency causes destabilization of many mRNAs that encode key factors for OL differentiation and myelin synthesis (Li et al., 2000). Presumably, Src-PTK-dependent phosphorylation of QKI-5 may release nuclear retention of mRNA ligands, while phosphorylation of cytoplasmic QKIs may influence translation levels. Fyn is the only Src-PTK member whose activity and expression are increased upon OL differentiation (Osterhout et al., 1999). This is accompanied by a general down regulation of the rest of the Src-PTKs (Lu et al., 2005). Fyn is essential for early OL differentiation as shown by pharmacological inhibition and siRNA-mediated knockdown of Fyn attenuate OL differentiation (Osterhout et al., 1999; Colognato et al., 2004). Initiation of active myelin formation results in decline in Fyn activity (Umemori et al., 1994). Lack of the Fyn-QKI mediated acceleration mechanism leads to slow

accumulation of the MBP mRNA, delayed myelin development and hypomyelination in both the Fyn knockout mice and the Qk^V mutant (Li et al., 2000; Lu et al., 2005).

The QKI locus is frequently deleted in a subpopulation of human glioma (Mulholland et al., 2006; Yin et al., 2009). Even when it is not deleted, QKI mRNA is severely diminished (Li et al., 2002b) which suggests that post-transcriptional dysregulation of QKI may occur. It is possible it acts through p27^{KIP1} dysregulation in glioma (Kirla et al., 2003; Zagzag et al., 2003). Reduced QKI expression has also reported in human colon cancer, partly due to hypermethylation of the QKI promoter (Yang et al., 2010). The same study also found that forced expression of QKI blocks cell cycle progression and reduces proliferation and tumorigenesis ability of colon epithelia (Yang et al., 2010). Loss-of-function of QKI has recently been linked with white matter impairment and myelin deficits in a number of cognitive disorders, including schizophrenics, major depression patients and suicide populations (Aberg et al., 2006b; Klempan et al., 2009). No deletion of QKI promoter or coding region is found in the above diseases. Instead, a single nucleotide polymorphism (SNP) in the intron upstream of an alternatively spliced exon for QKI-5 was reported to segregate with probands in a large schizophrenia family (Aberg et al., 2006a). This could possibly be due to epigenetic mechanisms affecting transcription. SNPs in the Fyn gene and aberrant Fyn signaling are also found to be associated with schizophrenia (Rybakowski et al., 2007; Hattori et al., 2009).

2.3.3   *Roles of Quaking in Mammalian Embryonic Development*

The role of QKI in myelination has been the main focus of study, mainly due to the circumstances surrounding the discovery of the gene in Qk^V mutant mice. However, a series of ENU-induced point mutations have also been found to cause embryonic death at midgestation due to cardiovascular failure (Cox et al., 1999; Li et al., 2003). The

majority of these point mutations were embryonically lethal, with the time of arrest for each allele ranging between E8.5 to E13.5, suggesting a broader role for QKI in development beyond myelination. The *qk*^{l-1} allele results in an A to G nucleotide conversion, which results in the generation of a new splice site upstream of the QKI-5 nuclear localization signal, resulting in the elimination of the QKI-5 isoform and embryonic lethality (Cox et al., 1999). The *qk*^{k2} allele features a T to A conversion in the KH domain of all three isoforms resulting in an amino acid change from a valine to a glutamic acid which negatively affects RNA-binding (Cox et al., 1999). Homozygous *qk*^{k2}/*qk*^{k2} embryos show defective blood vessel formation prior to the presentation of neural defects (Noveroske et al., 2002), suggesting an essential role for QKI during vascular development.

Vasculogenesis is the formation of mammalian blood vessels through differentiation of endothelial cells. It initiates shortly after gastrulation in the yolk sac mesoderm which lies adjacent to the visceral endoderm (Tam et al., 2001). The visceral endoderm sends cues to mesodermal progenitors to direct their differentiation into primitive endothelial and hematopoietic cells (Flamme et al., 1997). Later stages of vasculogenesis result in the formation of vascular channels and a capillary plexus, which is then remodeled via angiogenesis, into a circulatory network composed of specialized endothelial cell types (i.e., arterial, venous) (Hopper and Hart 1985; Lucitti et al., 2007). By E9.5, wildtype mice yolk sacs have a well-developed vascular system composed of epithelial cell tubes surrounded by mural cells. QKI-5 is not expressed in endothelial or smooth muscle cells that form the vasculature, but rather is expressed in the endoderm adjacent to vascular cells in the yolk sac at E8.5 and E9.5, thus a cell autonomous role in endothelial and/or mural cell development for QKI-5 is not likely. In *qk*^{k2} mutant mice, which contain a T to A transition in the KH domain and are embryonically lethal by E11.5 at the latest (Cox et al., 1999), cardiac function and heart

34

tissue differentiation occurs normally, with the primary defect being vascular development (Noveroske et al., 2002). Closer examination of qk^{k2} mutants as well as qk^{l-1} mutants, which does not express QKI-5 due to loss of the QKI-5 splice site (Cox et al., 1999), using whole-mount immunostaining revealed a lack of mature vascular definition in both the head and in between the somites. Vessel structures were disorganized and lacking definition, with large vitelline vessels not forming, as well as failure of the capillaries to remodel (Bohnsack et al., 2006). Defects in the vascular network were eventually traced back to a defect in local retinoic acid production due to a decrease in expression of *Raldh2*, an enzyme necessary for retinoic acid (RA) production (Mic et al., 2002). Closer examination of E8.5 qk^{k2} mutants showed a 2-fold increase in mitotic cells in the yolk sac compared to wild-type littermates, with the majority of the proliferating cells being identified as endothelial cells (Bohnsack et al., 2006). The addition of biologically active retinoic acid to the food of pregnant qk^{k2}/qk^{k2} mutants restored the number of mitotic cells to wildtype levels and promoted proper endothelial cell maturation without having an effect on mesenchymal differentiation. However, retinoic acid was not able to rescue vascular patterning nor was it able to affect the survivability of qk^{k2}/qk^{k2} mutants despite the integrity of the visceral endoderm being restored. The ability of QKI, an intracellular protein, to potentially regulate RA synthesis may also have effects on developmental processes of the surrounding mesodermal cells through the activation of retinoic acid receptors. Defects in QKI protein may thus result in a secondary deficiency in RA leading to improper endothelial cell growth and maturation. This suggests that QKI has direct targets within the visceral endoderm which are independent of retinoic acid-mediated signaling in the mesoderm, that are necessary and required for vascular patterning and embryonic development.

Another aspect of embryonic development that QKI is potentially involved in is angiogenesis. The discovery that QKI-6 and QKI-7 is expressed in both the endothelial

cells as well as the vascular smooth muscle cells (Van Mil et al., 2012) suggests that QKI has a role to play in both vascular patterning and angiogenesis. A deficiency in QKI resulted in a decrease in both vascular endothelial growth factor A (VEGFA) and basic fibroblast growth factor (Bohnsack et al., 2006). QKI down regulation also resulted in a decrease in endothelial cell sprout length as well as a reduction in the release of angiogenic growth factors including the above mentioned VEGFA, basic fibroblast growth factor, and platelet-derived growth factor (Van Mil et al., 2012). As well, miR-214 has been shown to directly target QKI and is able to efficiently repress the translation and affect the mRNA stability of all three QKI isoforms (Van Mil et al., 2012). Co-transfection of endothelial cells with both QKI siRNA and anti-miR-214 was not able to rescue the reduction in sprouting length, suggesting that the ability of miR-214 to target QKI is largely responsible (Van Mil et al., 2012). However, Van Mil et al., (2012) were not able to demonstrate direct binding of QKI to VEGFA mRNA, which does not rule out the possibility of QKI binding to various other molecules such as transcription factors or protein kinases.

It has been observed that in schizophrenia patients, there is a decrease in OL density in the white matter of the cortex as well as in the hippocampus (Haroutunian et al., 2006). Many of the defects observed in Qk^V mutant mice such as a lack of compaction of the myelin sheath and a reduction in the number of myelin lamellae have also been observed in patients with schizophrenia (Stewart and Davis 2004). As well, several myelin-associated genes were down regulated in the white matter of schizophrenia patients, including MBP, *Plp* and QKI (Aberg et al., 2006a; Aberg et al., 2006b)

It was observed that myelin and OL defects may contribute to the development of schizophrenia (Stewart and Davis 2004). A decreased OL density in the white matter of schizophrenia patients and other alterations in schizophrenia brains resemble those observed in the Qk^V mice (Haroutunian et al., 2006). A schizophrenia susceptibility locus

was mapped to chromosome 6q25-6q26, the location of the QKI gene (Aberg et al., 2006a; Aberg et al., 2006b; Haroutunian et al., 2006). The QKI isoforms link ataxia with the Qk^V and Qk^{e5} mice and show Purkinje cell axonal swelling, indicative of neuronal degeneration (Noveroske et al., 2005).

In conclusion, the recent discovery of a QKI-6-*Plp* pathway, the link between *Plp* and *Sirt2*, as well as the role of *Sirt2* in OL differentiation, provides a novel pathway through which QKI-6 is able to influence OL differentiation. This in addition to the ability of QKI to influence cell cycle factors provides many interesting possibilities regarding the role of QKI and glial cell development. As well, the limited research that has been completed on QKI-5, the potential difference in function and temporal expression profiles between QKI-5 and QKI-6, lead to the potential for QKI-5 to play a prominent role in early glial cell development as well as overall embryonic development.

III MATERIALS & METHODS

3.1 CLONING OF FULL LENGTH QKI-5 MRNA AND PLASMID CONSTRUCTION

CG4 cells were grown to confluency as mentioned below. Cells were harvested once they reached confluency and RNA was isolated from the harvested CG4 cells using TRIZOL reagent according to manufacturer's instructions. cDNA was generated by Reverse Transcriptase II (Invitrogen, Burlington, Ontario) according to manufacturer's instructions. Full length QKI-5 sequence was cloned *in vitro* from cDNA generated from total RNA isolates of CG4 cells. The QKI-5 sequence was analyzed using the Primer-BLAST software available through NCBI. Identified PCR primer pairs were used to directly clone the full length QKI-5 mRNA sequence.

The primers used are:

QK1 Forward	(5′-GGATCCATGGTCGGGGAAATGGAAACG-3′)
QK3 Reverse	(5′-GAATTCTCATAGGTTAGTTGCCGGTGG-3′)

Pfx polymerase was used in all PCR reactions as it has higher fidelity than Taq polymerase and there would be fewer errors introduced into the amplified sequence. PCR reaction mixtures were prepared according to manufacturer's instructions with 100 ng of DNA template and 0.1 μm of each primer set. PCR cycling parameters: "hot start" at 95°C for 5 min, followed by 25 cycles of denaturation at 94°C for 40 sec, annealing at 54°C for 30 sec, extension at 68°C for 90 sec, and a final extension at 72°C for 10 min. In order to generate poly A+ ends, all PCR amplified products were incubated with 1 U Taq and 150 μm dATP for 2 h at 72°C. Purified PCR products were ligated with 50 ng pGEM T-easy vector and 1 U T4 DNA ligase in 5X reaction buffer [250 mM Tris-HCl (pH 7.6), 50 mM $MgCl_2$, 5 mM ATP, 5 mM DTT, 25% (w/v) polyethylene glycol-8000] at 15°C overnight. Ligase was heat inactivated by incubating the sample for 10 min at

70°C. DH5α *E.coli* cells (Invitrogen) were transformed according to manufacturer's instructions with the ligation products to generate large amounts of plasmid and to facilitate long-term storage. Recombinant DNA was purified using PureLink™ Gel Extraction Kit (Invitrogen) according to manufacturer's instructions. Recovered plasmid was verified to be the correct size by restriction digest with EcoRI in 10X REact® 3 Buffer (Invitrogen) at 37°C for 1.5 h and enzyme inactivation by addition of 10X DNA loading buffer [Bromophenol Blue, EDTA, glycerol]. Accuracy of cDNA sequence was confirmed by DNA sequencing using ABI 3730XL capillary electrophoresis DNA analyzer (PBI, Saskatoon, Saskatchewan). Plasmids that contained the gene of interest were then digested with EcoRI and BamHI in 1X REact® 3 Buffer (Invitrogen) at 37°C for 1.5 h to generate sequences with directional specificity for ligation into the expression vector pLEGFP-C1 (Clontech, Mountainview, California). Digestion with XhoI and SalI in 1X REact® 2 Buffer (Invitrogen) at 37°C for 1.5 h for ligation into pIRES2-EGFP expression vector (BD Biosciences, Mississauga, Ontario). All ligation reactions were performed according to manufacturer's instructions and similar to above.

3.2 CG4 CELL CULTURE AND TRANSFECTION

CG4 cells were previously obtained from Dr. Doucettes's laboratory, with a stable line established and maintained in our own lab. In all experiments, wild-type CG4 cells were cultured and maintained according to protocols previously described (Wang et al., 2011). For detection of the expression level of both protein and mRNA, wild-type CG4 cells (2×10^5 cells) were seeded onto three 15 mm² coverslips on Poly-D-Lysine (Sigma, Oakville, Ontario) coated 60mm dishes. Each dish was cultured overnight in growth media (GM) composed of DMEM (Sigma), 50 µg/mL transferrin (Sigma), 5 µg/mL insulin (Sigma), 10 pg/mL biotin (Sigma), 50 ng/mL selenium (Sigma) and 30% B104 conditioned medium. The B104 conditioned medium is crucial for

39

maintenance of the CG4 cells in an early, proliferative developmental state. Details regarding the production and composition of B104 conditioned medium were taken from Wang et al., (2011). Briefly, for the production of B104 conditioned medium, B104 neuroblastoma cells were plated in DMEM:F12 (1:1) with 10% FBS until they reached 90% confluency. Once the cells reached confluency, the medium was switched to defined medium composed of DMEM (Dulbecco's modified eagle medium) and 1% TPPS (1 mg of holo-transferrin bovine; 1.0 mM of putrescine; 2 mM of progesterone and 30 µM of sodium selenite). After incubation for 3 days, the serum-free defined medium was collected and stored at -80 °C.

CG4 cells were transfected the following morning with the appropriate vector (5.5 µg plasmid DNA per dish) or siRNA (220 pmol siRNA per dish). Cell culture media was changed after 6-8h following transfection to differentiation media (DM), composed of DMEM, 0.4% FBS (Sigma), 50 µg/mL of transferrin, 2.5 µg/mL of insulin, 10 pg/mL of biotin and 50 ng/mL of selenium. Cell culture media was replaced with fresh media every 24h. Transfected cells were cultured for up to 6 days in DM, with one dish being collected for samples on each day. Cells which were to be cultured for 4d, 5d, or 6d were transfected again on day 3 (Figure 4). All transfections were performed with Lipofectamine™ 2000 (Invitrogen) according to manufacturer's instructions. Plasmids used for transfection were purified using the EndoFree Plasmid Maxi Kit (Qiagen, Mississauga, Ontario).

QKI siRNA sequences		
	Sense	Anti-Sense
siRNA 1	5'-CCAAAGAUUCUGAGGUUUAUU-3'	5'-UAAACCUCAGAAUCUUUGGUU-3'
siRNA 2	5'-CCACCGGCAACUAACCUAUGACCUU-3'	5'-AAGGUCAUAGGUUAGUUGCCGGUGG-3'
siRNA 3	5'-AGUUCGAAGGCACGAUAUG-3'	5'-CAUAUCGUGCCUUCGAACU-3'

3.3   RNA Isolation and RT-PCR

In order to validate the efficacy and specificity of each plasmid and siRNA treatment, CG4 cells were seeded overnight in 6 separate 60mm dishes. Each dish was transfected with 5.5 µg of plasmid DNA in GM; the GM was changed 6-8h after transfection to DM (Figure 4).

Total RNA was obtained from cells using the RNeasy Mini Kit (Qiagen) and 1 µg of RNA for each sample was reverse transcribed into cDNAs using the Quantitect Reverse Transcription Kit (Qiagen). The synthesized cDNAs were then used as templates in PCR amplification using sequence specific primers for the genes of interest. PCR was carried out similar to protocols previously described by Brady et al. (2012) but PCR was only run for 25 cycles. PCR products were visualized on ethidium bromide stained 1% agarose gel. Integrated density values (the sum of the values of the pixels) were determined for each band with AlphaView® imaging software and normalized to β–actin levels, then again to the mean 1 day wildtype levels. All values are reported as mean ± SEM.

RT-PCR primer pairs		
	Forward	Reverse
QKI-5	5'-CCTTGCCTTTTCTCTTGCAG-3'	5'-CAGGCATGGTCAGGTCATCA-3'
QKI-6	5'-CCTTGCCTTTTCTCTTGCAG-3'	5'-GCCTTTCGTTGGGAAAGCCATA-3'
QKI-7	5'-CCTTGCCTTTTCTCTTGCAG-3'	5'-TAAAACAGTGGGGTTGCACA-3'
Plp	5'-TGCTCTGCTGTGCCTGTGTAC-3'	5'-TCTATGGGAGATCAGAACTTG-3'
Sirt2	5′-AGCAAGGCACCACTAGCCACC-3′	5′-TGTTCCTCTTTCTCTTTGGTC-3′
β-Actin	5'-ATTGTAACCAACTGGGACG-3'	5'-TTGCCGATAGTGATGACCT-3'

3.4 WESTERN BLOT ANALYSES

For detection of the expression level of QKI protein as well as PLP and SIRT2 protein, cells were cultured as above, harvested and lysed with RIPA buffer (150 mM NaCl, 0.5% SDS, 1% Trition-100, 0.1% deoxycholate, 10 mM Tris-HCl [pH 7.2], 5 mM EDTA). Protein quantification, electrophoresis, and subsequent protein detection was performed as described previously (Ji et al. 2011). Briefly, protein samples were separated on 12% SDS-PAGE. Proteins were then transferred to a PVDF membrane, blocked overnight with 3% skim milk solution, incubated for 1 h with primary antibody, washed with PBS, incubated with secondary antibody for 1 h and then visualized with Immobilon™ Western HRP Substrate (Millipore, Billerica, Massachusetts). The following primary antibodies were used: anti-QKI (1:1000, Proteintech Group, Chicago, Illinois), β-Actin (1:1000, Santa Cruz, Dallas, Texas), *Plp* (1:500, Santa Cruz), and *Sirt2* (1:1000, Acris antibodies GmbH, San Diego, California). Secondary antibodies utilized include Pierce® goat anti-mouse Poly-HRP (1:3000, Thermo Scientific, Lafayette, Colorado), goat anti-rabbit IgG-HRP conjugate (1:3000, BioRad, Mississauga, Ontario), and rabbit anti-goat IgG-HRP conjugate (1:3000, BioRad).

3.5 IMMUNOCYTOCHEMISTRY

Immunocytochemistry was carried as previously described (Wang et al., 2011). CG4 cells were sub-cultured from the same passage and seeded onto 15mm^2 coverslips at 2 x 10^5 cells per 60mm dish. Cells were cultured in the same dishes as those used to collect protein and RNA samples. Cells were fixed to coverslips using 4% paraformaldehyde solution and then incubated for 1h with the primary antibody. Coverslips were then incubated for 1h with the secondary antibody and finally stained with Hoescht® stain. All coverslips were washed with PBS in between each staining step. The following primary antibodies used were; A2B5 (1:100, ATCC, Manassas,

Virginia), anti-galactocerebroside (GalC) (1:100, hybridoma (Ranscht et al. 1982), anti-GFP (1:100, Novus Biologicals, Oakville, Ontario). The secondary antibodies utilized include Alexa Fluor® 488 goat anti-rabbit IgG (1:100, Molecular Probes, Eugene, Oregon), Alexa Fluor® 594 goat anti-mouse IgG (1:100, Molecular Probes) and Alexa Fluor® 488 goat anti-mouse IgG (1:100, Molecular Probes). In all immunocytochemical stainings, nuclei were visualized with Hoechst® stain (Sigma).

3.6   BLINDED CELL COUNTS

Upon completion of the immunofluorescent staining, each cell group was assigned an alphanumeric code and all cell counts were done blindly (Wang et al., 2011). For immunostaining experiments, 10–12 microscopic fields on each coverslip were selected for each cell group (A2B5[+], GalC[+], GFP[+] or Hoescht^{+} cells), with cell count data collected (>1500 cells) from three replicates. Total number of A2B5[+], GalC[+], and GFP^{+} cells was determined for each image. The total number of Hoechst[+] nuclei was also determined for each image. These cell counts were done using the software program Image Pro® Plus 6.2 (Olympus Canada Inc., Markham, Ontario).

3.7   STATISTICS

All assays were performed in triplicate and quantitative data were statistically compared using a two-way analysis of variance (ANOVA) (Prism® Software Corporation). For the RT-PCR data, the optical density ratio between each target band and the internal control band (β-actin) was obtained using the AlphaImager™ Gel Imaging Software. Multiple post hoc comparisons were performed with Bonferonni's multiple comparisons post-test (Prism software program). The significance level for

both the ANOVA and the post-test was set at $p < 0.05$. Mean data values are expressed as mean ± standard error mean (SEM).

IV   RESULTS

4.1   CLONING

The full length QKI-5 mRNA sequence was cloned into both the pLEGFP-C1 vector and pIRES2-EGFP vector. This was confirmed through a double restriction digest to confirm proper orientation of the insert as well as through DNA sequencing to confirm insert sequence was correct (Figure 3). The pLEGFP-C1 retroviral vector was originally the first choice vector for over expression of QKI-5 in CG4 cells due to the carboxy-terminal fusion of EGFP to QKI-5. pIRES2-EGFP allows for both QKI-5 and EGFP to be translated from a single bicistronic mRNA. This allows for specific selection of transiently transfected cells, but it can be difficult to determine whether EGFP is expressed in the same cellular location as the target gene due to processing of mRNA prior to translation. However, it can be advantageous to use a bicistronic vector since there is no fusion of GFP to the target protein. This minimizes any interaction between GFP and the target protein that might impact the proper function and localization of the target protein. Eventually, the pIRES2-QKI5 construct was chosen due to difficulties encountered with transfecting using the pLEGFP-C1 vector.

A

```
GGTGACTTATTATTGGGCGATTGGGCCCGACGTCGCATGCTCCCGGCCGCCATGGCGCCGCGGGAATTCGATTG
GATCCATGGTCGGGGAAATGGAAACGAAGGAGAAGCCGAAGCCCACCCCAGATTACTTGATGCAGCTGATGAACG
ACAAGAAGCTTATGAGCAGCGTATGACGGAAAGACATTAAATGCAAGGAGTGCAGAATTGCCTGACG
TAGCAGAGTACGGAAAGACACATTAAATGCAAGAGAAACTTTATGTGCCTGTAAAGAATACCCTGATTTAATTTGTTGGGA
CGGTGGGACCCATTGTTCAGTTACAAGAGAAACTTTATGTGCCTGTAAAGAATACCCTGATTTAATTTGTTGGGCAAA
GAATCCTTGGACCTAGAGGACTTACAGTAAACAACTTGAAGCAGAAACAGGATGTAAAATAATGGTCCGAGGCAAA
GGCTCCATGAGGGATAAAAAGAAGGAGGGCAAAATAGAGGCAAACCCAATTGGGAGCATCTAAATGAAGATTTACA
TGTACTAATCACTGTGGAAGATGCTCAAAACAGAGCAGAAATCAAGCTGAAGAGAGCGGTTGAAGAAGTGAAGAAG
TTACTGGTACCTGCAGCTGAAGGAGAAGACAGCCTGAAGAAGATGCAGCTGATGGAGCTTGCAATTCTGAATGGCA
CCTACAGAGACGCCAACAATTAAATCACCAGCCCTTGCCTTTTCTTGCGTACACCCACGCCCAGCTGGCCCTACCATAATGCC
CATCACTGGGCCCGGCCCTGTCTCCCACCAGCTGCTCTGCGTACACCCACGCCCAGCTGGCCCTACCATAGTCCCTCCAGGG
TTTGATGACAGATTCAGACCGCTGTCATGCCAAACGGAACTCCTCACCCTGCACCAGCTACGCACGTCAATCCTTGAGTACCC
CCTGAAGCTGGGTAATCTCACACACCCCTATGAGTCGCGGTGGCTACTAAAGTTCGAAGGCACGATATGCGTGTCCATCCTTACCAA
AGGATTGTGACCGCAGACCGAGCCGCCACCGCAACTAACTAGTGAATTCACTAGTGAATTCGCGGCCGCCTGCAGGT
CGACCCATATGGGAGAGCTCCCAACGCGTTGGGATGCCATAGCTTCTATAGTTCCACCCAAATTTGGATACCC
```

B

1043bp QKI-5

6892bp pLEGFP-C1
7935bp pLEGFP-C1+QKI-5

pLEGFP-C1+QKI5
dbl cut - EcoRI + BamHI

pLEGFP-C1+QKI5
uncut

pIRES2-EGFP+QKI5
dbl cut - XhoI + SalI

pIRES2-EGFP+QKI5
uncut

pIRES2-EGFP 5300bp
pIRES2-EGFP+QKI5 6343bp
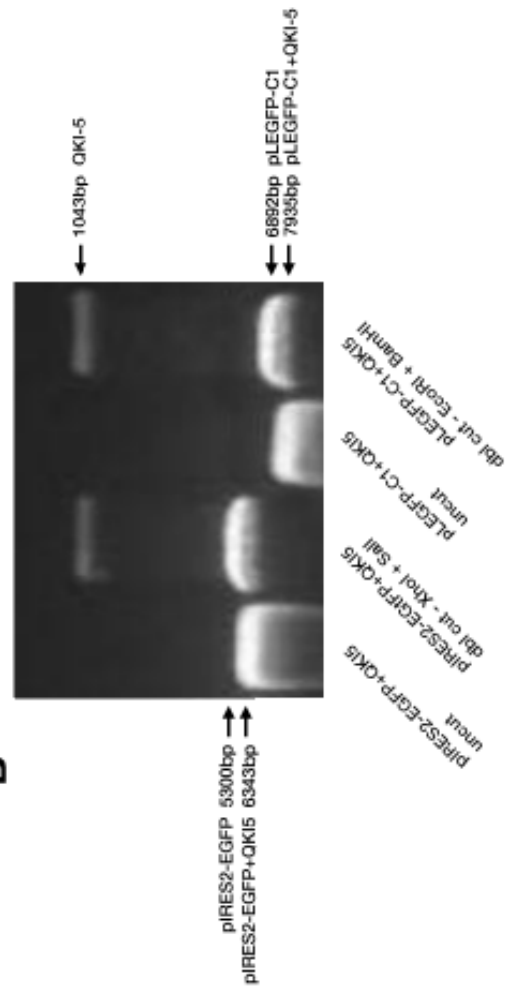
Figure 3. *Cloning QKI-5 mRNA sequence into two separate expression vectors*. **A)** Sequencing results from pIRES2-EGFP+QKI-5 construct. Primers used to sequence the construct were QK1 and QK3. The underlined indicates the coding sequence of QKI-5. **B)** 1% Agarose gel electrophoresis of pIRES22-EGFP+QKI-5 and pLEGFP-C1+QKI-5 plasmid constructs, visualized by ethidium bromide-staining. Plasmid constructs were run either uncut, double cut with XhoI + SalI for pIRES2-EGFP+QKI-5 or double cut with EcoRI + BamHI for pLEGFP-C1+QKI-5. A ~1kb band corresponding to the expected size of the QKI-5 coding sequence was isolated from both plasmid constructs.

4.2   TRANSFECTION EFFICIENCY

Initial culture of CG4 oligodendroglial cells were grown to confluency (~90-95%) in growth media. Upon reaching confluency, CG4 cells were passed into 6 separate 60mm dishes at a density of 2×10^5 cells per dish (Figure 4). Cells were cultured overnight in GM and then transfected with the appropriate plasmid or siRNA the following day. Media was removed and replaced with DM after 16 h. Each day three coverslips, total protein and total RNA was collected from a single dish. After the 3rd day, the remaining 3 dishes, representing the 4d, 5d, and 6d time points, were transfected for a second time (Figure 4). Each time point was grown in a separate dish.

Initial cell culture

Cells were passed into 6 separate dishes | 2 x 10^5 cells per 60mm dish

0d   0d   0d   0d   0d   0d

Growth media

all 6 dishes were transfected

1d   2d   3d   4d   5d   6d

Differentiation media

4-6d dishes were transfected again on the 3rd day

Total Protein   Total RNA   Immunocytochemistry
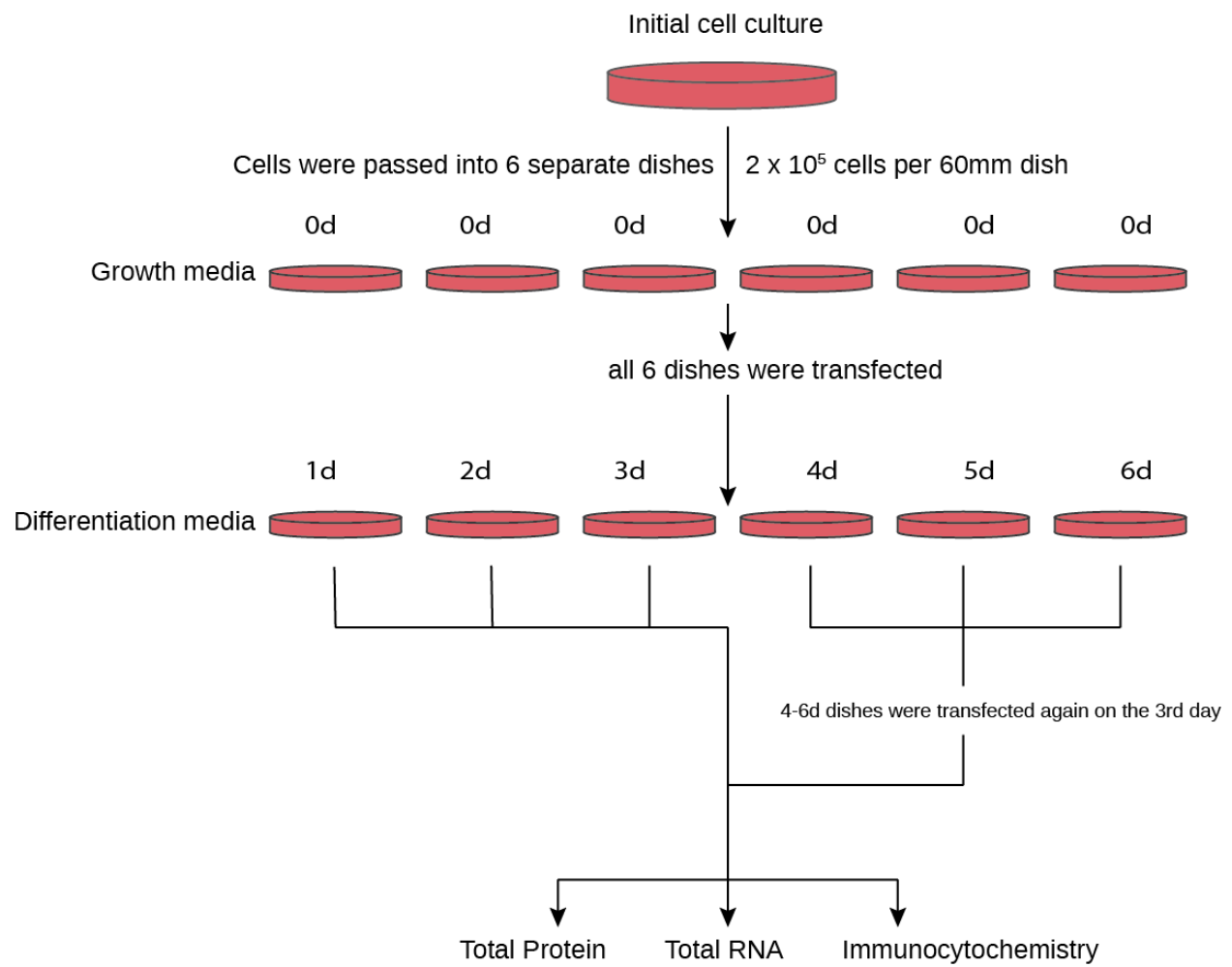
Figure 4. *Schematic diagram of the experimental design.* Initial culture of CG4 oligodendroglial cells were grown to confluency (~90-95%) in growth media. Upon reaching confluency, CG4 cells were passed into 6 separate 60mm dishes at a density of 2×10^5 cells per dish. Cells were cultured overnight in growth media and then transfected the following day. Media was removed and replaced with differentiation media after 16 h. Each day coverslips, total protein and total RNA was collected from a single dish. After the 3rd day, the remaining 3 dishes, representing the 4d, 5d, and 6d time points, were transfected for a second time. Each treatment was done in triplicate.

To determine the efficiency of transfection, GFP⁺ cells from blank pIRES2 plasmid transfected and pIRES2-QKI5 plasmid transfected were imaged and counted using fluorescence microscopy (Figure 5). Transfection efficiency was determined the day after transfection using the formula, (# GFP⁺/ # Hoechst⁺)(100). Transfection efficiency was determined as 37.74 ± 4.86 % in blank pIRES2 plasmid transfected cultures, 1d after transfection (Figure 5). In 1d pIRES2-QKI5 transfected cultures, the transfection efficiency was determined as 38.51 ± 3.61 %. The transfection efficiency was maintained following the second round of transfection after 3d; 38.11 ± 5.98 % in the 4d blank pIRES2 plasmid transfected cultures and 37.89 ± 4.47 % in 4d pIRES2-QKI5 plasmid transfected cultures (Figure 5). While the transfection efficiency was not optimal, our attempts to increase the transfection efficiency resulted in an increase in cell death (data not shown) which made it difficult to properly evaluate total RNA and protein as well as have sufficient cell numbers for immunocytochemistry.

blank pIRES2 vector

pIRES2-QKI5

GFP

GFP+Hoescht

GFP

GFP+Hoescht

1d

4d

100 μm
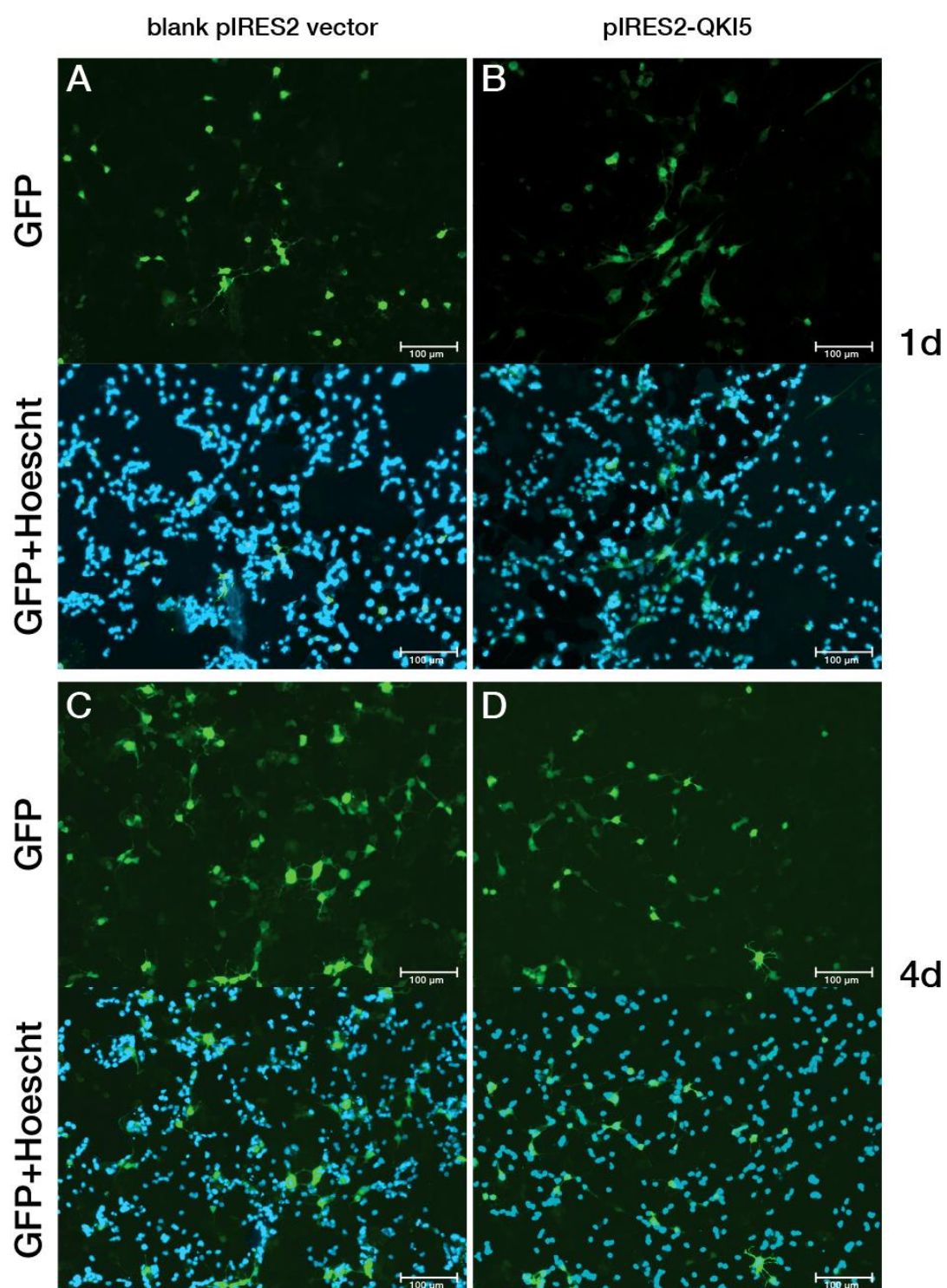
Figure 5. *Transfection efficiency of pIRES2 plasmid.* The transfection efficiency of **A)** 1d and **B)** 4d blank pIRES2 plasmid as well as **C)** 1d and **D)** 4d pIRES2-QKI5 plasmid was determined using immunocytochemistry. GFP staining is shown on the top, with GFP+Hoescht staining shown on the bottom. Transfection efficiency was determined by (# GFP$^+$/ # Hoechst$^+$)(100) (n=3). Scale bar = 100 μm.

4.3 QKI-5 AND QKI-6 MRNA LEVELS INCREASE OVER TIME

To assess the efficacy of the pIRES2-QKI5 recombinant vector, CG4 cells were transfected with 5.5 µg of DNA and cultured for up to 6d in DM. Following transfection, total RNA was collected after each day and RT-PCR was performed to determine mRNA levels of the three QKI isoforms. A 4-fold increase in QKI-5 mRNA levels was observed one day following transfection in pIRES2-QKI5 transfected cell cultures compared to 1d wildtype untreated CG4 cell cultures (Figure 6A). QKI-5 mRNA expression showed almost a 3-fold increase over 6 days in pIRES2-QKI5 transfected cells versus 6d wildtype untreated CG4 cell cultures (8-fold increase versus 3-fold increase, compared to day 1 wildtype) (Figure 6A). Culturing the CG4 cells for 6d in DM, did not significantly affect QKI-6 and -7 mRNA levels by either the transfection reagent (1.98 ± 0.06 and 1.19 ± 0.06, respectively, $p < 0.05$) or the addition of the pIRES2-QKI5 plasmid (2.15 ± 0.07 and 1.10 ± 0.11, respectively, $p < 0.05$) compared to the wildtype untreated CG4 cell cultures (1.91 ± 0.08 and 0.99 ± 0.06, respectively, $p < 0.05$) (Figure 6B & 6C). Transfection with pIRES2-QKI5 recombinant vector was able to significantly increase QKI-5 mRNA levels without affecting either QKI-6 or QKI-7 mRNA expression.

There was also a significant increase observed in QKI-5 and QKI-6 mRNA levels over the course of cell differentiation, when QKI-5 was not upregulated. By day 4 there was a 2.5-fold increase in wildtype QKI-5 mRNA levels compared to day 1 (1.01 ± 0.18 increasing to 2.73 ± 0.18, $p < 0.05$) which eventually rose to a 3-fold increase by day 6 (3.11 ± 0.22, $p < 0.05$) (Figure 6A). This trend was mirrored in both blank pIRES2 plasmid transfected and to a lesser extent in the pIRES-QKI5 plasmid transfected CG4 cell cultures. This increase during cell differentiation was also seen in QKI-6 mRNA levels, with an eventual 2-fold increase being observed by the 6 day time point (1.00 ± 0.08 increasing to 1.91 ± 0.08, $p < 0.05$) (Figure 6B). There was no significant change in QKI-7

mRNA expression over the course of differentiation (Figure 6C). Thus, during CG4 cellular differentiation, QKI-5 and QKI-6 mRNA levels increase, but not QKI-7 mRNA. Upon transfection with the pIRES2-QKI5 plasmid, QKI-5 mRNA levels were significantly increased without affecting either QKI-6 or QKI-7 mRNA levels.

QKI-5 mRNA expression

wildtype
negative control (blank pIRES2 plasmid)
pIRES2-QKI5

A

QKI-6 mRNA expression

C

QKI-7 mRNA expression

E

B

QKI-5

D

QKI-6

F

QKI-7

56
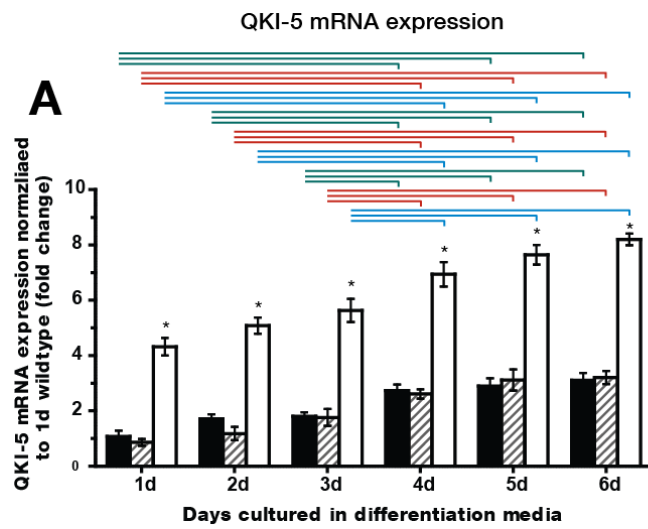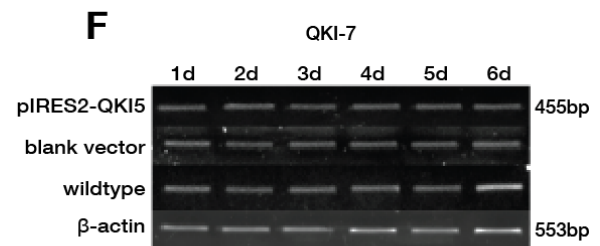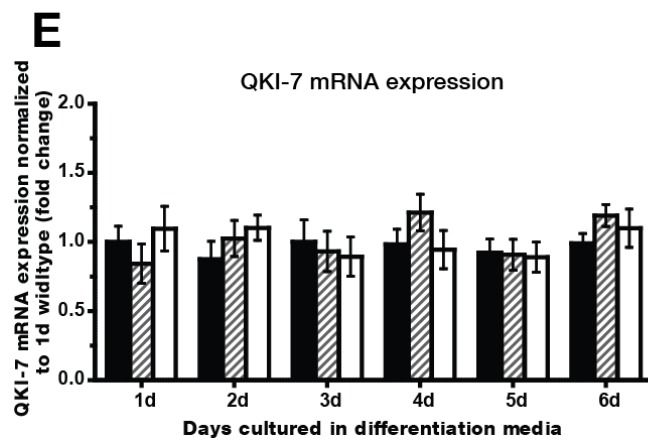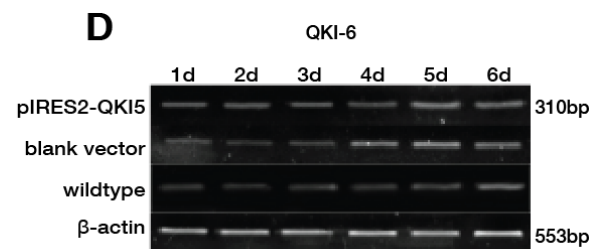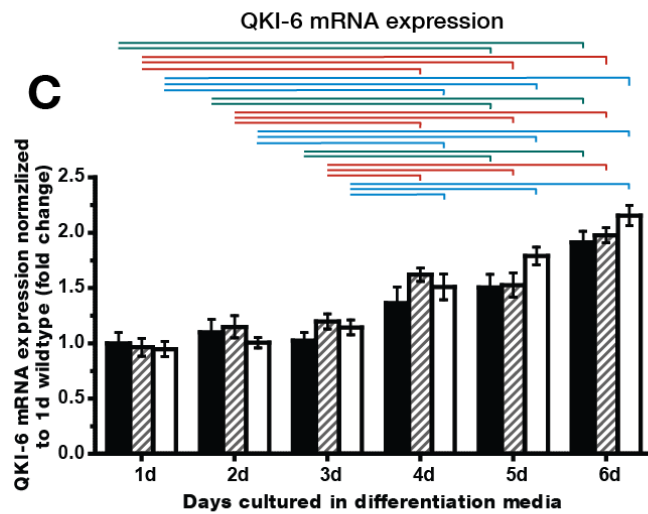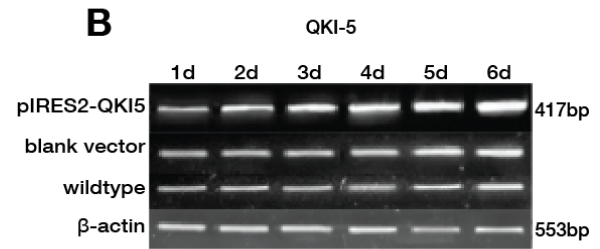
Figure 6. *QKI-5 mRNA is up regulated following transfection with pIRES2-QKI5.* CG4 cells were cultured for 6d in differentiation media, total RNA was collected and then RT-PCR for QKI-5, QKI-6, and QKI-7 was performed. **A)** QKI-5 mRNA levels were significantly higher at each day in pIRES2-QKI5 transfected cultures versus wildtype or blank pIRES2 plasmid transfected cultures. **B)** QKI-6 mRNA levels showed no change following transfection with either plasmid but there was in time-dependent increase. **C)** QKI-7 mRNA levels were unchanged regardless of culture time or up regulation of QKI-5 mRNA. Densitometer measurements were performed using AlphaImager software in order to quantify mRNA levels. Measurements were first normalized to the β-actin measurement for that day, and then all days were normalized to 1d wildtype and plotted as histograms. Representative gel images are shown on the right. Error bars indicate mean ± SEM (n=3). Asterisks denote significance compared to wildtype and control blank plasmid mean values ($p < 0.05$). The colored brackets indicate time-dependent significance within the same treatment groups (*green* = wildtype, *red* = blank vector, *blue* = plasmid treated) (Bonferroni's post-test; $p < 0.05$).

Treatment with QKI-5 specific siRNA was sufficient to knockdown QKI-5 mRNA levels compared to wild-type and control siRNA treatment (Figure 7). A 0.7-fold change in QKI-5 mRNA levels was observed one day following siRNA transfection (0.31 ± 0.10 compared to 1.00 ± 0.09 in the wildtype, $p < 0.05$). By day 6, the difference had grown to a 2.2-fold change in QKI-5 mRNA expression (0.34 ± 0.06 compared to 2.54 ± 0.15, $p < 0.05$) (Figure 7A). Treatment with the QKI-5 specific siRNA abolished the time dependent increase seen in the control treated cells. Similar to the blank vector controls, treatment with control siRNA resulted in a time dependent increase in QKI-5 mRNA levels (2.70 ± 0.10 at 6d compared to 1.25 ± 0.10, $p<0.05$) (Figure 7A). However, in the siRNA treated cells this increase during differentiation was not present, with the 6d siRNA treated cells not significantly different from the 1d siRNA treated cells (0.34 ± 0.06 at 6d compared to 0.36 ± 0.10, $p<0.05$) (Figure 7A). The siRNA treatment was specific to QKI-5 as both QKI-6 and QKI-7 mRNA levels were not significantly different from control siRNA treated levels at any time point (Figure 7B & C). An increase during differentiation was still evident in QKI-6 mRNA expression, (1.89 ± 0.09 at 6d siRNA treated compared to 0.96 ± 0.07 at 1d siRNA treated, $p<0.05$) (Figure 7B), with a similar trend being seen in both wildtype and control siRNA treated cells. Treatment with QKI-5 specific siRNA was sufficient to down regulate QKI-5 mRNA levels at all time points without having an effect on QKI-6 or QKI-7 mRNA expression levels.

QKI-5 mRNA expression

A

B QKI-5

C QKI-6 mRNA expression

D QKI-6

E QKI-7 mRNA expression

F QKI-7
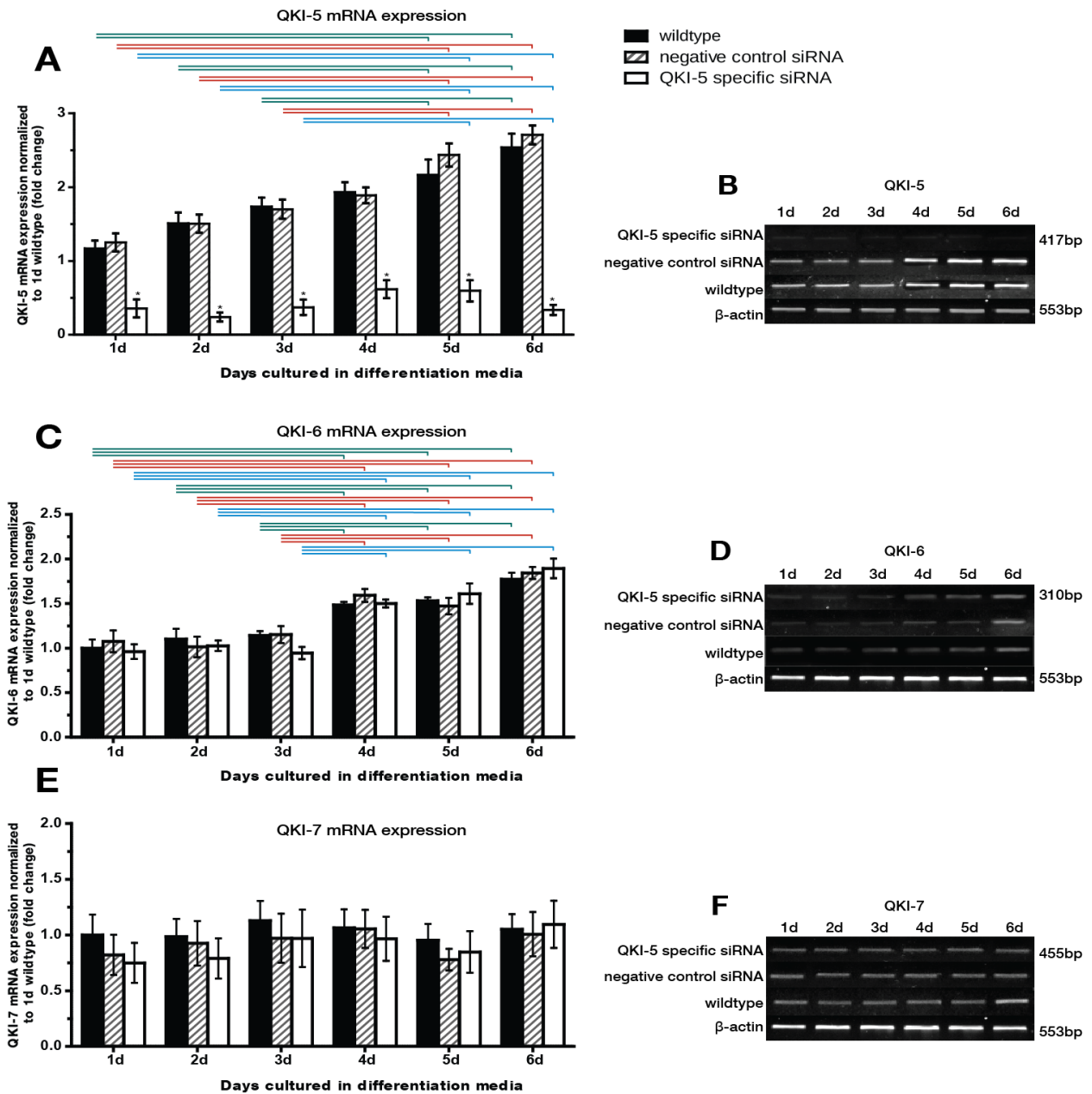
Figure 7. *QKI-5 specific siRNA is able to decrease QKI-5 mRNA levels but not QKI-6 or -7.* CG4 cells were cultured for 6d in differentiation media, total RNA was collected and then RT-PCR for QKI-5, QKI-6, and QKI-7 was performed. **A)** QKI-5 mRNA levels were significantly lower at each day in QKI-5 specific siRNA transfected cultures versus wildtype or control siRNA transfected cultures. **B)** QKI-6 mRNA levels showed no change following transfection with siRNA but there was a time-dependent increase. **C)** QKI-7 mRNA levels were unchanged regardless of culture time or transfection with either siRNA. Densitometer measurements were performed using AlphaImager software in order to quantify mRNA levels. Measurements were first normalized to the β-actin measurement for that day, and then all days were normalized to 1d wildtype and plotted as histograms. Representative gel images are shown on the right. Error bars indicate mean ± SEM (n=3). Asterisks denote significance compared to wildtype and control siRNA mean values ($p < 0.05$). The colored brackets indicate time-dependent significance within the same treatment groups (*green* = wildtype, *red* = negative control, *blue* = siRNA treated) (Bonferroni's post-test; $p < 0.05$).

4.4 QKI-5 UP REGULATION RESULTED IN UP REGULATION OF *PLP* AND *SIRT2* MRNA

Changes in *Plp* and *Sirt2* mRNA levels were also examined following up regulation of QKI-5. Interestingly, *Plp* mRNA levels followed a similar pattern as QKI-5, with a significant increase in *Plp* mRNA levels following pIRES2-QKI5 transfection (p <0.05) (Figure 8A). A 2-fold increase in *Plp* mRNA levels was observed one day following transfection (2.28 ± 0.12 at 1d pIRES2-QKI5 versus 1.00 ± 0.15 at 1d blank vector, p <0.05) and rose to a 5.5-fold increase by day 6 (5.50 ± 0.23 at 6d pIRES2-QKI5 versus 0.97 ± 0.17 at 6d blank vector, p <0.05). This increase during differentiation in *Plp* mRNA levels, while present in all three treatment groups, was only significant in the pIRES2-QKI5 transfected cell cultures (Figure 8). In both the wildtype and control blank vector transfected cultures, there was no significant change in *Plp* mRNA levels following exposure to DM for 6d (1.46 ± 0.15 at 6d blank vector compared to 0.81 ± 0.11 at 1d blank vector, p<0.05). While culturing in DM was not sufficient to increase *Plp* mRNA expression, transfection with pIRES2-QKI5 along with exposure to DM did significantly increase *Plp* mRNA levels.

Sirt2 mRNA levels in pIRES2-QKI-5 transfected CG4 cells were also elevated but only starting at 4d and onwards. At day 1 and day 2, there was no significant change in *Sirt2* mRNA levels following transfection with pIRES2-QKI5 vector but at day 3 a 2-fold increase was observed (2.23 ± 0.23 at 2d pIRES2-QKI5 compared to 1.38 ± 0.18 at 2d blank vector, p <0.05). By day 6 a five-fold increase in *Sirt2* mRNA was observed (5.45 ± 0.24 at 6d pIRES2-QKI5 compared to 1.16 ± 0.15 at 6d blank vector, p <0.05) (Figure 8B). There was an increase during differentiation in *Sirt2* mRNA levels but only in the pIRES2-QKI5 transfected cell cultures (Figure 8B). In both the wildtype and control blank vector transfected cultures, there was no significant change in mRNA levels following exposure to DM for 6d (1.19 ± 0.20 at 6d blank vector compared to 1.09 ± 0.23

at 1d blank vector, $p<0.05$). Similar to *Plp*, up regulation of QKI-5 is able to significantly increase *Sirt2* mRNA levels during differentiation.

A PLP mRNA expression

B PLP

C SIRT2 mRNA expression

D SIRT2

63
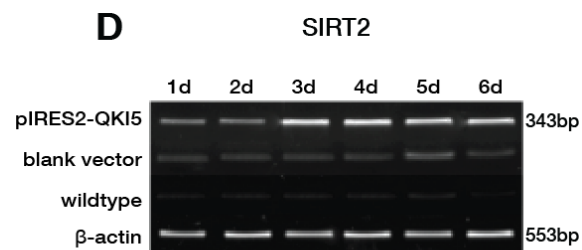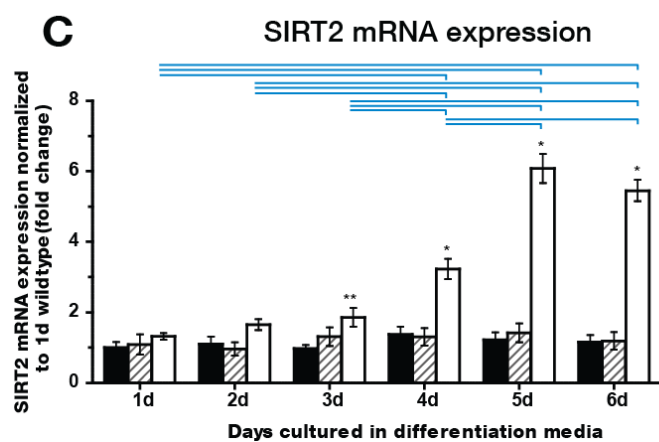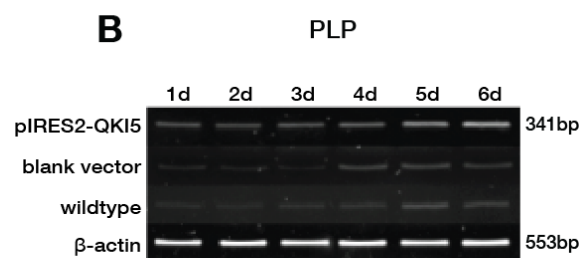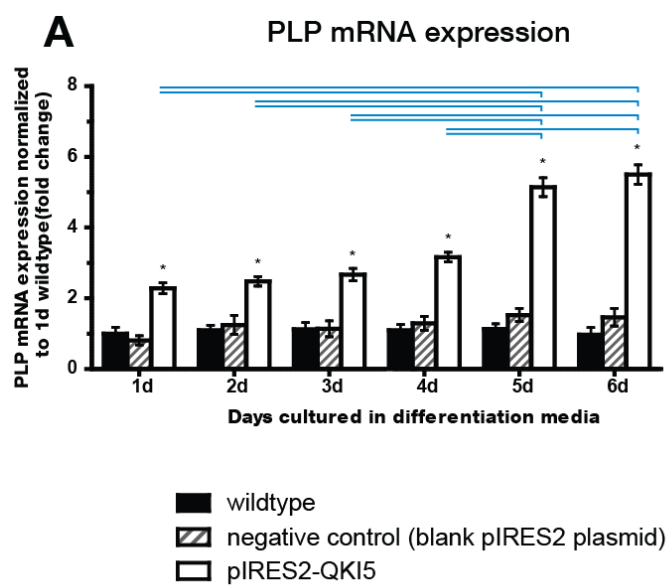
Figure 8. *Plp* and *Sirt2 mRNA is up regulated following transfection with pIRES2-QKI5.* CG4 cells were cultured for 6d in differentiation media, total RNA was collected and then RT-PCR for *Plp* and *Sirt2* was performed. **A)** *Plp* mRNA levels were significantly higher at each day in pIRES2-QKI5 transfected cultures versus wildtype or blank pIRES2 plasmid transfected cultures. **B)** *Sirt2* mRNA levels were significantly higher at each day in pIRES2-QKI5 transfected cultures versus wildtype or blank pIRES2 plasmid transfected cultures. Densitometer measurements were performed using AlphaImager software in order to quantify mRNA levels. Measurements were first normalized to the β-actin measurement for that day, and then all days were normalized to 1d wildtype and plotted as histograms. Representative gel images are shown on the right. Error bars indicate mean ± SEM (n=3). Asterisks denote significance compared to wildtype and control blank plasmid mean values ($p < 0.05$). Double asterisks indicate significance compared to only the wildtype mean ($p < 0.05$). The colored brackets indicate time-dependent significance within the same treatment groups (*blue* = plasmid treated) (Bonferroni's post-test; $p < 0.05$).

Treatment with QKI-5 specific siRNA, had no effect on either *Plp* or *Sirt2* mRNA levels at any time point ($p < 0.05$) (Figure 9). This is interesting to note as up regulation of QKI-5 was able to increase both *Plp* and *Sirt2* mRNA levels. However, when QKI-5 was down regulated, there was no effect on either *Plp* or *Sirt2* mRNA expression levels. This suggests either that QKI-5 is not necessary for transcription of *Plp* or *Sirt2* or that another protein is able to compensate for the loss of QKI-5. Since QKI-6 expression is not affected by down regulation of QKI-5, it is likely that QKI-6 is able to compensate for the lack of QKI-5 expression. There was also no effect on *Plp* or *Sirt2* mRNA levels during differentiation when CG4 cells were treated with either control siRNA or QKI-5 specific siRNA ($p < 0.05$) (Figure 9). Thus, the loss of QKI-5 does not appear to affect transcription of either *Plp* or *Sirt2*, but elevated QKI-5 levels can increase mRNA levels for both genes.

A

PLP mRNA expression

B

PLP

C

SIRT2 mRNA expression

D
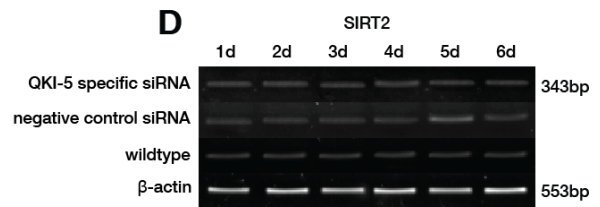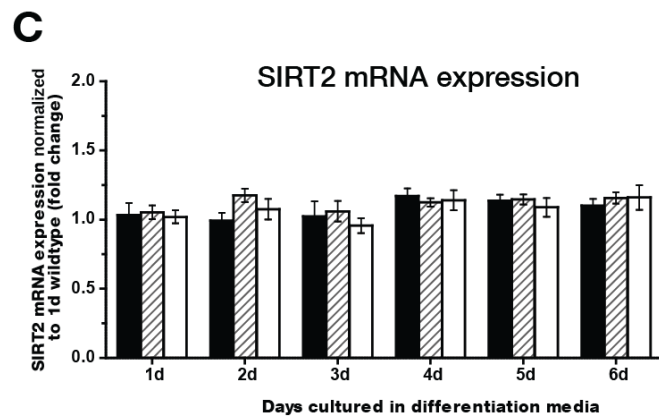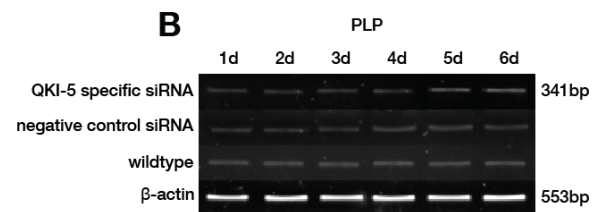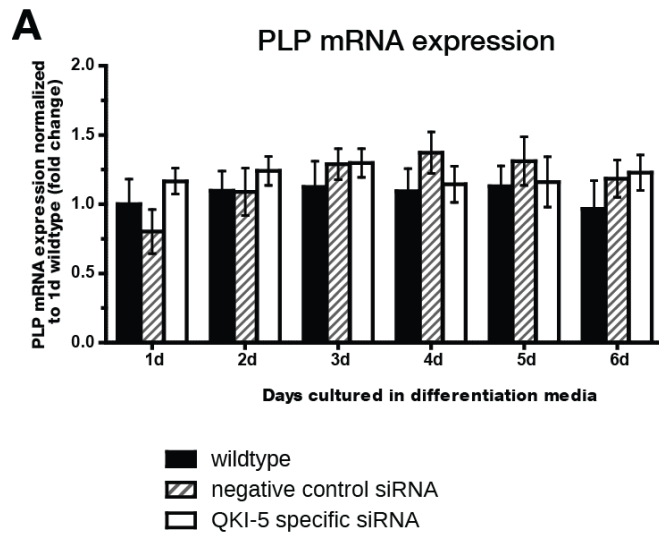
SIRT2

Figure 9. *QKI-5 specific siRNA has no effect on Plp or Sirt2 mRNA expression levels.* CG4 cells were cultured for 6d in differentiation media, total RNA was collected and then RT-PCR for *Plp* and *Sirt2* was performed. **A)** *Plp* mRNA levels were not significantly different between QKI-5 specific siRNA treated cell cultures versus wildtype or control siRNA transfected cultures. **B)** *Sirt2* mRNA levels were not significantly different between QKI-5 specific siRNA treated versus wildtype or control siRNA transfected cultures. There was also no increase in either *Plp* or *Sirt2* mRNA levels over time. Densitometer measurements were performed using AlphaImager software in order to quantify mRNA levels. Measurements were first normalized to the β-actin measurement for that day, and then all days were normalized to 1d wildtype and plotted as histograms. Representative gel images are shown on the right. Error bars indicate mean ± SEM (N=3).

4.5 QKI-5 PROTEIN LEVELS INCREASE FOLLOWING pIRES-QKI-5 TRANSFECTION

To determine if protein levels followed the mRNA expression levels, western blots were performed on protein lysates from each time point for each treatment. Similar to mRNA levels, following transfection with pIRES2-QKI5, QKI-5 protein levels were also elevated at each time point (day 1 to day 6) compared to wildtype levels. The greatest change observed was a 3-fold increase at day 6 (p <0.05)(Figure 10), although QKI-5 protein levels were elevated at all time points compared to wildtype and blank vector transfected cells. However, QKI-6 and QKI-7 levels showed no significant change in protein levels which is consistent with their mRNA expression levels. QKI-7 migrates at the same molecular weight as QKI-5, which is why only 2 bands are observed following Western blot. Curiously enough, the increase during differentiation in both QKI-5 and QKI-6 mRNA expression in wildtype CG4 cells (Figure 6) did not result in a corresponding increase in either QKI-5 or QKI-6 protein levels (Figure 10). However, treatment with the pIRES2-QKI5 plasmid resulted in a significant increase over the 6 day time period, following a similar pattern as QKI-5 mRNA levels (Figure 10). Transfection with pIRES2-QKI5 is able to cause a significant increase in QKI-5 protein levels over the course of differentiation. However, differentiation by itself is not sufficient to increase QKI-5, QKI-6, or QKI-7 protein levels.

A QKI-5 & QKI-7 protein expression

QKI-5 protein expression normalized to 1d wildtype (fold change)

Days cultured in differentiation media

■ wildtype
▨ negative control (blank pIRES2 plasmid)
□ pIRES2-QKI5

B

pIRES2-QKI5 → QKI-5 & 7 (45 kDa)
→ QKI-6 (38 kDa)
blank vector
wildtype
β-actin → 42 kDa

C QKI-6 protein expression

QKI-6 protein expression normalized to 1d wildtype (fold change)

Days cultured in differentiation media

Figure 10. *QKI-5 protein levels are elevated following pIRES2-QKI5 transfection*. CG4 cells were cultured for 6d in differentiation media. Protein lysates were collected following cell lysis. Protein samples were separated out on 12% polyacrylamide gels using SDS-PAGE. Following the transfer of proteins to a PVDF membrane, membranes were probed with a QKI antibody. **A)** QKI-5 & 7 protein levels were elevated following transfection with pIRES2-QKI5 at all time points compared to wildtype and control blank pIRES2 vector transfected cultures. **B)** QKI-6 protein levels were unaffected by transfection with blank pIRES2 vector or by time. A representative blot showing QKI-5 and QKI-6 protein levels following transfection with either blank pIRES2 plasmid or pIRES2-QKI5 plasmid is shown on the right. Protein levels were quantified using AlphaImager software and normalized to β–actin levels. This value was again normalized to the 1d wildtype value and plotted as histograms. Note the different y-axis in **A)** and **B)**. Error bars indicate mean ± SEM (n=3). Asterisks denote significance compared to either wildtype or control blank plasmid transfected cells ($p < 0.05$). The colored brackets indicate time-dependent significance within the same treatment groups (*blue* = plasmid treated) (Bonferroni's post-test; $p < 0.05$).

QKI-5 protein was specifically down regulated throughout the duration of the experiment (day 1 to 6) following QKI-5 siRNA treatment, with a consistent 0.5 to 0.75-fold change in protein levels (0.56 ± 0.06 at day 6 siRNA treated samples compared to 1.28 ± 0.03 in the day 6 wildtype samples, $p < 0.05$) (Figure 11). While the QKI-5 specific siRNA was able to successfully down regulate QKI-5 mRNA and protein levels, there was no significant effect on either QKI-6 or QKI-7 protein levels (Figure 11A & 11B). In contrast to treatment with pIRES2-QKI-5 which resulted in a gradual increase in QKI-5 protein levels during differentiation, treatment with the QKI-5 specific siRNA maintained QKI-5 protein levels below both corresponding wildtype and control siRNA levels. There was no increase in either QKI-5 or QKI-6 and QKI-7 protein levels, regardless of treatment (Figure 11). Thus, the QKI-5 specific siRNA was sufficient and specifically able to knock down QKI-5 protein levels without affecting QKI-6 or QKI-7 protein levels. The culturing of CG4 cells in DM is not able to significantly increase the protein levels of any of the three QKI isoforms.

A QKI-5 & QKI-7 protein expression

B

	1d	2d	3d	4d	5d	6d

QKI-5 specific siRNA ← QKI-5 & 7 (45 kDa) ← QKI-6 (38 kDa)

negative control siRNA

wildtype

β-actin 42 kDa

C QKI-6 protein expression
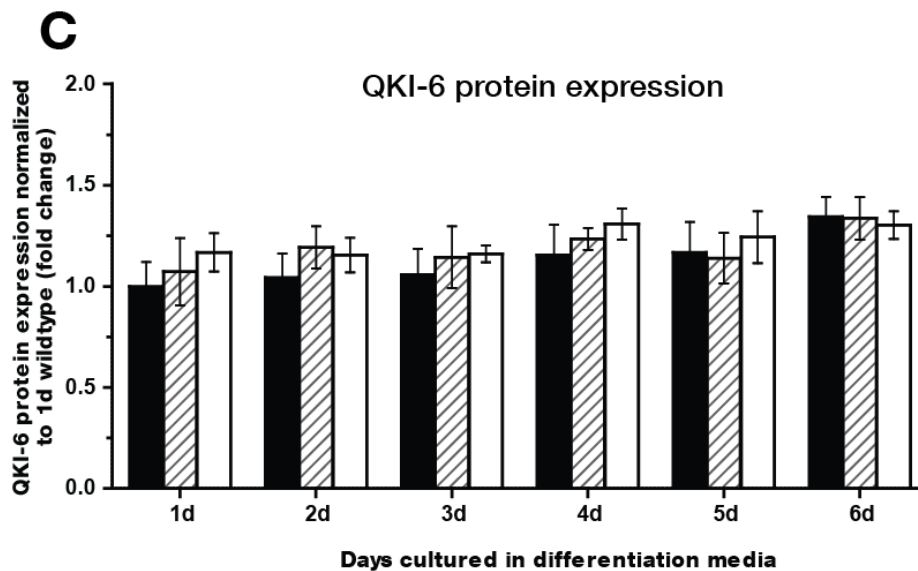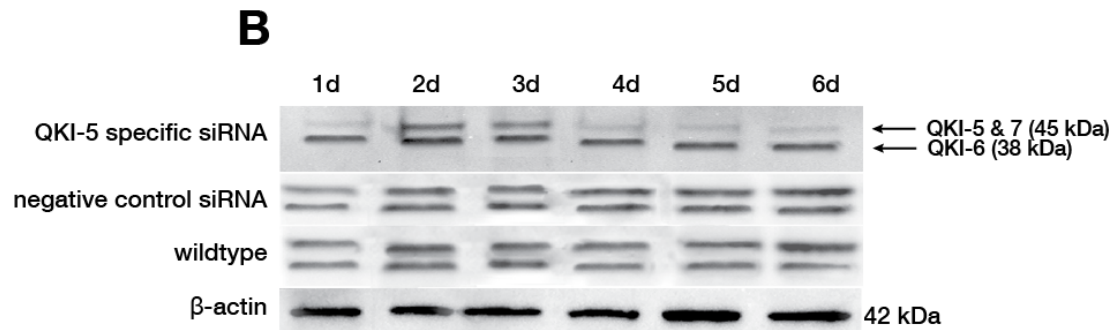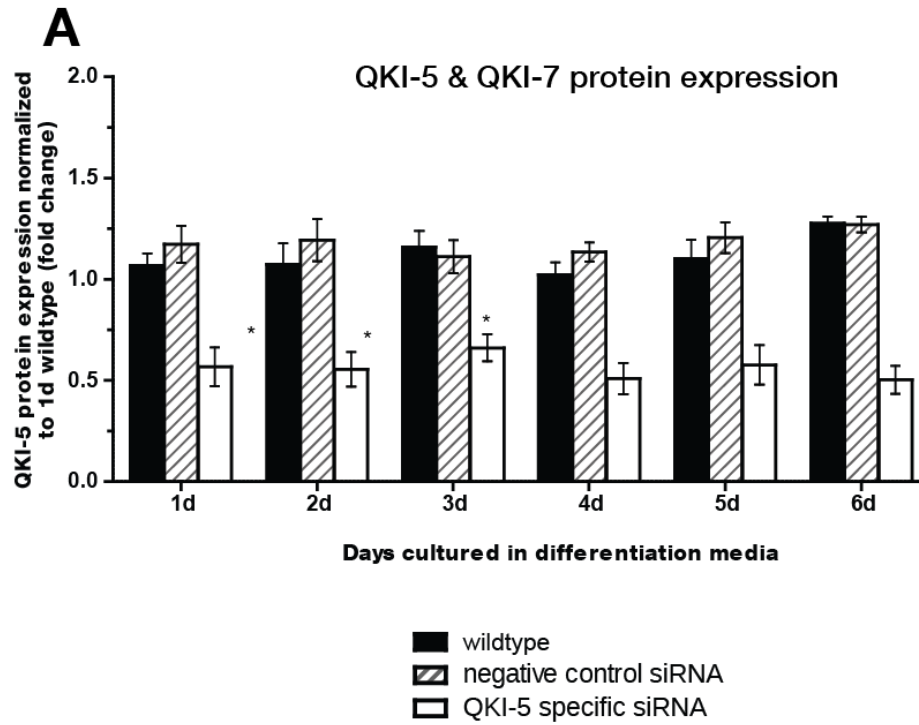
Figure 11. *QKI-5 protein levels are reduced following QKI-5 specific siRNA transfection*. CG4 cells were cultured for 6d in differentiation media. Protein lysates were collected following cell lysis. Protein samples were separated out on 12% polyacrylamide gels using SDS-PAGE. Following the transfer of proteins to a PVDF membrane, membranes were probed with a QKI antibody. A) QKI-5 protein levels were reduced following transfection with QKI-5 specific siRNA at all time points compared to wildtype and control siRNA transfected cultures. B) Neither time nor siRNA transfection had any effect on QKI-6 protein levels. A representative blot showing QKI-5 and QKI-6 protein levels following transfection with either control siRNA or QKI-5 specific siRNA is shown on the right. Protein levels were quantified using AlphaImager software and normalized to β–actin levels. This value was again normalized to the 1d wildtype value and plotted as histograms. Error bars indicate mean ± SEM (n=3). Asterisks denote significance compared to either wildtype or blank plasmid transfected cells (p < 0.05).

4.6 INCREASE IN PLP AND SIRT2 PROTEIN EXPRESSION DURING DIFFERENTIATION

Since QKI-5 was able to increase both *Plp* and *Sirt2* mRNA expression, we next examined the ability of QKI-5 up regulation to affect PLP and SIRT2 protein expression. Similar to the above experiments, total protein was collected from each day from cells transfected with pIRES2-QKI5 and cultured up to 6d in DM. Western blots were then performed to examine both PLP and SIRT2 protein levels. An increase during differentiation in both PLP and SIRT2 protein was observed in cultures from day 1 to day 6 which was not affected by either up or down regulation of QKI-5 (p <0.05) (Figure 12 and Figure 13). PLP and SIRT2 protein levels showed approximately 2.5-fold and 2.75-fold increase, respectively, in untreated wild-type by day 6 (Figure 12). This increase was also seen in blank pIRES2 and pIRES2-QKI5 transfected CG4 cells. However, transfection with either vector did not significantly affect PLP or SIRT2 protein levels during differentiation compared to wildtype levels. This is interesting to note, as an increase in mRNA levels is generally associated with an increase in protein levels. In contrast, both *Plp* and *Sirt2* mRNA levels did not exhibit a significant increase in mRNA levels (p >0.05) during differentiation. Thus, during the course of differentiation, *Plp* and *Sirt2* mRNA levels do not increase but PLP and SIRT2 protein levels do show a significant increase.

PLP protein expression

A

PLP protein expression normalized to 1d wildtype (fold change)

Days cultured in differentiation media

■ wildtype
▨ negative control (blank pIRES2 plasmid)
▭ pIRES2-QKI5

B   PLP protein
1d 2d 3d 4d 5d 6d

pIRES2-QKI5   30 kDa
blank vector
wildtype
β-actin   42 kDa

D   SIRT2 protein
1d 2d 3d 4d 5d 6d

pIRES2-QKI5   40 kDa
blank vector
wildtype
β-actin   42 kDa

C   SIRT2 protein expression

SIRT2 protein expression normalized to 1d wildtype (fold change)

Days cultured in differentiation media

Figure 12. *PLP and SIRT2 protein levels increase over time during culture* and *are not affected following pIRES-QKI-5 transfection.* CG4 cells were cultured for 6d in differentiation media. Protein lysates were collected following cell lysis. Protein samples were separated out on 12% polyacrylamide gels using SDS-PAGE. Following the transfer of proteins to a PVDF membrane, membranes were probed with either a **A)** *Plp*-specific or **B)** *Sirt2*-specific antibody. Neither *Plp* nor *Sirt2* protein levels were affected by pIRES-QKI-5 transfection. However, protein levels were elevated over time. A representative blot showing PLP and SIRT2 protein levels following transfection with either blank pIRES2 plasmid or pIRES2-QKI5 plasmid is shown on the right. Protein levels were quantified using AlphaImager software and normalized to β–actin levels. This value was again normalized to the 1d wildtype value and plotted as histograms. Error bars indicate mean ± SEM (n=3). Asterisks denote significance compared to either wildtype or control blank plasmid transfected cells ($p < 0.05$). The colored brackets indicate time-dependent significance within the same treatment groups (*green* = wildtype, *red* = blank vector, *blue* = plasmid treated) (Bonferroni's post-test; $p < 0.05$).

4.7 QKI-5 DOES NOT IMPACT PLP OR SIRT2 PROTEIN LEVELS

QKI-5 protein levels increased following transfection with the pIRES2-QKI5 plasmid (Figure 10), although this did not result in a significant change in either PLP or SIRT2 protein levels (Figure 12) between treatments with blank vector or untreated wildtype cells at similar time points. This is in contrast to both *Plp* and *Sirt2* mRNA, as both showed significant increases following transfection with pIRES2-QKI5 (Figure 8). Thus, while QKI-5 is able to increase mRNA levels of both *Plp* and *Sirt2*, this increase in mRNA does not translate into a similar increase in protein levels for both genes.

Additionally, following QKI-5 siRNA treatment, QKI-6, QKI-7, *Plp* or *Sirt2* protein did not exhibit a change in expression levels from wild-type or control siRNA treated cells ($p < 0.05$)(Figure 11 and Figure 13).

A

PLP protein expression

PLP protein expression normalized to 1d wildtype (fold change)

Days cultured in differentiation media

■ wildtype
▨ negative control siRNA
☐ QKI-5 specific siRNA

B PLP protein

| | 1d | 2d | 3d | 4d | 5d | 6d | |
QKI-5 specific siRNA ... 30 kDa
negative control siRNA
wildtype
β-actin ... 42 kDa

C

SIRT2 protein expression

SIRT2 protein expression normalized to 1d wildtype (fold change)

Days cultured in differentiation media

D SIRT2 protein

| | 1d | 2d | 3d | 4d | 5d | 6d | |
QKI-5 specific siRNA ... 40 kDa
negative control siRNA
wildtype
β-actin ... 42 kDa

Figure 13. *PLP and SIRT2 protein levels increase over time regardless of QKI-5 specific siRNA transfection.* CG4 cells were cultured for 6d in differentiation media. Protein lysates were collected following cell lysis. Protein samples were separated out on 12% polyacrylamide gels using SDS-PAGE. Following the transfer of proteins to a PVDF membrane, membranes were probed with either a **A)** *Plp*-specific or **B)** *Sirt2*-specific antibody. Neither *Plp* nor *Sirt2* protein levels were affected by QKI-5 specific siRNA transfection. However, protein levels were elevated over time. A representative blot showing PLP and SIRT2 protein levels following transfection with either negative control siRNA or QKI-5 specific siRNA is shown on the right. Protein levels were quantified using AlphaImager software and normalized to β–actin levels. This value was again normalized to the 1d wildtype value and plotted as histograms. Error bars indicate mean ± SEM (n=3). The colored brackets indicate time-dependent significance within the same treatment groups (*green* = wildtype, *red* = control siRNA, *blue* = siRNA treated) (Bonferroni's post-test; $p < 0.05$).

4.8 QKI-5 UP REGULATION INHIBITS GALC EXPRESSION AND PROMOTES A2B5 EXPRESSION

In order to evaluate differentiation in the entire cell population, CG4 cells were probed with either A2B5 or GalC antibodies and stained. A2B5 is a cell surface ganglioside epitope expressed on OPCs (Raff et al., 1983). A2B5 is commonly used as an early stage cellular marker for OPCs while GalC is used to mark OPCs that have differentiated into pre-myelinating OLs and is still present on myelinating OLs. The percentage of cells expressing A2B5 increased following QKI-5 up regulation (Figure 14). From day one to day three there was little change in the percentage of cells expressing A2B5 between treatments. Starting at day 4, in CG4 cells transfected with pIRES2-QKI5, there was a significantly higher percentage of A2B5+ve cells ($60.4 \pm 4.4\%$) versus blank plasmid transfected cells ($35.5 \pm 2.2\%$) ($p<0.05$). By day 6 the percentages had dropped ($44.6 \pm 2.7\%$) in pIRES2-QKI5 transfected CG4 cells but was still significantly higher than the percentage of A2B5+ve ($26.4 \pm 1.9\%$) in blank plasmid transfected CG4 cells ($p<0.05$). Conversely, the percentage of cells expressing GalC, the major glycolipid in myelin (Marcus and Popko 2002), decreased following QKI-5 up regulation (Figure 15). Starting at day 3 the percentage of GalC$^+$ ($11.9 \pm 1.3\%$) in pIRES2-QKI5 transfected was significantly lower than blank plasmid transfected cells ($25.2 \pm 1.6\%$) ($p<0.05$). The percentage of GalC$^+$ cells stayed consistently lower than controls, all the way through day 6; 43.2 ± 3.7 % compared to 58.5 ± 4.5 % ($p<0.05$) in control 6d blank plasmid transfected cultures. Up regulation of QKI-5 appears to drive cells to express A2B5 for a longer period of time, suggesting that QKI-5 serves to inhibit differentiation in CG4 cells.

wildtype   blank pIRES2 vector   pIRES2-QKI5

control siRNA   QKI-5 specific siRNA

A2B5 expression following QKI-5 upregulation

A2B5 expression following down regulation of QKI-5
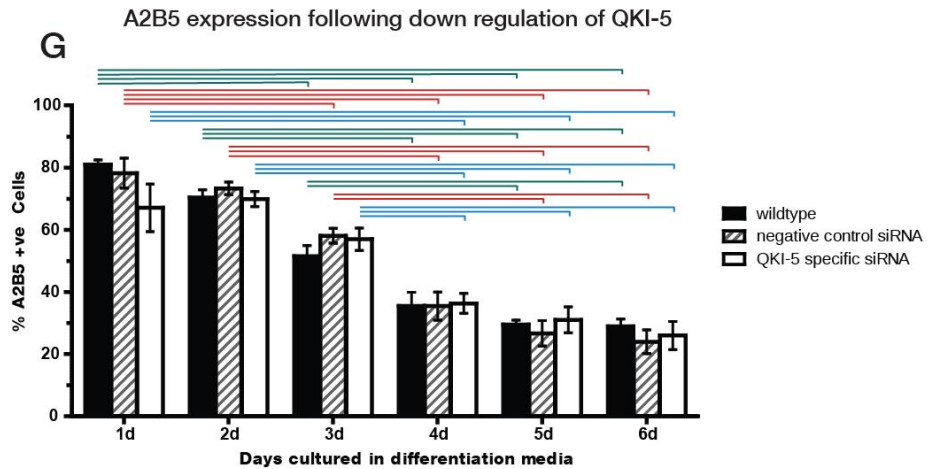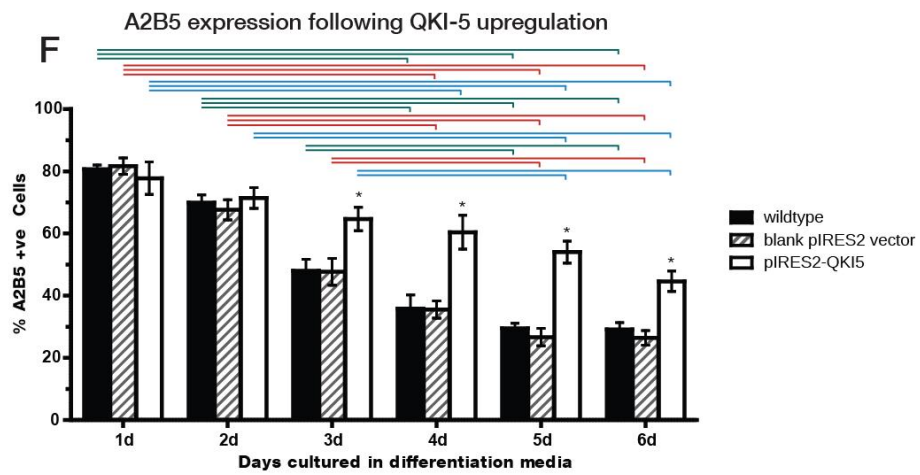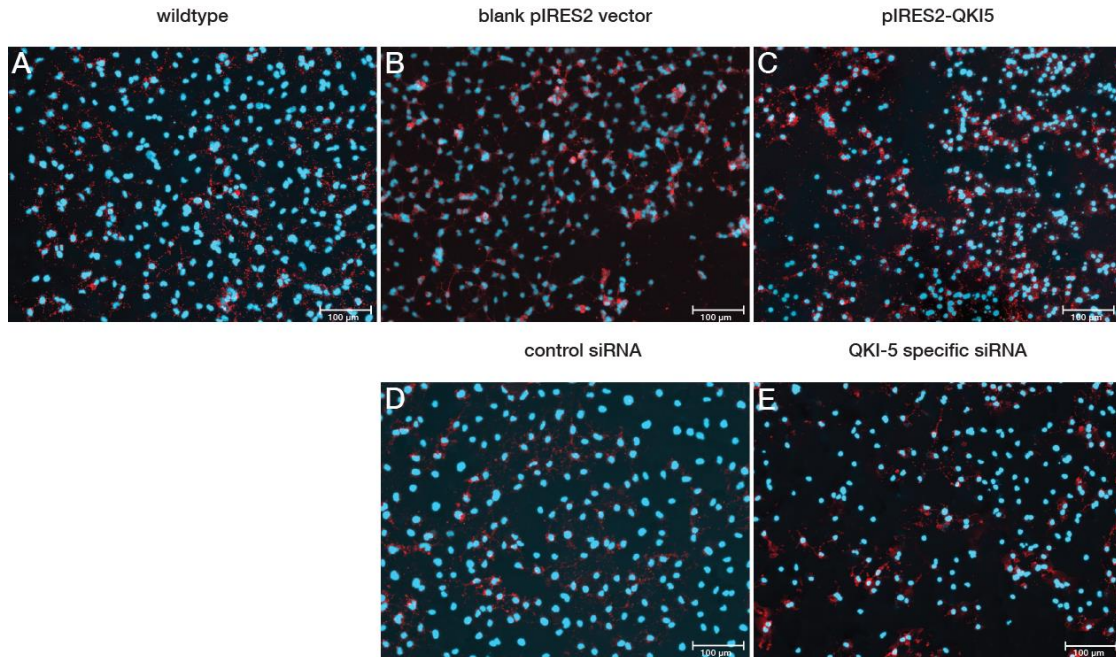
Figure 14. *Cell counts of A2B5⁺ cells after 6d in DM.* CG4 cells were either **A)** untransfected (wildtype) and transfected with either **B)** blank pIRES2 plasmid (negative control), **C)** pIRES2-QKI5 plasmid, **D)** control siRNA, or **E)** QKI-5 specific siRNA, and cultured for 6d in DM on coverslips. After fixing coverslips were stained with antibodies against A2B5. Hoechst stain was used to visualize the cell nuclei. Fluorescent microscope images taken at 100X resolution. Cell counts were performed blind, as previously described in Nicolay, 2004. A2B5 is stained red and Hoechst is stained blue. Scale bar = 100 μm. Average cell counts (n=3) are graphed in **F)** and **G).** Error bars indicate mean ± SEM (n=3). Asterisks denote significance compared to either wildtype or negative control transfected cells ($p < 0.05$). The colored brackets indicate time-dependent significance within the same treatment groups (*green* = wildtype, *red* = blank pIRES2/negative control, *blue* = plasmid/siRNA treated) (Bonferroni's post-test; $p < 0.05$). Approximately 1500 cells were counted from each experiment time point.

wildtype   blank pIRES2 vector   pIRES2-QKI5

control siRNA   QKI-5 specific siRNA

GalC expression following up regulation of QKI-5

GalC expression following down regulation of QKI-5

83

Figure 15. *Cell density of GalC⁺ cells after 6d in DM.* CG4 cells were either **A)** untransfected (wildtype) and transfected with either **B)** blank pIRES2 plasmid (negative control), **C)** pIRES2-QKI5 plasmid, **D)** control siRNA, or **E)** QKI-5 specific siRNA, and cultured for 6d in DM on coverslips. After fixing coverslips were stained with antibodies against A2B5. Hoechst stain was used to visualize the cell nuclei. Fluorescence microscope images taken at 100X resolution. Cell counts were performed blind, as previously described in Nicolay, 2004. A2B5 is stained red and Hoechst is stained blue. Scale bar = 100 μm. Average cell counts (n=3) are graphed in **F)** and **G).** Error bars indicate mean ± SEM (n=3). Asterisks denote significance compared to either wildtype or negative control transfected cells ($p < 0.05$). The colored brackets indicate time-dependent significance within the same treatment groups (*green* = wildtype, *red* = blank pIRES2/negative control, *blue* = plasmid/siRNA treated) (Bonferroni's post-test; *p* < 0.05). Approximately 1500 cells were counted from each experiment time point.

Down regulation of QKI-5 did not have a significant effect on the number of cells expressing A2B5 (Figure 14). At day 6 the percentage of A2B5$^+$ cells in cultures transfected with QKI-5 specific siRNA was 26.0 ± 3.7 % compared to 24.0 ± 3.1 % ($p<0.05$) in the 6d control siRNA sample. However, GalC$^+$ cell counts were affected by QKI-5 specific siRNA transfection (Figure 15). Starting at day 4, the percentage of GalC$^+$ cells in the QKI-5 specific siRNA treated cultures was significantly higher (40.4 ± 1.8 %) compared to control siRNA treated cultures (27.7 ± 1.7 %) ($p<0.05$). This trend continued to day 6 with the percentage rising to 67.7 ± 4.3 % compared to 55.1 ± 3.4 % ($p<0.05$) in the 6d control siRNA sample.

V   DISCUSSION

A significant role for QKI in myelination has been well established. Additionally, more recent research has begun to highlight the importance of QKI in embryonic development. This is not surprising as other STAR proteins regulate a variety of developmental processes including bone metabolism, germline differentiation, and male fertility. However, the function of QKI in early embryonic development has not been well described. There are three mechanisms by which QKI is able to regulate mRNA metabolism, stabilization, localization, and proper generation of mRNA variants via alternative splicing. All of these mechanisms affect translation of mRNA targets. In this context, the aim of this research project was to further expand on the role of QKI-5 in oligodendrocyte development.

In the course of this work, I established that there is an increase in QKI-5 and QKI-6 mRNA, but not in QKI-7, *Plp* or *Sirt2* mRNA, during cell differentiation in wildtype CG4 cells. In contrast to the mRNA expression profile, QKI-5 protein does not increase during CG4 cell differentiation. However, QKI-6, PLP and SIRT2 protein levels all increased during differentiation of wildtype CG4 cells. QKI-7 protein levels are difficult to examine as it migrates at the same size as QKI-5. Following transfection with pIRES2-QKI5, QKI-5 mRNA and protein levels were elevated throughout the experimental time course, from day 1 through til day 6. Over expression of QKI-5 resulted in an increase in both *Plp* and *Sirt2* mRNA but did not result in an increase in either PLP or SIRT2 protein levels. Whereas treatment with QKI-5 siRNA, while able to significantly and specifically decrease QKI-5 mRNA and protein levels, it did not impact QKI-6, QKI-7, *Plp* or *Sirt2* mRNA and protein levels. As well, up regulation of QKI-5 induced an increase in A2B5$^+$ cells and decrease in GalC$^+$ cells, suggesting that QKI-5 inhibits CG4 OL cell differentiation.

5.1 EFFECT OF OVER-EXPRESSION OF QKI-5 ON MRNA EXPRESSION LEVELS

An increase in QKI-5 and QKI-6 levels has been shown to correlate with OL differentiation (Chen et al. 2007; Larocque et al. 2009). Since the CG4 OL cells were cultured in DM, it was expected that both QKI-5 and QKI-6 mRNA levels would increase over the 6d time period. In both wildtype and control transfected cell cultures, QKI-5 and QKI-6 mRNA levels did in fact increase when cultured for 6d in DM. However, QKI-7 mRNA levels remained stable even after 6d of growth in DM. When CG4 cells were transfected with pIRES2-QKI5, there was a significant increase in QKI-5 mRNA levels at every time point although there was no change in QKI-6 or QKI-7 mRNA levels. Likewise, when CG4 cells were transfected with a QKI-5 specific siRNA, there was a significant decrease observed in QKI-5 mRNA levels but QKI-6 and QKI-7 mRNA levels were not affected.

During differentiation of wildtype or control CG4 cells, *Plp* or *Sirt2* mRNA levels did not change even after 6 days in DM. However, overexpression of QKI-5 induced an increase in *Plp* and in *Sirt2* mRNA levels. Increases in PLP and SIRT2 protein levels have been associated with OL differentiation (Ji et al., 2011) although it would appear that an increase in *Plp* or *Sirt2* mRNA levels are not needed in order for protein levels to increase. There is evidence that QKI-6 can stabilize mRNA targets, preventing their degradation (Li et al., 2000; Lakiza et al., 2005). Hence, it is possible that CG4 OL growth in DM results in stabilization of *Plp* and/or *Sirt2* mRNA, negating the need for an increase in transcription during differentiation. Another explanation for this would be the ability of QKI-5 to sequester *Plp* and *Sirt2* mRNA to the nucleus. Elevation of QKI-5 levels may cause an increase in *Plp* and *Sirt2* transcription but then restrict the export of *Plp* and *Sirt2* mRNA into the cytoplasm. So while the pIRES2-QKI5 transfected cultures show elevated *Plp* and *Sirt2* mRNA levels, the amount of mRNA that is available to be translated is similar to the wildtype and control CG4 cells. However, treatment with a

QKI-5 specific siRNA did not affect *Plp* or *Sirt2* mRNA and protein levels, this may imply that while QKI-5 is able to increase transcription of these target genes, it is not essential for proper transcription or translation. It has been shown that *Sirt2* expression proceeds normally even in the absence of *Plp* in pre-myelinating OLs (Zhu et al. 2012). However, a QRE has been identified in the 3' UTR of *Plp* transcripts (Macklin et al. 1987) as well as a QRE in *Sirt2* (unpublished data), leaving open the possibility that QKI-5 may regulate availability and translation of *Plp* and *Sirt2* mRNA through binding of the QREs.

5.2 EFFECT OF OVER-EXPRESSION OF QKI-5 ON PROTEIN LEVELS

After demonstrating that QKI-5 expression can affect both *Plp* and *Sirt2* mRNA levels, we wanted to examine the effect of QKI-5 on protein levels. First we looked at protein levels for the three QKI isoforms. Protein levels for QKI-5 correlated with the increase in mRNA following differentiation of the CG4 cells, regardless of treatment. However, QKI-6 protein levels did not follow the increase in QKI-6 mRNA levels during differentiation. The fact that QKI-6 protein did not increase during CG4 cell differentiation may indicate that the CG4 cells were not fully differentiated. The antibody we used is unable to differentiate between QKI-5 and QKI-7 protein levels, however, QKI-6 and QKI-7 have similar expression profiles, are both negatively affected in the Qk^V/Qk^V mutant, and have similar effects on both Schwann cells and OLs (Hardy et al., 1996; Larocque et al., 2009) . We also observed no change in QKI-7 mRNA levels. One possible explanation is that QKI-5 is binding the excess QKI-6 mRNA, sequestering it in the nucleus and preventing its transport out into the cytoplasm, thereby indirectly inhibiting translation. Another possibility is the stabilization of QKI-6 mRNA by QKI-5 protein. Thus, even though transcription proceeds normally, there is reduced degradation resulting in accumulation of QKI-6 mRNA.

Plp is a four transmembrane domain protein that acts as a major scaffolding protein within the myelin sheath. It is encoded by the *Plp1* gene, which codes for 7 exons and generates two isoforms, *Plp* and DM20. DM20 is missing exon 3B which is crucial for axo-glial interaction (Stecca et al., 2000). *Plp* is expressed in differentiated OLs which explains the increase in PLP and SIRT2 protein levels we observed during CG4 cell differentiation. While protein levels for PLP and SIRT2 were observed to increase during growth in DM they were not affected by QKI-5 over expression. Regardless of treatment, both PLP and SIRT2 protein levels show a time dependent increase during differentiation from day 1 to day 6. However, over expression of QKI-5 did not significantly increase *Plp* or *Sirt2* protein levels compared to wildtype or control culture levels. This is in contrast to changes observed in mRNA expression for both genes, where over expression of QKI-5 resulted in an increase in both *Plp* and *Sirt2* mRNA levels although normal cellular differentiation did not appear to have an effect on mRNA levels. Generally, when mRNA levels increase, protein levels similarly increase. One explanation is that QKI-6 activity is responsible for the increase in *Plp* and *Sirt2* mRNA, as QKI-6 has been previously described to play a regulatory role in mRNA translation and stabilization (Lakiza et al. 2005; Saccomanno et al. 1999). An alternative explanation is that, similar to QKI-6 mRNA, QKI-5 binds to and sequesters *Plp* and *Sirt2* mRNA within the nucleus, thus resulting in mRNA accumulation without a subsequent increase in protein levels.

Transfection with a QKI-5 specific siRNA did not impact QKI-6, QKI-7, *Plp*, or *Sirt2* mRNA and protein levels. A possible explanation is that baseline transcription of these genes are still able to proceed with transcription even when QKI-5 levels are low, suggesting that while QKI-5 may not be essential for *Plp* or *Sirt2* transcription. Although it is still able to induce transcription of both genes. While QKI-5 expression was impacted by siRNA treatment, QKI-6 and QKI-7 mRNA levels were still at

wildtype levels. Thus it is possible that QKI-6 and -7 are able to compensate for a reduction in QKI-5. However, when ENU-induced alleles examined loss of function by abolishing QKI dimerization or through the loss of a splice site necessary for proper QKI-5 transcript production, there was either a loss of QKI protein function or a complete absence of the nuclear isoform, QKI-5. In contrast, our study only diminished QKI-5 expression and was unable to completely remove QKI-5 expression. It is possible that low levels of QKI-5 are sufficient to maintain OL viability without negatively impacting differentiation.

Plp and Sirt2 mRNA are affected by QKI-5 over expression but not by normal growth in wildtype CG4 cells in DM. There was a significant increase in both Plp and Sirt2 mRNA levels following over expression of QKI-5. However, protein levels for Plp and Sirt2 were not affected by QKI-5 over expression but were observed to increase during normal growth in wildtype CG4 cells in DM. One explanation for this is, perhaps sequestering of Plp and Sirt2 mRNA in the nucleus by QKI-5. Elevation of QKI-5 levels may cause an increase in Plp and Sirt2 transcription but then restrict the export of Plp and Sirt2 mRNA into the cytoplasm. So while the pIRES2-QKI5 transfected cultures show elevated Plp and Sirt2 mRNA levels, the amounts of mRNA that is available to be translated is similar to the wildtype and control cultures. However, treatment with a QKI-5 specific siRNA was unable to affect Plp and Sirt2 mRNA and protein levels indicating that while QKI-5 is able to increase transcription of these target genes, it is not essential for proper transcription or translation. It has been shown that Sirt2 expression proceeds normally even in the absence of Plp in pre-myelinating OLs (Zhu et al. 2012). However, a QRE has been identified in the 3' UTR of Plp transcripts (Macklin et al. 1987) as well as a QRE in Sirt2 (our laboratory unpublished data), leaving open the possibility that QKI-5 may regulate availability and translation of Plp and Sirt2 mRNA through binding and sequestering within the nucleus.

5.3   IMPACT OF UP-REGULATION OF QKI ON OL DIFFERENTIATION

In order to evaluate the effect of QKI-5 on OL differentiation, CG4 cells were transfected with pIRES2-QKI5 and immunostained with antibodies against A2B5 and GalC. A2B5 is an antibody that recognizes an epitope on a cell surface ganglioside expressed by OPCs. GalC is a glycosphingolipid that is highly expressed in the myelin sheath. GalC is expressed later than A2B5 and is specific to differentiated OLs. The percentage of cells expressing A2B5 provides us with a baseline while percentage of cells expressing GalC was used to evaluate differentiation of CG4 cells. Transfection of CG4 OL with the pIRES2-QKI5 plasmid resulted in a higher percentage of A2B5+ cells, compared to wildtype or control vector transfected cells. As well, the percentage of GalC+ cells was lower compared to wildtype and control cultures. The increase in A2B5+ cells coupled with a decrease in GalC+ cells points to the ability of QKI-5 to delay differentiation when over expressed in CG4 OL cells. It is possible that QKI-5 can bind to mRNAs that encode for enhancers of OPC differentiation, thus retaining them within the nucleus and inhibiting OPC differentiation.

The increase in *Plp* and *Sirt2* mRNA expression may be an indirect result of the delay in differentiation. A delay in differentiation could drive increased transcription of *Plp* and *Sirt2* mRNA as a feedback mechanism or result in accumulation of mRNA transcripts. Also, since PLP and SIRT2 protein levels remain unchanged, it is possible that the change in timing of OL differentiation is due to a separate pathway. Up regulation of *Sirt2* has been found to enhance differentiation (Ji et al. 2011). As well, Ji et al. found that knockdown of *Sirt2* inhibited MBP expression. While the up regulation of QKI-5 did not have an effect on SIRT2 protein levels, the increase observed in all treatment groups during the 6d time course can be attributed to growth in DM and subsequent differentiation.

There was no change in the percentage of A2B5^{+} cells following siRNA treatment. One explanation why a decrease in the number of A2B5^{+} cells is not observed is that A2B5 is one of the earliest markers of OPCs and the fate of some cells have already been determined. However, the percentage of GalC^{+} cells was significantly increased from 4d onward. Since the knockdown of QKI-5 is unable to impact QKI-6, QKI-7, PLP, or SIRT2 protein levels, it is likely that the baseline transcription, mentioned previously, is similarly able to compensate for the decrease in QKI-5 protein. Also, the markers examined are mainly end stage differentiation markers, so it is possible that the cells are differentiating but have not reached the point at which *Plp*, *Sirt2* mRNA or GalC are up regulated. Examination of a differentiation marker that is expressed in between A2B5 and GalC may provide insight to the rate at which knockdown of QKI-5 impacts cellular differentiation.

While QKI-5 has been shown to have alternative splicing activity (Wu et al., 2002), QKI-6 has been implicated in cellular differentiation through mediation of mRNA translation and stabilization. While this role has not been described for QKI-5, it is possible that it could mediate mRNA translation since all QKI isoforms contain the same RNA binding domain and thus can bind the same targets. In contrast to QKI-6, which stabilizes mRNAs by binding and preventing degradation via RNases, QKI-5 likely prevents translation by sequestering target mRNAs in the nucleus. This would allow the cell to quickly respond to extracellular signals by rapidly translating the large pool of available mRNAs, thereby producing a large number of proteins in a short period of time. That QKI-5 protein levels steadily increases up until shortly after the onset of myelination (Hardy et al., 1996), suggests the ability of OLs to stockpile necessary myelin mRNAs in the nucleus prior to the onset of myelination. The fact that QKI-6 levels increase once QKI-5 levels begin to decline suggests that competition between the two differentially localized isoforms controls the availability of target

92

mRNAs and is one mechanism by which OLs can tightly regulate the translation of mRNAs required for myelinogenesis.

The ability of QKI-5 to bind to both *Plp* and *Sirt2* mRNA combined with the presence of a nuclear localization signal could result in the sequestering of *Plp* and *Sirt2* mRNA to the nucleus. By sequestering mRNA in the nucleus, it would prevent translation of the target mRNA. This would explain the stockpiling of mRNA with little change in protein levels. Indeed, QKI-5 has been shown to retain MBP mRNA in the nucleus (Larocque et al. 2002) and it is conceivable that QKI-5 can retain other mRNA targets. Since QKI-5 and QKI-6 have differing expression profiles over time, it is possible that the cell may use QKI as an aid in the proper timing of cell cycle progression through switching expression from QKI-5 to QKI-6 resulting in the release and translation of a large quantity of mRNA in a short period of time. QKI may also act through other downstream targets, such as p27[KIP1] (Larocque et al. 2005), to regulate cell cycle progression and cellular differentiation.

Table 1. <u>Summary of gene expression changes following changes in QKI-5 expression</u>

Up regulation of QKI-5	Knock down of QKI-5
QKI-5 mRNA levels increase	QKI-5 mRNA levels similar to wildtype
QKI-5/QKI-7 protein levels increase	QKI-5/QKI-7 protein levels similar to wildtype
QKI-6 mRNA and protein levels similar to wildtype	QKI-6 mRNA and protein levels similar to wildtype
Plp mRNA levels increase	Plp mRNA levels similar to wildtype
Sirt2 mRNA levels increase	Sirt2 mRNA levels similar to wildtype
PLP protein levels similar to wildtype	PLP protin levels similar to wildtype
SIRT2 protein levels similar to wildtype	SIRT2 protein levels similar to wildtype
Increase in % of A2B5+ve cells	% of A2B5+ve cells similar to wildtype
Decrease in % of GalC+ve cells	Increase in % of GalC+ve cells

Table 1. *Summary of gene expression changes following changes in QKI-5 expression.* Summary of various gene expression changes including mRNA and protein levels following either upregulation or knockdown of QKI-5 expression. Genes examined include QKI-6, *Plp*, *Sirt2* as well as ganglioside markers A2B5 and GalC.

5.4   FUTURE DIRECTIONS

In the present work, I focused mainly on the impact of elevated QKI-5 on CG4 OL cell differentiation. Down regulation of QKI-5 was also examined but results were limited compared to the up regulation studies. The first is that CG4 cells were allowed to differentiate for up to 6 days in DM. The experiment did not go beyond 6 days because of cell confluency and the inability to stain and count individual cells. Based on previous studies from our lab (Ji et al., 2011), 6 days was determined to be the appropriate time to allow for CG4 cells to differentiate to a stage of maturity where they would begin to express MBP proteins. While (Ji et al.,) was able to show an increase in MBP after growth for 6d in DM, I was unable to detect MBP using either western blots or immunocytochemistry after a similar time period. This could either be an issue with the DM or else the cells just need to be cultured for a longer period of time. These culture problems are important to overcome in order to fully describe the effect of QKI-5 on PLP and SIRT2 protein expression patterns. Another aspect of the study that could be improved would be the use of primary OL cells or perhaps even QKI-5 over expression *in vivo*, to both validate and expand upon the results presented here.

There is evidence linking QKI to cell cycling machinery and it would be interesting to further investigate the relationships between cell cycle components and QKI-5. A recent study has also linked QKI with glioblastoma via microRNA (miRNA) regulation (Chen et al., 2012). The study by Chen et al., described the association of QKI with miRNA-20a, leading to stabilization of the miRNA target and the discovery of a novel tumor suppression mechanism. Another study also discovered that U343 cells that were deficient in QKI had elevated levels of miRNA-7 which resulted in defects in cellular proliferation (Wang et al., 2013). Further investigation of the links between miRNA and QKI would provide insight into another mechanism by which QKI may regulate glial cell proliferation and function.

In addition, further experiments that describe the mRNA targets that QKI is able to bind directly are needed. Initial RNA coimmunoprecipitation studies performed in our lab (unpublished) have provided us with a clearer picture of the interaction between QKI protein and *Plp* and *Sirt2* mRNA. CG4 cells that were fully differentiated showed higher levels of *Plp* mRNA were bound to QKI protein compared to IgG controls. In cells cultured in GM, *Plp* expression is lower and this is reflected in lower levels of mRNA precipitating out with QKI protein. In the CG4 cells grown in DM, we again see increased binding of QKI protein to *Sirt2* mRNA when compared to IgG controls. This demonstrates the ability of QKI protein to directly bind both *Plp* and *Sirt2* mRNA in CG4 OL cells. The cellular location of binding has yet to be determined and will provide greater insight on the role of QKI on *Plp* and *Sirt2* mRNA. It will be interesting to see if the majority of binding occurs in the nucleus or cytoplasm and if QKI-5 is able to shuttle back and forth between the nucleus and cytoplasm while bound to either *Plp* or *Sirt2* mRNA. As well, the investigation of a greater number of mRNA targets bound by QKI-5 will also provide further insight into the role of QKI-5 and glial cell proliferation. Previous bioinformatics studies have highlighted some potential targets of QKI (Galarneau and Richard 2005) but outside of one or two popular targets (MBP and MAG) there is a lack of data on both the *in vitro* and *in vivo* binding targets of QKI. The recent discovery that QKI can also regulate miRNA metabolism has further increased the number of possible binding targets (Wang et al., 2013).

VI REFERENCES

Aberg, K., Saetre, P., Jareborg, N. and Jazin, E. (2006a). Human QKI, a potential regulator of mRNA expression of human oligodendrocyte-related genes involved in schizophrenia. Proc Natl Acad Sci U S A **103**(19): 7482-7487.

Aberg, K., Saetre, P., Lindholm, E., Ekholm, B., Pettersson, U., Adolfsson, R. and Jazin, E. (2006b). Human QKI, a new candidate gene for schizophrenia involved in myelination. Am J Med Genet B Neuropsychiatr Genet **141B**(1): 84-90.

Aggarwal, S., Yurlova, L. and Simons, M. (2011). Central nervous system myelin: structure, synthesis and assembly. Trends Cell Biol **21**(10): 585-593.

Artzt, K. and Wu, J.I. (2010). STAR trek: An introduction to STAR family proteins and review of quaking (QKI). Adv Exp Med Biol **693**: 1-24.

Bansal, R. and Pfeiffer, S.E. (1989). Reversible inhibition of oligodendrocyte progenitor differentiation by a monoclonal antibody against surface galactolipids. Proc Natl Acad Sci U S A **86**(16): 6181-6185.

Bansal, R. and Pfeiffer, S.E. (1994). Regulation of gene expression in mature oligodendrocytes by the specialized myelin-like membrane environment: antibody perturbation in culture with the monoclonal antibody R-mAb. Glia **12**(3): 173-179.

Baracskay, K.L., Kidd, G.J., Miller, R.H. and Trapp, B.D. (2007). NG2-positive cells generate A2B5-positive oligodendrocyte precursor cells. Glia **55**(10): 1001-1010.

Baron, W., Metz, B., Bansal, R., Hoekstra, D. and de Vries, H. (2000). PDGF and FGF-2 signaling in oligodendrocyte progenitor cells: regulation of proliferation and differentiation by multiple intracellular signaling pathways. Mol Cell Neurosci **15**(3): 314-329.

Bartzokis, G. (2004a). Age-related myelin breakdown: a developmental model of cognitive decline and Alzheimer's disease. Neurobiol Aging **25**(1): 5-18; author reply 49-62.

Bartzokis, G. (2004b). Quadratic trajectories of brain myelin content: unifying construct for neuropsychiatric disorders. Neurobiol Aging **25**(1): 49-62.

Bartzokis, G., Sultzer, D., Lu, P.H., Nuechterlein, K.H., Mintz, J. and Cummings, J.L. (2004). Heterogeneous age-related breakdown of white matter structural

integrity: implications for cortical "disconnection" in aging and Alzheimer's disease. <u>Neurobiol Aging</u> **25**(7): 843-851.

Ben Fredj, N., Grange, J., Sadoul, R., Richard, S., Goldberg, Y. and Boyer, V. (2004). Depolarization-induced translocation of the RNA-binding protein Sam68 to the dendrites of hippocampal neurons. <u>J Cell Sci</u> **117**(Pt 7): 1079-1090.

Bhat, N.R., Zhang, P. and Mohanty, S.B. (2007). p38 MAP kinase regulation of oligodendrocyte differentiation with CREB as a potential target. <u>Neurochem Res</u> **32**(2): 293-302.

Bockbrader, K. and Feng, Y. (2008). Essential function, sophisticated regulation and pathological impact of the selective RNA-binding protein QKI in CNS myelin development. <u>Future Neurol</u> **3**(6): 655-668.

Boggs, J.M., Gao, W. and Hirahara, Y. (2008). Myelin glycosphingolipids, galactosylceramide and sulfatide, participate in carbohydrate-carbohydrate interactions between apposed membranes and may form glycosynapses between oligodendrocyte and/or myelin membranes. <u>Biochim Biophys Acta</u> **1780**(3): 445-455.

Boggs, J.M., Gao, W., Zhao, J., Park, H.-J., Liu, Y. and Basu, A. (2010). Participation of galactosylceramide and sulfatide in glycosynapses between oligodendrocyte or myelin membranes. <u>FEBS Lett</u> **584**(9): 1771-1778.

Boggs, J.M. and Wang, H. (2001). Effect of liposomes containing cerebroside and cerebroside sulfate on cytoskeleton of cultured oligodendrocytes. <u>J Neurosci Res</u> **66**(2): 242-253.

Boggs, J.M. and Wang, H. (2004). Co-clustering of galactosylceramide and membrane proteins in oligodendrocyte membranes on interaction with polyvalent carbohydrate and prevention by an intact cytoskeleton. <u>J Neurosci Res</u> **76**(3): 342-355.

Boggs, J.M., Wang, H., Gao, W., Arvanitis, D.N., Gong, Y. and Min, W. (2004). A glycosynapse in myelin? <u>Glycoconj J</u> **21**(3-4): 97-110.

Bohnsack, B.L., Lai, L., Northrop, J.L., Justice, M.J. and Hirschi, K.K. (2006). Visceral endoderm function is regulated by quaking and required for vascular development. <u>Genesis</u> **44**(2): 93-104.

Bosio, A., Binczek, E. and Stoffel, W. (1996). Functional breakdown of the lipid bilayer of the myelin membrane in central and peripheral nervous system by disrupted galactocerebroside synthesis. <u>Proceedings of the National Academy of Sciences</u> **93**(23): 13280-13285.

Busa, R., Paronetto, M.P., Farini, D., Pierantozzi, E., Botti, F., Angelini, D.F., Attisani, F., Vespasiani, G. and Sette, C. (2007). The RNA-binding protein Sam68 contributes to proliferation and survival of human prostate cancer cells. <u>Oncogene</u> **26**(30): 4372-4382.

Campagnoni, A.T. and Skoff, R.P. (2001). The pathobiology of myelin mutants reveal novel biological functions of the MBP and PLP genes. <u>Brain Pathol</u> **11**(1): 74-91.

Chawla, G., Lin, C.H., Han, A., Shiue, L., Ares, M., Jr. and Black, D.L. (2009). Sam68 regulates a set of alternatively spliced exons during neurogenesis. <u>Mol Cell Biol</u> **29**(1): 201-213.

Chen, A.J., Paik, J.H., Zhang, H., Shukla, S.A., Mortensen, R., Hu, J., Ying, H., Hu, B., Hurt, J., Farny, N., Dong, C., Xiao, Y., Wang, Y.A., Silver, P.A., Chin, L., Vasudevan, S. and Depinho, R.A. (2012). STAR RNA-binding protein Quaking suppresses cancer via stabilization of specific miRNA. <u>Genes Dev</u> **26**(13): 1459-1472.

Chen, T. and Richard, S. (1998). Structure-function analysis of Qk1: a lethal point mutation in mouse quaking prevents homodimerization. <u>Mol Cell Biol</u> **18**(8): 4863-4871.

Chen, Y., Tian, D., Ku, L., Osterhout, D.J. and Feng, Y. (2007). The selective RNA-binding protein quaking I (QKI) is necessary and sufficient for promoting oligodendroglia differentiation. <u>J Biol Chem</u> **282**(32): 23553-23560.

Chenard, C.A. and Richard, S. (2008). New implications for the QUAKING RNA binding protein in human disease. <u>J Neurosci Res</u> **86**(2): 233-242.

Chew, L.J., Coley, W., Cheng, Y. and Gallo, V. (2010). Mechanisms of regulation of oligodendrocyte development by p38 mitogen-activated protein kinase. <u>J Neurosci</u> **30**(33): 11011-11027.

Coetzee, T., Fujita, N., Dupree, J., Shi, R., Blight, A., Suzuki, K., Suzuki, K. and Popko, B. (1996a). Myelination in the Absence of Galactocerebroside and Sulfatide: Normal Structure with Abnormal Function and Regional Instability. <u>Cell</u> **86**(2): 209-219.

Coetzee, T., Li, X., Fujita, N., Marcus, J., Suzuki, K., Francke, U. and Popko, B. (1996b). Molecular cloning, chromosomal mapping, and characterization of the mouse UDP-galactose:ceramide galactosyltransferase gene. Genomics **35**(1): 215-222.

Colognato, H., Ramachandrappa, S., Olsen, I.M. and ffrench-Constant, C. (2004). Integrins direct Src family kinases to regulate distinct phases of oligodendrocyte development. J Cell Biol **167**(2): 365-375.

Cox, R.D., Hugill, A., Shedlovsky, A., Noveroske, J.K., Best, S., Justice, M.J., Lehrach, H. and Dove, W.F. (1999). Contrasting effects of ENU induced embryonic lethal mutations of the quaking gene. Genomics **57**(3): 333-341.

Coyle, J.H., Guzik, B.W., Bor, Y.C., Jin, L., Eisner-Smerage, L., Taylor, S.J., Rekosh, D. and Hammarskjold, M.L. (2003). Sam68 enhances the cytoplasmic utilization of intron-containing RNA and is functionally regulated by the nuclear kinase Sik/BRK. Mol Cell Biol **23**(1): 92-103.

Denu, J.M. (2005). The Sir 2 family of protein deacetylases. Curr Opin Chem Biol **9**(5): 431-440.

Derry, J.J., Prins, G.S., Ray, V. and Tyner, A.L. (2003). Altered localization and activity of the intracellular tyrosine kinase BRK/Sik in prostate tumor cells. Oncogene **22**(27): 4212-4220.

Derry, J.J., Richard, S., Valderrama Carvajal, H., Ye, X., Vasioukhin, V., Cochrane, A.W., Chen, T. and Tyner, A.L. (2000). Sik (BRK) phosphorylates Sam68 in the nucleus and negatively regulates its RNA binding ability. Mol Cell Biol **20**(16): 6114-6126.

Doetsch, F., Garcia-Verdugo, J.M. and Alvarez-Buylla, A. (1997). Cellular composition and three-dimensional organization of the subventricular germinal zone in the adult mammalian brain. J Neurosci **17**(13): 5046-5061.

Donmez, G. and Guarente, L. (2010). Aging and disease: connections to sirtuins. Aging Cell **9**(2): 285-290.

Dryden, S.C., Nahhas, F.A., Nowak, J.E., Goustin, A.S. and Tainsky, M.A. (2003). Role for human SIRT2 NAD-dependent deacetylase activity in control of mitotic exit in the cell cycle. Mol Cell Biol **23**(9): 3173-3185.

Dubois-Dalcq, M., Behar, T., Hudson, L. and Lazzarini, R.A. (1986). Emergence of three myelin proteins in oligodendrocytes cultured without neurons. J Cell Biol **102**(2): 384-392.

Dupree, J.L., Girault, J.-A. and Popko, B. (1999). Axo-Glial Interactions Regulate the Localization of Axonal Paranodal Proteins. J Cell Biol **147**(6): 1145-1152.

Ebersole, T., Rho, O. and Artzt, K. (1992). The proximal end of mouse chromosome 17: new molecular markers identify a deletion associated with quakingviable. Genetics **131**(1): 183-190.

Ebersole, T.A., Chen, Q., Justice, M.J. and Artzt, K. (1996). The quaking gene product necessary in embryogenesis and myelination combines features of RNA binding and signal transduction proteins. Nat Genet **12**(3): 260-265.

Flamme, I., Frolich, T. and Risau, W. (1997). Molecular mechanisms of vasculogenesis and embryonic angiogenesis. J Cell Physiol **173**(2): 206-210.

Fragoso, G., Haines, J.D., Roberston, J., Pedraza, L., Mushynski, W.E. and Almazan, G. (2007). p38 mitogen-activated protein kinase is required for central nervous system myelination. Glia **55**(15): 1531-1541.

Fragoso, G., Robertson, J., Athlan, E., Tam, E., Almazan, G. and Mushynski, W.E. (2003). Inhibition of p38 mitogen-activated protein kinase interferes with cell shape changes and gene expression associated with Schwann cell myelination. Exp Neurol **183**(1): 34-46.

Friedrich, V.L., Jr. (1975). Hyperplasia of oligodendrocytes in quaking mice. Anat Embryol (Berl) **147**(3): 259-271.

Fumagalli, S., Totty, N.F., Hsuan, J.J. and Courtneidge, S.A. (1994). A target for Src in mitosis. Nature **368**(6474): 871-874.

Fusaki, N., Iwamatsu, A., Iwashima, M. and Fujisawa, J. (1997). Interaction between Sam68 and Src family tyrosine kinases, Fyn and Lck, in T cell receptor signaling. J Biol Chem **272**(10): 6214-6219.

Galarneau, A. and Richard, S. (2005). Target RNA motif and target mRNAs of the Quaking STAR protein. Nat Struct Mol Biol **12**(8): 691-698.

Galarneau, A. and Richard, S. (2009). The STAR RNA binding proteins GLD-1, QKI, SAM68 and SLM-2 bind bipartite RNA motifs. BMC Mol Biol **10**: 47.

Garcia-Mayoral, M.F., Hollingworth, D., Masino, L., Diaz-Moreno, I., Kelly, G., Gherzi, R., Chou, C.F., Chen, C.Y. and Ramos, A. (2007). The structure of the C-terminal

KH domains of KSRP reveals a noncanonical motif important for mRNA degradation. <u>Structure</u> **15**(4): 485-498.

Grange, J., Belly, A., Dupas, S., Trembleau, A., Sadoul, R. and Goldberg, Y. (2009). Specific interaction between Sam68 and neuronal mRNAs: implication for the activity-dependent biosynthesis of elongation factor eEF1A. <u>J Neurosci Res</u> **87**(1): 12-25.

Gray, S.G. and Ekstrom, T.J. (2001). The human histone deacetylase family. <u>Exp Cell Res</u> **262**(2): 75-83.

Griffiths, I., Klugmann, M., Anderson, T., Yool, D., Thomson, C., Schwab, M.H., Schneider, A., Zimmermann, F., McCulloch, M., Nadon, N. and Nave, K.A. (1998). Axonal swellings and degeneration in mice lacking the major proteolipid of myelin. <u>Science</u> **280**(5369): 1610-1613.

Gudz, T.I., Schneider, T.E., Haas, T.A. and Macklin, W.B. (2002). Myelin proteolipid protein forms a complex with integrins and may participate in integrin receptor signaling in oligodendrocytes. <u>J Neurosci</u> **22**(17): 7398-7407.

Hansen, D. and Schedl, T. (2006). The regulatory network controlling the proliferation-meiotic entry decision in the Caenorhabditis elegans germ line. <u>Curr Top Dev Biol</u> **76**: 185-215.

Hardy, R.J. (1998). Molecular defects in the dysmyelinating mutant quaking. <u>J Neurosci Res</u> **51**(4): 417-422.

Hardy, R.J., Loushin, C.L., Friedrich, V.L., Jr., Chen, Q., Ebersole, T.A., Lazzarini, R.A. and Artzt, K. (1996). Neural cell type-specific expression of QKI proteins is altered in quakingviable mutant mice. <u>J Neurosci</u> **16**(24): 7941-7949.

Haroutunian, V., Katsel, P., Dracheva, S. and Davis, K.L. (2006). The human homolog of the QKI gene affected in the severe dysmyelination "quaking" mouse phenotype: downregulated in multiple brain regions in schizophrenia. <u>Am J Psychiatry</u> **163**(10): 1834-1837.

Hattori, K., Fukuzako, H., Hashiguchi, T., Hamada, S., Murata, Y., Isosaka, T., Yuasa, S. and Yagi, T. (2009). Decreased expression of Fyn protein and disbalanced alternative splicing patterns in platelets from patients with schizophrenia. <u>Psychiatry Res</u> **168**(2): 119-128.

Hong, W., Resnick, R.J., Rakowski, C., Shalloway, D., Taylor, S.J. and Blobel, G.A. (2002). Physical and functional interaction between the transcriptional cofactor CBP and the KH domain protein Sam68. Mol Cancer Res **1**(1): 48-55.

Hopper, A.F. and Hart, N.H. (1985). Foundations of animal development, Oxford University Press.

Hubbert, C., Guardiola, A., Shao, R., Kawaguchi, Y., Ito, A., Nixon, A., Yoshida, M., Wang, X.F. and Yao, T.P. (2002). HDAC6 is a microtubule-associated deacetylase. Nature **417**(6887): 455-458.

Ichimura, K., Mungall, A.J., Fiegler, H., Pearson, D.M., Dunham, I., Carter, N.P. and Collins, V.P. (2006). Small regions of overlapping deletions on 6q26 in human astrocytic tumours identified using chromosome 6 tile path array-CGH. Oncogene **25**(8): 1261-1271.

Jan, E., Motzny, C.K., Graves, L.E. and Goodwin, E.B. (1999). The STAR protein, GLD-1, is a translational regulator of sexual identity in Caenorhabditis elegans. EMBO J **18**(1): 258-269.

Ji, S., Doucette, J.R. and Nazarali, A.J. (2011). Sirt2 is a novel in vivo downstream target of Nkx2.2 and enhances oligodendroglial cell differentiation. J Mol Cell Biol **3**(6): 351-359.

Justice, M.J. and Bode, V.C. (1988). Three ENU-induced alleles of the murine quaking locus are recessive embryonic lethal mutations. Genet Res **51**(2): 95-102.

Karim, S.A., Barrie, J.A., McCulloch, M.C., Montague, P., Edgar, J.M., Iden, D.L., Anderson, T.J., Nave, K.A., Griffiths, I.R. and McLaughlin, M. (2010). PLP/DM20 expression and turnover in a transgenic mouse model of Pelizaeus-Merzbacher disease. Glia **58**(14): 1727-1738.

Kirla, R.M., Haapasalo, H.K., Kalimo, H. and Salminen, E.K. (2003). Low expression of p27 indicates a poor prognosis in patients with high-grade astrocytomas. Cancer **97**(3): 644-648.

Klempan, T.A., Ernst, C., Deleva, V., Labonte, B. and Turecki, G. (2009). Characterization of QKI gene expression, genetics, and epigenetics in suicide victims with major depressive disorder. Biol Psychiatry **66**(9): 824-831.

Lakiza, O., Frater, L., Yoo, Y., Villavicencio, E., Walterhouse, D., Goodwin, E.B. and Iannaccone, P. (2005). STAR proteins quaking-6 and GLD-1 regulate translation

of the homologues GLI1 and tra-1 through a conserved RNA 3'UTR-based mechanism. <u>Dev Biol</u> **287**(1): 98-110.

Larocque, D., Fragoso, G., Huang, J., Mushynski, W.E., Loignon, M., Richard, S. and Almazan, G. (2009). The QKI-6 and QKI-7 RNA binding proteins block proliferation and promote Schwann cell myelination. <u>PLoS One</u> **4**(6): e5867.

Larocque, D., Galarneau, A., Liu, H.N., Scott, M., Almazan, G. and Richard, S. (2005). Protection of p27(Kip1) mRNA by quaking RNA binding proteins promotes oligodendrocyte differentiation. <u>Nat Neurosci</u> **8**(1): 27-33.

Larocque, D., Pilotte, J., Chen, T., Cloutier, F., Massie, B., Pedraza, L., Couture, R., Lasko, P., Almazan, G. and Richard, S. (2002). Nuclear retention of MBP mRNAs in the quaking viable mice. <u>Neuron</u> **36**(5): 815-829.

Laursen, L.S., Chan, C.W. and Ffrench-Constant, C. (2011). Translation of myelin basic protein mRNA in oligodendrocytes is regulated by integrin activation and hnRNP-K. <u>J Cell Biol</u> **192**(5): 797-811.

Le Bras, B., Chatzopoulou, E., Heydon, K., Martinez, S., Ikenaka, K., Prestoz, L., Spassky, N., Zalc, B. and Thomas, J.L. (2005). Oligodendrocyte development in the embryonic brain: the contribution of the plp lineage. <u>Int J Dev Biol</u> **49**(2-3): 209-220.

Levine, J.M., Reynolds, R. and Fawcett, J.W. (2001). The oligodendrocyte precursor cell in health and disease. <u>Trends in Neurosciences</u> **24**(1): 39-47.

Li, J., Liu, Y., Kim, B.O. and He, J.J. (2002a). Direct participation of Sam68, the 68-kilodalton Src-associated protein in mitosis, in the CRM1-mediated Rev nuclear export pathway. <u>J Virol</u> **76**(16): 8374-8382.

Li, W., Zhang, B., Tang, J., Cao, Q., Wu, Y., Wu, C., Guo, J., Ling, E.A. and Liang, F. (2007). Sirtuin 2, a mammalian homolog of yeast silent information regulator-2 longevity regulator, is an oligodendroglial protein that decelerates cell differentiation through deacetylating alpha-tubulin. <u>J Neurosci</u> **27**(10): 2606-2616.

Li, Z., Takakura, N., Oike, Y., Imanaka, T., Araki, K., Suda, T., Kaname, T., Kondo, T., Abe, K. and Yamamura, K. (2003). Defective smooth muscle development in qkI-deficient mice. <u>Dev Growth Differ</u> **45**(5-6): 449-462.

Li, Z., Zhang, Y., Li, D. and Feng, Y. (2000). Destabilization and mislocalization of myelin basic protein mRNAs in quaking dysmyelination lacking the QKI RNA-binding proteins. J Neurosci **20**(13): 4944-4953.

Li, Z.Z., Kondo, T., Murata, T., Ebersole, T.A., Nishi, T., Tada, K., Ushio, Y., Yamamura, K. and Abe, K. (2002b). Expression of Hqk encoding a KH RNA binding protein is altered in human glioma. Jpn J Cancer Res **93**(2): 167-177.

Lockhart, P.J., O'Farrell, C.A. and Farrer, M.J. (2004). It's a double knock-out! The quaking mouse is a spontaneous deletion of parkin and parkin co-regulated gene (PACRG). Mov Disord **19**(1): 101-104.

Lorenzetti, D., Antalffy, B., Vogel, H., Noveroske, J., Armstrong, D. and Justice, M. (2004a). The neurological mutant quaking(viable) is Parkin deficient. Mamm Genome **15**(3): 210-217.

Lorenzetti, D., Bishop, C.E. and Justice, M.J. (2004b). Deletion of the Parkin coregulated gene causes male sterility in the quaking(viable) mouse mutant. Proc Natl Acad Sci U S A **101**(22): 8402-8407.

Lu, Z., Ku, L., Chen, Y. and Feng, Y. (2005). Developmental abnormalities of myelin basic protein expression in fyn knock-out brain reveal a role of Fyn in posttranscriptional regulation. J Biol Chem **280**(1): 389-395.

Lucitti, J.L., Jones, E.A., Huang, C., Chen, J., Fraser, S.E. and Dickinson, M.E. (2007). Vascular remodeling of the mouse yolk sac requires hemodynamic force. Development **134**(18): 3317-3326.

Lukong, K.E., Larocque, D., Tyner, A.L. and Richard, S. (2005). Tyrosine phosphorylation of sam68 by breast tumor kinase regulates intranuclear localization and cell cycle progression. J Biol Chem **280**(46): 38639-38647.

Lukong, K.E. and Richard, S. (2003). Sam68, the KH domain-containing superSTAR. Biochim Biophys Acta **1653**(2): 73-86.

Luthi-Carter, R., Taylor, D.M., Pallos, J., Lambert, E., Amore, A., Parker, A., Moffitt, H., Smith, D.L., Runne, H., Gokce, O., Kuhn, A., Xiang, Z., Maxwell, M.M., Reeves, S.A., Bates, G.P., Neri, C., Thompson, L.M., Marsh, J.L. and Kazantsev, A.G. (2010). SIRT2 inhibition achieves neuroprotection by decreasing sterol biosynthesis. Proc Natl Acad Sci U S A **107**(17): 7927-7932.

Marcus, J. and Popko, B. (2002). Galactolipids are molecular determinants of myelin development and axo-glial organization. <u>Biochim Biophys Acta</u> **1573**(3): 406-413.

Matsumoto, K., Shiraishi, T., Rikimaru, T., Mimori, Y., Kinoshita, M., Oizumi, K., Kajimura, K. and Kondo, S. (1999). [Resistance against oral antibiotics to Streptococcus pneumoniae isolated from adult respiratory tract infections]. <u>Kansenshogaku Zasshi</u> **73**(12): 1187-1193.

Matsuyama, A., Shimazu, T., Sumida, Y., Saito, A., Yoshimatsu, Y., Seigneurin-Berny, D., Osada, H., Komatsu, Y., Nishino, N., Khochbin, S., Horinouchi, S. and Yoshida, M. (2002). In vivo destabilization of dynamic microtubules by HDAC6-mediated deacetylation. <u>EMBO J</u> **21**(24): 6820-6831.

Matter, N., Herrlich, P. and Konig, H. (2002). Signal-dependent regulation of splicing via phosphorylation of Sam68. <u>Nature</u> **420**(6916): 691-695.

Maxwell, M.M., Tomkinson, E.M., Nobles, J., Wizeman, J.W., Amore, A.M., Quinti, L., Chopra, V., Hersch, S.M. and Kazantsev, A.G. (2011). The Sirtuin 2 microtubule deacetylase is an abundant neuronal protein that accumulates in the aging CNS. <u>Hum Mol Genet</u> **20**(20): 3986-3996.

Messina, V., Meikar, O., Paronetto, M.P., Calabretta, S., Geremia, R., Kotaja, N. and Sette, C. (2012). The RNA binding protein SAM68 transiently localizes in the chromatoid body of male germ cells and influences expression of select microRNAs. <u>PLoS One</u> **7**(6): e39729.

Mic, F.A., Haselbeck, R.J., Cuenca, A.E. and Duester, G. (2002). Novel retinoic acid generating activities in the neural tube and heart identified by conditional rescue of Raldh2 null mutant mice. <u>Development</u> **129**(9): 2271-2282.

Michan, S. and Sinclair, D. (2007). Sirtuins in mammals: insights into their biological function. <u>Biochem J</u> **404**(1): 1-13.

Miskimins, R., Srinivasan, R., Marin-Husstege, M., Miskimins, W.K. and Casaccia-Bonnefil, P. (2002). p27(Kip1) enhances myelin basic protein gene promoter activity. <u>J Neurosci Res</u> **67**(1): 100-105.

Mulholland, P.J., Fiegler, H., Mazzanti, C., Gorman, P., Sasieni, P., Adams, J., Jones, T.A., Babbage, J.W., Vatcheva, R., Ichimura, K., East, P., Poullikas, C., Collins, V.P., Carter, N.P., Tomlinson, I.P. and Sheer, D. (2006). Genomic profiling identifies discrete deletions associated with translocations in glioblastoma multiforme. <u>Cell Cycle</u> **5**(7): 783-791.

Nabel-Rosen, H., Volohonsky, G., Reuveny, A., Zaidel-Bar, R. and Volk, T. (2002). Two isoforms of the Drosophila RNA binding protein, how, act in opposing directions to regulate tendon cell differentiation. Dev Cell **2**(2): 183-193.

Nave, K.A., Lai, C., Bloom, F.E. and Milner, R.J. (1987). Splice site selection in the proteolipid protein (PLP) gene transcript and primary structure of the DM-20 protein of central nervous system myelin. Proc Natl Acad Sci U S A **84**(16): 5665-5669.

Nishiyama, A., Lin, X.H., Giese, N., Heldin, C.H. and Stallcup, W.B. (1996). Co-localization of NG2 proteoglycan and PDGF alpha-receptor on O2A progenitor cells in the developing rat brain. J Neurosci Res **43**(3): 299-314.

North, B.J., Marshall, B.L., Borra, M.T., Denu, J.M. and Verdin, E. (2003). The human Sir2 ortholog, SIRT2, is an NAD+-dependent tubulin deacetylase. Mol Cell **11**(2): 437-444.

Noveroske, J.K., Hardy, R., Dapper, J.D., Vogel, H. and Justice, M.J. (2005). A new ENU-induced allele of mouse quaking causes severe CNS dysmyelination. Mamm Genome **16**(9): 672-682.

Noveroske, J.K., Lai, L., Gaussin, V., Northrop, J.L., Nakamura, H., Hirschi, K.K. and Justice, M.J. (2002). Quaking is essential for blood vessel development. Genesis **32**(3): 218-230.

Osterhout, D.J., Wolven, A., Wolf, R.M., Resh, M.D. and Chao, M.V. (1999). Morphological differentiation of oligodendrocytes requires activation of Fyn tyrosine kinase. J Cell Biol **145**(6): 1209-1218.

Outeiro, T.F., Kontopoulos, E., Altmann, S.M., Kufareva, I., Strathearn, K.E., Amore, A.M., Volk, C.B., Maxwell, M.M., Rochet, J.C., McLean, P.J., Young, A.B., Abagyan, R., Feany, M.B., Hyman, B.T. and Kazantsev, A.G. (2007). Sirtuin 2 inhibitors rescue alpha-synuclein-mediated toxicity in models of Parkinson's disease. Science **317**(5837): 516-519.

Owens, G.C. and Bunge, R.P. (1990). Schwann cells depleted of galactocerebroside express myelin-associated glycoprotein and initiate but do not continue the process of myelination. Glia **3**(2): 118-124.

Pandithage, R., Lilischkis, R., Harting, K., Wolf, A., Jedamzik, B., Luscher-Firzlaff, J., Vervoorts, J., Lasonder, E., Kremmer, E., Knoll, B. and Luscher, B. (2008). The

regulation of SIRT2 function by cyclin-dependent kinases affects cell motility. J Cell Biol **180**(5): 915-929.

Paronetto, M.P., Achsel, T., Massiello, A., Chalfant, C.E. and Sette, C. (2007). The RNA-binding protein Sam68 modulates the alternative splicing of Bcl-x. J Cell Biol **176**(7): 929-939.

Paronetto, M.P., Farini, D., Sammarco, I., Maturo, G., Vespasiani, G., Geremia, R., Rossi, P. and Sette, C. (2004). Expression of a truncated form of the c-Kit tyrosine kinase receptor and activation of Src kinase in human prostatic cancer. Am J Pathol **164**(4): 1243-1251.

Paronetto, M.P., Messina, V., Barchi, M., Geremia, R., Richard, S. and Sette, C. (2011). Sam68 marks the transcriptionally active stages of spermatogenesis and modulates alternative splicing in male germ cells. Nucleic Acids Res **39**(12): 4961-4974.

Paronetto, M.P., Messina, V., Bianchi, E., Barchi, M., Vogel, G., Moretti, C., Palombi, F., Stefanini, M., Geremia, R., Richard, S. and Sette, C. (2009). Sam68 regulates translation of target mRNAs in male germ cells, necessary for mouse spermatogenesis. J Cell Biol **185**(2): 235-249.

Paronetto, M.P., Zalfa, F., Botti, F., Geremia, R., Bagni, C. and Sette, C. (2006). The nuclear RNA-binding protein Sam68 translocates to the cytoplasm and associates with the polysomes in mouse spermatocytes. Mol Biol Cell **17**(1): 14-24.

Pfister, J.A., Ma, C., Morrison, B.E. and D'Mello, S.R. (2008). Opposing effects of sirtuins on neuronal survival: SIRT1-mediated neuroprotection is independent of its deacetylase activity. PLoS One **3**(12): e4090.

Poliak, S., Gollan, L., Salomon, D., Berglund, E.O., Ohara, R., Ranscht, B. and Peles, E. (2001). Localization of Caspr2 in myelinated nerves depends on axon-glia interactions and the generation of barriers along the axon. Journal of Neuroscience **21**(19): 7568-7575.

Raff, M.C., Miller, R.H. and Noble, M. (1983). A glial progenitor cell that develops in vitro into an astrocyte or an oligodendrocyte depending on culture medium. Nature **303**(5916): 390-396.

Rajan, P., Gaughan, L., Dalgliesh, C., El-Sherif, A., Robson, C.N., Leung, H.Y. and Elliott, D.J. (2008a). Regulation of gene expression by the RNA-binding protein Sam68 in cancer. Biochem Soc Trans **36**(Pt 3): 505-507.

Rajan, P., Gaughan, L., Dalgliesh, C., El-Sherif, A., Robson, C.N., Leung, H.Y. and Elliott, D.J. (2008b). The RNA-binding and adaptor protein Sam68 modulates signal-dependent splicing and transcriptional activity of the androgen receptor. J Pathol **215**(1): 67-77.

Ranscht, B., Clapshaw, P.A., Price, J., Noble, M. and Seifert, W. (1982). Development of oligodendrocytes and Schwann cells studied with a monoclonal antibody against galactocerebroside. Proc Natl Acad Sci U S A **79**(8): 2709-2713.

Ranscht, B., Wood, P.M. and Bunge, R.P. (1987). Inhibition of in vitro peripheral myelin formation by monoclonal anti-galactocerebroside. Journal of Neuroscience **7**(9): 2936-2947.

Regis, S., Grossi, S., Corsolini, F., Biancheri, R. and Filocamo, M. (2009). PLP1 gene duplication causes overexpression and alteration of the PLP/DM20 splicing balance in fibroblasts from Pelizaeus-Merzbacher disease patients. Biochim Biophys Acta **1792**(6): 548-554.

Rosenbluth, J., Liu, Z., Guo, D. and Schiff, R. (1994). Inhibition of CNS myelin development in vivo by implantation of anti-GalC hybridoma cells. Journal of Neurocytology **23**(11): 699-707.

Roth, H.J., Hunkeler, M.J. and Campagnoni, A.T. (1985). Expression of myelin basic protein genes in several dysmyelinating mouse mutants during early postnatal brain development. J Neurochem **45**(2): 572-580.

Rybakowski, J.K., Borkowska, A., Skibinska, M. and Hauser, J. (2007). Polymorphisms of the Fyn kinase gene and a performance on the Wisconsin Card Sorting Test in schizophrenia. Psychiatr Genet **17**(3): 201-204.

Ryder, S.P., Frater, L.A., Abramovitz, D.L., Goodwin, E.B. and Williamson, J.R. (2004). RNA target specificity of the STAR/GSG domain post-transcriptional regulatory protein GLD-1. Nat Struct Mol Biol **11**(1): 20-28.

Ryder, S.P. and Williamson, J.R. (2004). Specificity of the STAR/GSG domain protein Qk1: implications for the regulation of myelination. RNA **10**(9): 1449-1458.

Saccomanno, L., Loushin, C., Jan, E., Punkay, E., Artzt, K. and Goodwin, E.B. (1999). The STAR protein QKI-6 is a translational repressor. Proc Natl Acad Sci U S A **96**(22): 12605-12610.

Schaeren-Wiemers, N., Van der Bijl, P. and Schwab, M.E. (1995). The UDP-galactose:ceramide galactosyltransferase: Expression pattern in oligodendrocytes and Schwann cells during myelination and substrate preference for hydroxyceramide. J Neurochem **65**(5): 2267-2278.

Sette, C., Messina, V. and Paronetto, M.P. (2010). Sam68: a new STAR in the male fertility firmament. J Androl **31**(1): 66-74.

Sidman, R.L., Dickie, M.M. and Appel, S.H. (1964). Mutant Mice (Quaking and Jimpy) with Deficient Myelination in the Central Nervous System. Science **144**(3616): 309-311.

Siegel, G., Brady, S., Albers, R.W. and Price, D. (2011). Basic Neurochemistry: Principles of Molecular, Cellular, and Medical Neurobiology, Elsevier Science.

Sorg, B.A., Smith, M.M. and Campagnoni, A.T. (1987). Developmental expression of the myelin proteolipid protein and basic protein mRNAs in normal and dysmyelinating mutant mice. J Neurochem **49**(4): 1146-1154.

Sorg, B.J., Agrawal, D., Agrawal, H.C. and Campagnoni, A.T. (1986). Expression of myelin proteolipid protein and basic protein in normal and dysmyelinating mutant mice. J Neurochem **46**(2): 379-387.

Southwood, C.M., Peppi, M., Dryden, S., Tainsky, M.A. and Gow, A. (2007). Microtubule deacetylases, SirT2 and HDAC6, in the nervous system. Neurochem Res **32**(2): 187-195.

Stariha, R.L. and Kim, S.U. (2001). Mitogen-activated protein kinase signalling in oligodendrocytes: a comparison of primary cultures and CG-4. Int J Dev Neurosci **19**(4): 427-437.

Stecca, B., Southwood, C.M., Gragerov, A., Kelley, K.A., Friedrich, V.L., Jr. and Gow, A. (2000). The evolution of lipophilin genes from invertebrates to tetrapods: DM-20 cannot replace proteolipid protein in CNS myelin. J Neurosci **20**(11): 4002-4010.

Stewart, D.G. and Davis, K.L. (2004). Possible contributions of myelin and oligodendrocyte dysfunction to schizophrenia. Int Rev Neurobiol **59**: 381-424.

Stolt, C.C., Rehberg, S., Ader, M., Lommes, P., Riethmacher, D., Schachner, M., Bartsch, U. and Wegner, M. (2002). Terminal differentiation of myelin-forming oligodendrocytes depends on the transcription factor Sox10. Genes Dev **16**(2): 165-170.

111

Suzuki, K. and Koike, T. (2007). Mammalian Sir2-related protein (SIRT) 2-mediated modulation of resistance to axonal degeneration in slow Wallerian degeneration mice: a crucial role of tubulin deacetylation. Neuroscience **147**(3): 599-612.

Tam, P.P., Gad, J.M., Kinder, S.J., Tsang, T.E. and Behringer, R.R. (2001). Morphogenetic tissue movement and the establishment of body plan during development from blastocyst to gastrula in the mouse. Bioessays **23**(6): 508-517.

Tang, B.L. and Chua, C.E. (2008). SIRT2, tubulin deacetylation, and oligodendroglia differentiation. Cell Motil Cytoskeleton **65**(3): 179-182.

Thomas, J.L., Spassky, N., Perez Villegas, E.M., Olivier, C., Cobos, I., Goujet-Zalc, C., Martinez, S. and Zalc, B. (2000). Spatiotemporal development of oligodendrocytes in the embryonic brain. J Neurosci Res **59**(4): 471-476.

Umemori, H., Sato, S., Yagi, T., Aizawa, S. and Yamamoto, T. (1994). Initial events of myelination involve Fyn tyrosine kinase signalling. Nature **367**(6463): 572-576.

van Mil, A., Grundmann, S., Goumans, M.-J., Lei, Z., Oerlemans, M.I., Jaksani, S., Doevendans, P.A. and Sluijter, J.P.G. (2012). MicroRNA-214 inhibits angiogenesis by targeting Quaking and reducing angiogenic growth factor release. Cardiovascular Research **93**(4): 655-665.

Ventura, J.J., Tenbaum, S., Perdiguero, E., Huth, M., Guerra, C., Barbacid, M., Pasparakis, M. and Nebreda, A.R. (2007). p38alpha MAP kinase is essential in lung stem and progenitor cell proliferation and differentiation. Nat Genet **39**(6): 750-758.

Vernet, C. and Artzt, K. (1997). STAR, a gene family involved in signal transduction and activation of RNA. Trends Genet **13**(12): 479-484.

Volk, T., Israeli, D., Nir, R. and Toledano-Katchalski, H. (2008). Tissue development and RNA control: "HOW" is it coordinated? Trends Genet **24**(2): 94-101.

Wang, E., Dimova, N., Sperle, K., Huang, Z., Lock, L., McCulloch, M.C., Edgar, J.M., Hobson, G.M. and Cambi, F. (2008). Deletion of a splicing enhancer disrupts PLP1/DM20 ratio and myelin stability. Exp Neurol **214**(2): 322-330.

Wang, L.L., Richard, S. and Shaw, A.S. (1995). P62 association with RNA is regulated by tyrosine phosphorylation. J Biol Chem **270**(5): 2010-2013.

Wang, M., Doucette, J.R. and Nazarali, A.J. (2011). Conditional Tet-regulated over-expression of Hoxa2 in CG4 cells increases their proliferation and delays their differentiation into oligodendrocyte-like cells expressing myelin basic protein. Cell Mol Neurobiol **31**(6): 875-886.

Wang, Y., Vogel, G., Yu, Z. and Richard, S. (2013). The QKI-5 and QKI-6 RNA binding proteins regulate the expression of microRNA 7 in glial cells. Mol Cell Biol **33**(6): 1233-1243.

Wei, Q., Miskimins, W.K. and Miskimins, R. (2004). Sox10 acts as a tissue-specific transcription factor enhancing activation of the myelin basic protein gene promoter by p27Kip1 and Sp1. J Neurosci Res **78**(6): 796-802.

Werner, H.B., Kuhlmann, K., Shen, S., Uecker, M., Schardt, A., Dimova, K., Orfaniotou, F., Dhaunchak, A., Brinkmann, B.G., Mobius, W., Guarente, L., Casaccia-Bonnefil, P., Jahn, O. and Nave, K.A. (2007). Proteolipid protein is required for transport of sirtuin 2 into CNS myelin. J Neurosci **27**(29): 7717-7730.

White, R., Gonsior, C., Kramer-Albers, E.M., Stohr, N., Huttelmaier, S. and Trotter, J. (2008). Activation of oligodendroglial Fyn kinase enhances translation of mRNAs transported in hnRNP A2-dependent RNA granules. J Cell Biol **181**(4): 579-586.

Wu, H.Y., Dawson, M.R., Reynolds, R. and Hardy, R.J. (2001). Expression of QKI proteins and MAP1B identifies actively myelinating oligodendrocytes in adult rat brain. Mol Cell Neurosci **17**(2): 292-302.

Wu, J., Zhou, L., Tonissen, K., Tee, R. and Artzt, K. (1999). The quaking I-5 protein (QKI-5) has a novel nuclear localization signal and shuttles between the nucleus and the cytoplasm. J Biol Chem **274**(41): 29202-29210.

Wu, J.I., Reed, R.B., Grabowski, P.J. and Artzt, K. (2002). Function of quaking in myelination: regulation of alternative splicing. Proc Natl Acad Sci U S A **99**(7): 4233-4238.

Yang, G., Fu, H., Zhang, J., Lu, X., Yu, F., Jin, L., Bai, L., Huang, B., Shen, L., Feng, Y., Yao, L. and Lu, Z. (2010). RNA-binding protein quaking, a critical regulator of colon epithelial differentiation and a suppressor of colon cancer. Gastroenterology **138**(1): 231-240 e231-235.

Yin, D., Ogawa, S., Kawamata, N., Tunici, P., Finocchiaro, G., Eoli, M., Ruckert, C., Huynh, T., Liu, G., Kato, M., Sanada, M., Jauch, A., Dugas, M., Black, K.L. and Koeffler, H.P. (2009). High-resolution genomic copy number profiling of

glioblastoma multiforme by single nucleotide polymorphism DNA microarray. Mol Cancer Res **7**(5): 665-677.

Yin, X., Baek, R.C., Kirschner, D.A., Peterson, A., Fujii, Y., Nave, K.A., Macklin, W.B. and Trapp, B.D. (2006). Evolution of a neuroprotective function of central nervous system myelin. J Cell Biol **172**(3): 469-478.

Zagzag, D., Blanco, C., Friedlander, D.R., Miller, D.C. and Newcomb, E.W. (2003). Expression of p27KIP1 in human gliomas: relationship between tumor grade, proliferation index, and patient survival. Hum Pathol **34**(1): 48-53.

Zearfoss, N.R., Clingman, C.C., Farley, B.M., McCoig, L.M. and Ryder, S.P. (2011). Quaking Regulates *Hnrnpa1* Expression through Its 3′ UTR in Oligodendrocyte Precursor Cells. PLoS Genet **7**(1): e1001269.

Zetser, A., Gredinger, E. and Bengal, E. (1999). p38 mitogen-activated protein kinase pathway promotes skeletal muscle differentiation. Participation of the Mef2c transcription factor. J Biol Chem **274**(8): 5193-5200.

Zhang, R., Murakami, S., Coustry, F., Wang, Y. and de Crombrugghe, B. (2006). Constitutive activation of MKK6 in chondrocytes of transgenic mice inhibits proliferation and delays endochondral bone formation. Proc Natl Acad Sci U S A **103**(2): 365-370.

Zhang, Y., Li, N., Caron, C., Matthias, G., Hess, D., Khochbin, S. and Matthias, P. (2003a). HDAC-6 interacts with and deacetylates tubulin and microtubules in vivo. EMBO J **22**(5): 1168-1179.

Zhang, Y., Lu, Z., Ku, L., Chen, Y., Wang, H. and Feng, Y. (2003b). Tyrosine phosphorylation of QKI mediates developmental signals to regulate mRNA metabolism. EMBO J **22**(8): 1801-1810.

Zhao, L., Ku, L., Chen, Y., Xia, M., LoPresti, P. and Feng, Y. (2006a). QKI binds MAP1B mRNA and enhances MAP1B expression during oligodendrocyte development. Mol Biol Cell **17**(10): 4179-4186.

Zhao, L., Mandler, M.D., Yi, H. and Feng, Y. (2010). Quaking I controls a unique cytoplasmic pathway that regulates alternative splicing of myelin-associated glycoprotein. Proc Natl Acad Sci U S A **107**(44): 19061-19066.

Zhao, L., Tian, D., Xia, M., Macklin, W.B. and Feng, Y. (2006b). Rescuing qkV dysmyelination by a single isoform of the selective RNA-binding protein QKI. J Neurosci **26**(44): 11278-11286.

Zhu, H., Zhao, L., Wang, E., Dimova, N., Liu, G., Feng, Y. and Cambi, F. (2012). The QKI-PLP pathway controls SIRT2 abundance in CNS myelin. Glia **60**(1): 69-82.
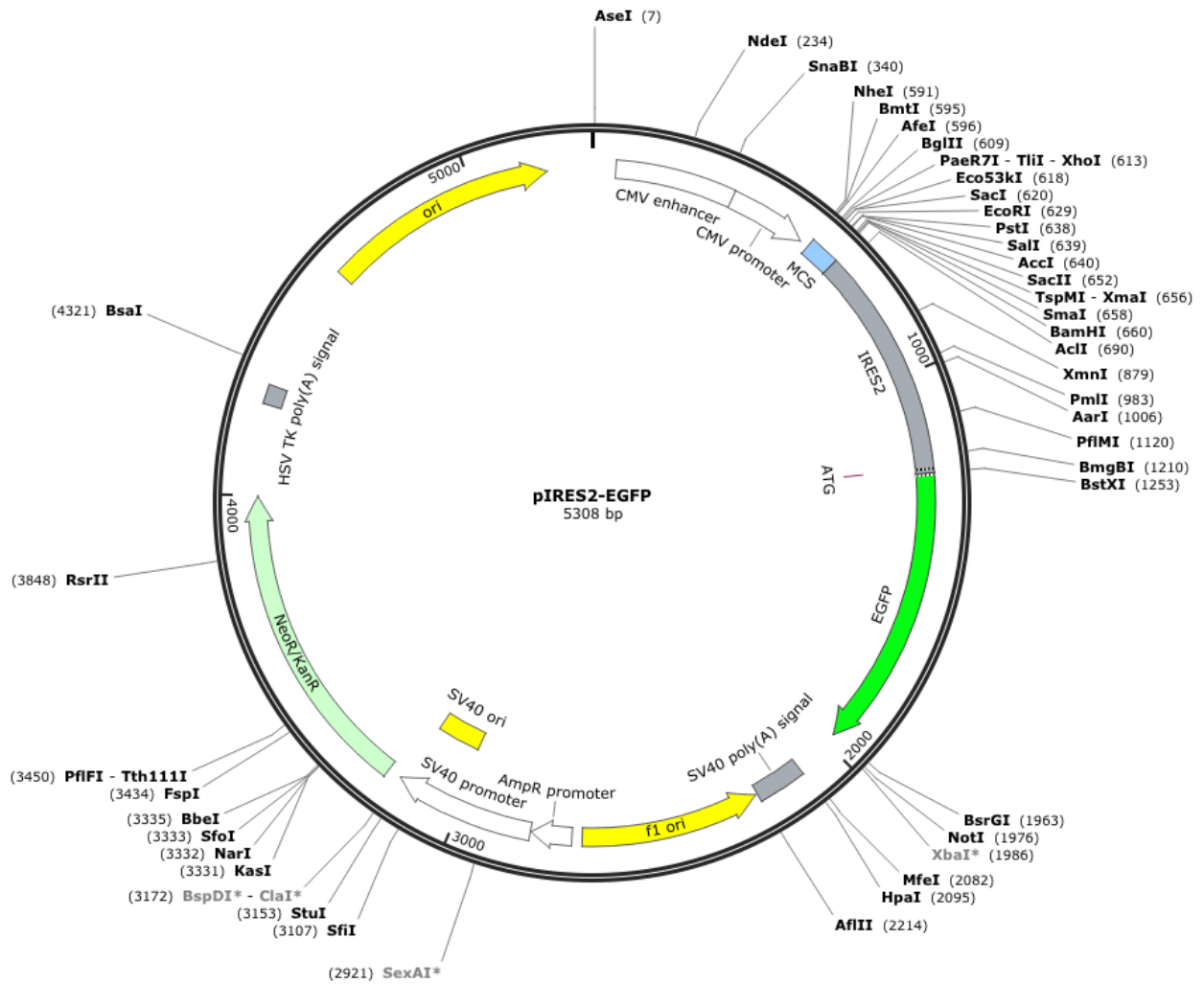
Two way ANOVA test for RT-PCR data of QKI-5 in DM (Figure 6)				
Source of Variation	**% of total variation**	**P value**		
Interaction	1.68	0.0184		
Time	20.22	< 0.0001		
Treatment	74.97	< 0.0001		
Subjects (matching)	1.2409	0.0132		
Source of Variation	**P value summary**	**Significant?**		
Interaction	*	Yes		
Time	***	Yes		
Treatment	***	Yes		
Subjects (matching)	*	Yes		
Source of Variation	**Df**	**Sum-of-squares**	**Mean square**	**F**
Interaction	10	4.582	0.4582	2.666
Time	5	55.22	11.04	64.26
Treatment	2	204.7	102.4	181.2
Subjects (matching)	6	3.389	0.5648	3.287
Residual	30	5.156	0.1719	
Number of missing values	0			

Bonferroni post hoc test				
wildtype vs blank plasmid				
Treatment	wildtype	blank plasmid	Difference	95% CI of diff.
1d	1.070	0.8612	-0.2092	-1.487 to 1.068
2d	1.710	1.181	-0.5284	-1.806 to 0.7492
3d	1.801	1.761	-0.04044	-1.318 to 1.237
4d	2.731	2.611	-0.1200	-1.398 to 1.158
5d	2.898	3.114	0.2158	-1.062 to 1.493
6d	3.105	3.203	0.09829	-1.179 to 1.376
Treatment	Difference	t	P value	Summary
1d	-0.2092	0.5260	P > 0.05	ns
2d	-0.5284	1.328	P > 0.05	ns
3d	-0.04044	0.1017	P > 0.05	ns

Treatment			P value	Summary
4d	-0.1200	0.3018	P > 0.05	ns
5d	0.2158	0.5426	P > 0.05	ns
6d	0.09829	0.2471	P > 0.05	ns

wildtype vs plasmid

Treatment	wildtype	plasmid	Difference	95% CI of diff.
1d	1.070	4.317	3.247	1.969 to 4.524
2d	1.710	5.082	3.372	2.095 to 4.650
3d	1.801	5.628	3.827	2.549 to 5.105
4d	2.731	6.936	4.205	2.927 to 5.483
5d	2.898	7.642	4.744	3.466 to 6.021
6d	3.105	8.197	5.092	3.815 to 6.370

Treatment	Difference	t	P value	Summary
1d	3.247	8.162	P<0.001	***
2d	3.372	8.478	P<0.001	***
3d	3.827	9.621	P<0.001	***
4d	4.205	10.57	P<0.001	***
5d	4.744	11.92	P<0.001	***
6d	5.092	12.80	P<0.001	***

blank plasmid vs plasmid

Treatment	blank plasmid	plasmid	Difference	95% CI of diff.
1d	0.8612	4.317	3.456	2.178 to 4.734
2d	1.181	5.082	3.901	2.623 to 5.178
3d	1.761	5.628	3.867	2.590 to 5.145
4d	2.611	6.936	4.325	3.047 to 5.603
5d	3.114	7.642	4.528	3.250 to 5.805
6d	3.203	8.197	4.994	3.716 to 6.271

Treatment	Difference	t	P value	Summary
1d	3.456	8.688	P<0.001	***
2d	3.901	9.806	P<0.001	***
3d	3.867	9.722	P<0.001	***
4d	4.325	10.87	P<0.001	***
5d	4.528	11.38	P<0.001	***
6d	4.994	12.55	P<0.001	***

Two way ANOVA test for RT-PCR data of QKI-5; siRNA treatment in DM (Figure 7)				
Source of Variation	% of total variation	P value		
Interaction	6.92	0.0005		
Time	16.78	< 0.0001		
Treatment	71.11	< 0.0001		
Subjects (matching)	0.7562	0.5406		
Source of Variation	P value summary	Significant?		
Interaction	***	Yes		
Time	***	Yes		
Treatment	***	Yes		
Subjects (matching)	ns	No		
Source of Variation	Df	Sum-of-squares	Mean square	F
Interaction	10	2.487	0.2487	4.680
Time	5	6.029	1.206	22.69
Treatment	2	25.56	12.78	282.1
Subjects (matching)	6	0.2718	0.04529	0.8521
Residual	30	1.595	0.05315	
Number of missing values	0			

Bonferroni post hoc test				
wildtype vs control siRNA				
Treatment	wildtype	control siRNA	Difference	95% CI of diff.
1d	1.170	1.250	0.08017	-0.5169 to 0.6773
2d	1.509	1.505	-0.003751	-0.6008 to 0.5933
3d	1.734	1.700	-0.03382	-0.6309 to 0.5633
4d	1.931	1.888	-0.04233	-0.6394 to 0.5548
5d	2.167	2.434	0.2671	-0.3300 to 0.8642
6d	2.538	2.706	0.1688	-0.4283 to 0.7658
Treatment	Difference	t	P value	Summary
1d	0.08017	0.4312	P > 0.05	ns
2d	-0.003751	0.02017	P > 0.05	ns
3d	-0.03382	0.1819	P > 0.05	ns
4d	-0.04233	0.2277	P > 0.05	ns
5d	0.2671	1.437	P > 0.05	ns

6d	0.1688	0.9077	P > 0.05	ns
wildtype vs siRNA				
Treatment	wildtype	siRNA	Difference	95% CI of diff.
1d	1.170	0.3564	-0.8137	-1.411 to -0.2167
2d	1.509	0.2398	-1.269	-1.866 to -0.6717
3d	1.734	0.3726	-1.362	-1.959 to -0.7646
4d	1.931	0.6168	-1.314	-1.911 to -0.7170
5d	2.167	0.5957	-1.571	-2.168 to -0.9742
6d	2.538	0.3375	-2.200	-2.797 to -1.603
Treatment	Difference	t	P value	Summary
1d	-0.8137	4.377	P<0.001	***
2d	-1.269	6.825	P<0.001	***
3d	-1.362	7.325	P<0.001	***
4d	-1.314	7.068	P<0.001	***
5d	-1.571	8.452	P<0.001	***
6d	-2.200	11.83	P<0.001	***
control siRNA vs siRNA				
Treatment	control siRNA	siRNA	Difference	95% CI of diff.
1d	1.250	0.3564	-0.8939	-1.491 to -0.2968
2d	1.505	0.2398	-1.265	-1.862 to -0.6680
3d	1.700	0.3726	-1.328	-1.925 to -0.7308
4d	1.888	0.6168	-1.272	-1.869 to -0.6746
5d	2.434	0.5957	-1.838	-2.435 to -1.241
6d	2.706	0.3375	-2.369	-2.966 to -1.772
Treatment	Difference	t	P value	Summary
1d	-0.8939	4.808	P<0.001	***
2d	-1.265	6.805	P<0.001	***
3d	-1.328	7.143	P<0.001	***
4d	-1.272	6.841	P<0.001	***
5d	-1.838	9.888	P<0.001	***
6d	-2.369	12.74	P<0.001	***

Two way ANOVA test for RT-PCR data of QKI-6 in DM (Figure 6)				
Source of Variation	**% of total variation**	**P value**		
Interaction	3.65	0.2611		
Time	84.07	< 0.0001		
Treatment	1.37	0.2882		
Subjects (matching)	2.6733	0.1754		
Source of Variation	**P value summary**	**Significant?**		
Interaction	ns	No		
Time	***	Yes		
Treatment	ns	No		
Subjects (matching)	ns	No		
Source of Variation	**Df**	**Sum-of-squares**	**Mean square**	**F**
Interaction	10	0.3081	0.03081	1.328
Time	5	7.106	1.421	61.23
Treatment	2	0.1161	0.05806	1.542
Subjects (matching)	6	0.2259	0.03766	1.623
Residual	30	0.6963	0.02321	
Number of missing values	0			

Bonferroni post hoc test				
wildtype vs blank plasmid				
Treatment	wildtype	blank plasmid	Difference	95% CI of diff.
1d	1.000	0.9646	-0.03540	-0.4551 to 0.3843
2d	1.101	1.149	0.04787	-0.3719 to 0.4676
3d	1.024	1.198	0.1735	-0.2462 to 0.5933
4d	1.365	1.620	0.2554	-0.1643 to 0.6751
5d	1.507	1.526	0.01877	-0.4010 to 0.4385
6d	1.913	1.977	0.06414	-0.3556 to 0.4839
Treatment	Difference	t	P value	Summary
1d	-0.03540	0.2709	P > 0.05	ns
2d	0.04787	0.3663	P > 0.05	ns
3d	0.1735	1.328	P > 0.05	ns
4d	0.2554	1.954	P > 0.05	ns
5d	0.01877	0.1436	P > 0.05	ns

6d	0.06414	0.4908	P > 0.05	ns

wildtype vs plasmid				
Treatment	wildtype	plasmid	Difference	95% CI of diff.
1d	1.000	0.9489	-0.05107	-0.4708 to 0.3686
2d	1.101	1.005	-0.09597	-0.5157 to 0.3238
3d	1.024	1.143	0.1191	-0.3006 to 0.5389
4d	1.365	1.510	0.1446	-0.2752 to 0.5643
5d	1.507	1.789	0.2819	-0.1379 to 0.7016
6d	1.913	2.154	0.2408	-0.1790 to 0.6605
Treatment	Difference	t	P value	Summary
1d	-0.05107	0.3908	P > 0.05	ns
2d	-0.09597	0.7344	P > 0.05	ns
3d	0.1191	0.9116	P > 0.05	ns
4d	0.1446	1.106	P > 0.05	ns
5d	0.2819	2.157	P > 0.05	ns
6d	0.2408	1.842	P > 0.05	ns
blank plasmid vs plasmid				
Treatment	blank plasmid	plasmid	Difference	95% CI of diff.
1d	0.9646	0.9489	-0.01568	-0.4354 to 0.4040
2d	1.149	1.005	-0.1438	-0.5636 to 0.2759
3d	1.198	1.143	-0.05440	-0.4741 to 0.3653
4d	1.620	1.510	-0.1108	-0.5305 to 0.3089
5d	1.526	1.789	0.2631	-0.1566 to 0.6828
6d	1.977	2.154	0.1766	-0.2431 to 0.5963
Treatment	Difference	t	P value	Summary
1d	-0.01568	0.1200	P > 0.05	ns
2d	-0.1438	1.101	P > 0.05	ns
3d	-0.05440	0.4163	P > 0.05	ns
4d	-0.1108	0.8480	P > 0.05	ns
5d	0.2631	2.013	P > 0.05	ns
6d	0.1766	1.352	P > 0.05	ns

Two way ANOVA test for RT-PCR data of QKI-6; siRNA treatment in DM (Figure 7)				
Source of Variation	**% of total variation**	**P value**		
Interaction	2.87	0.6654		
Time	84.33	< 0.0001		

Treatment	0.18	0.6639		
Subjects (matching)	1.2574	0.7632		
Source of Variation	**P value summary**	**Significant?**		
Interaction	ns	No		
Time	***	Yes		
Treatment	ns	No		
Subjects (matching)	ns	No		
Source of Variation	**Df**	**Sum-of-squares**	**Mean square**	**F**
Interaction	10	0.1778	0.01778	0.7591
Time	5	5.220	1.044	44.57
Treatment	2	0.01139	0.005693	0.4389
Subjects (matching)	6	0.07783	0.01297	0.5538
Residual	30	0.7027	0.02342	
Number of missing values	0			

Bonferroni post hoc test				
wildtype vs control				
Treatment	wildtype	control	Difference	95% CI of diff.
1d	1.000	1.076	0.07637	-0.3098 to 0.4625
2d	1.101	1.014	-0.08754	-0.4737 to 0.2986
3d	1.143	1.152	0.008790	-0.3774 to 0.3949
4d	1.484	1.592	0.1083	-0.2778 to 0.4945
5d	1.531	1.472	-0.05903	-0.4452 to 0.3271
6d	1.771	1.842	0.07150	-0.3146 to 0.4576
Treatment	Difference	t	P value	Summary
1d	0.07637	0.6352	P > 0.05	ns
2d	-0.08754	0.7281	P > 0.05	ns
3d	0.008790	0.07311	P > 0.05	ns
4d	0.1083	0.9010	P > 0.05	ns
5d	-0.05903	0.4910	P > 0.05	ns
6d	0.07150	0.5947	P > 0.05	ns
wildtype vs siRNA				
Treatment	wildtype	siRNA	Difference	95% CI of diff.
1d	1.000	0.9607	-0.03932	-0.4255 to 0.3468
2d	1.101	1.026	-0.07542	-0.4616 to 0.3107
3d	1.143	0.9444	-0.1986	-0.5847 to 0.1875
4d	1.484	1.500	0.01627	-0.3699 to 0.4024

5d	1.531	1.611	0.07994	-0.3062 to 0.4661
6d	1.771	1.893	0.1226	-0.2636 to 0.5087
Treatment	Difference	t	P value	Summary
1d	-0.03932	0.3270	P > 0.05	ns
2d	-0.07542	0.6273	P > 0.05	ns
3d	-0.1986	1.652	P > 0.05	ns
4d	0.01627	0.1353	P > 0.05	ns
5d	0.07994	0.6649	P > 0.05	ns
6d	0.1226	1.020	P > 0.05	ns
control vs siRNA				
Treatment	control	siRNA	Difference	95% CI of diff.
1d	1.076	0.9607	-0.1157	-0.5018 to 0.2705
2d	1.014	1.026	0.01212	-0.3740 to 0.3983
3d	1.152	0.9444	-0.2074	-0.5935 to 0.1788
4d	1.592	1.500	-0.09205	-0.4782 to 0.2941
5d	1.472	1.611	0.1390	-0.2472 to 0.5251
6d	1.842	1.893	0.05107	-0.3351 to 0.4372
Treatment	Difference	t	P value	Summary
1d	-0.1157	0.9623	P > 0.05	ns
2d	0.01212	0.1008	P > 0.05	ns
3d	-0.2074	1.725	P > 0.05	ns
4d	-0.09205	0.7657	P > 0.05	ns
5d	0.1390	1.156	P > 0.05	ns
6d	0.05107	0.4248	P > 0.05	ns

Two way ANOVA test for RT-PCR data of QKI-7 in DM (Figure 6)				
Source of Variation	**% of total variation**	**P value**		
Interaction	15.49	0.4739		
Time	9.13	0.3489		
Treatment	1.37	0.8623		
Subjects (matching)	27.0410	0.0246		
Source of Variation	**P value summary**	**Significant?**		
Interaction	ns	No		
Time	ns	No		
Treatment	ns	No		
Subjects (matching)	*	Yes		
Source of Variation	**Df**	**Sum-of-squares**	**Mean square**	**F**
Interaction	10	0.3541	0.03541	0.9888
Time	5	0.2087	0.04174	1.166
Treatment	2	0.03130	0.01565	0.1519
Subjects (matching)	6	0.6183	0.1031	2.878
Residual	30	1.074	0.03581	
Number of missing values	0			

Bonferroni post hoc test				
wildtype vs blank plasmid				
Treatment	wildtype	blank plasmid	Difference	95% CI of diff.
1d	1.000	0.8430	-0.1570	-0.6987 to 0.3847
2d	0.8751	1.026	0.1505	-0.3912 to 0.6922
3d	1.002	0.9320	-0.06964	-0.6114 to 0.4721
4d	0.9830	1.213	0.2298	-0.3119 to 0.7716
5d	0.9225	0.9083	-0.01419	-0.5559 to 0.5275
6d	0.9901	1.191	0.2005	-0.3412 to 0.7423
Treatment	Difference	t	P value	Summary
1d	-0.1570	0.8869	P > 0.05	ns
2d	0.1505	0.8500	P > 0.05	ns
3d	-0.06964	0.3934	P > 0.05	ns
4d	0.2298	1.298	P > 0.05	ns
5d	-0.01419	0.08015	P > 0.05	ns
6d	0.2005	1.133	P > 0.05	ns

wildtype vs plasmid				
Treatment	wildtype	plasmid	Difference	95% CI of diff.
1d	1.000	1.097	0.09709	-0.4446 to 0.6388
2d	0.8751	1.103	0.2274	-0.3143 to 0.7691
3d	1.002	0.8934	-0.1083	-0.6500 to 0.4334
4d	0.9830	0.9445	-0.03846	-0.5802 to 0.5033
5d	0.9225	0.8898	-0.03267	-0.5744 to 0.5091
6d	0.9901	1.100	0.1098	-0.4319 to 0.6515
Treatment	Difference	t	P value	Summary
1d	0.09709	0.5484	P > 0.05	ns
2d	0.2274	1.284	P > 0.05	ns
3d	-0.1083	0.6117	P > 0.05	ns
4d	-0.03846	0.2172	P > 0.05	ns
5d	-0.03267	0.1845	P > 0.05	ns
6d	0.1098	0.6201	P > 0.05	ns

Two way ANOVA test for RT-PCR data of QKI-7; siRNA treatment in DM (Figure 7)				
Source of Variation	**% of total variation**	**P value**		
Interaction	2.79	0.9880		
Time	8.56	0.2139		
Treatment	3.85	0.8038		
Subjects (matching)	50.9816	< 0.0001		
Source of Variation	**P value summary**	**Significant?**		
Interaction	ns	No		
Time	ns	No		
Treatment	ns	No		
Subjects (matching)	***	Yes		
Source of Variation	**Df**	**Sum-of-squares**	**Mean square**	**F**
Interaction	10	0.1197	0.01197	0.2471
Time	5	0.3678	0.07356	1.518
Treatment	2	0.1654	0.08270	0.2265
Subjects (matching)	6	2.191	0.3651	7.536
Residual	30	1.454	0.04845	
Number of missing values	0			

Bonferroni post hoc test				
wildtype vs blank plasmid				
Treatment	wildtype	blank plasmid	Difference	95% CI of diff.
1d	1.000	0.8217	-0.1783	-0.9732 to 0.6166
2d	0.9855	0.9264	-0.05908	-0.8540 to 0.7358
3d	1.128	0.9710	-0.1571	-0.9520 to 0.6378
4d	1.065	1.055	-0.009672	-0.8046 to 0.7852
5d	0.9548	0.7803	-0.1745	-0.9694 to 0.6204
6d	1.052	1.008	-0.04416	-0.8391 to 0.7507
Treatment	Difference	t	P value	Summary
1d	-0.1783	0.6863	P > 0.05	ns
2d	-0.05908	0.2274	P > 0.05	ns
3d	-0.1571	0.6046	P > 0.05	ns
4d	-0.009672	0.03723	P > 0.05	ns
5d	-0.1745	0.6718	P > 0.05	ns
6d	-0.04416	0.1700	P > 0.05	ns
wildtype vs plasmid				
Treatment	wildtype	plasmid	Difference	95% CI of diff.
1d	1.000	0.7492	-0.2508	-1.046 to 0.5441
2d	0.9855	0.7904	-0.1951	-0.9900 to 0.5998
3d	1.128	0.9708	-0.1573	-0.9522 to 0.6376
4d	1.065	0.9666	-0.09840	-0.8933 to 0.6965
5d	0.9548	0.8482	-0.1066	-0.9015 to 0.6883
6d	1.052	1.096	0.04373	-0.7512 to 0.8386
Treatment	Difference	t	P value	Summary
1d	-0.2508	0.9656	P > 0.05	ns
2d	-0.1951	0.7511	P > 0.05	ns
3d	-0.1573	0.6054	P > 0.05	ns
4d	-0.09840	0.3788	P > 0.05	ns
5d	-0.1066	0.4103	P > 0.05	ns
6d	0.04373	0.1683	P > 0.05	ns

Two way ANOVA test for RT-PCR data of *Plp* in DM (Figure 8)				
Source of Variation	**% of total variation**	**P value**		
Interaction	17.32	< 0.0001		
Time	12.72	< 0.0001		
Treatment	65.97	< 0.0001		
Subjects (matching)	2.0132	0.0010		
Source of Variation	**P value summary**	**Significant?**		
Interaction	***	Yes		
Time	***	Yes		
Treatment	***	Yes		
Subjects (matching)	**	Yes		
Source of Variation	**Df**	**Sum-of-squares**	**Mean square**	**F**
Interaction	10	17.95	1.795	26.30
Time	5	13.18	2.636	38.61
Treatment	2	68.37	34.18	98.31
Subjects (matching)	6	2.086	0.3477	5.094
Residual	30	2.048	0.06826	
Number of missing values	0			

Bonferroni post hoc test				
wildtype vs blank plasmid				
Treatment	wildtype	blank plasmid	Difference	95% CI of diff.
1d	1.000	0.8101	-0.1899	-1.079 to 0.6988
2d	1.097	1.249	0.1511	-0.7376 to 1.040
3d	1.125	1.141	0.01589	-0.8728 to 0.9046
4d	1.093	1.294	0.2002	-0.6885 to 1.089
5d	1.130	1.523	0.3934	-0.4953 to 1.282
6d	0.9670	1.461	0.4939	-0.3948 to 1.383
Treatment	Difference	t	P value	Summary
1d	-0.1899	0.6863	P > 0.05	ns
2d	0.1511	0.5460	P > 0.05	ns
3d	0.01589	0.05744	P > 0.05	ns
4d	0.2002	0.7236	P > 0.05	ns
5d	0.3934	1.422	P > 0.05	ns
6d	0.4939	1.785	P > 0.05	ns

wildtype vs plasmid				
Treatment	wildtype	plasmid	Difference	95% CI of diff.
1d	1.000	2.283	1.283	0.3939 to 2.171
2d	1.097	2.479	1.381	0.4928 to 2.270
3d	1.125	2.669	1.544	0.6550 to 2.432
4d	1.093	3.162	2.068	1.180 to 2.957
5d	1.130	5.144	4.014	3.126 to 4.903
6d	0.9670	5.501	4.534	3.645 to 5.423
Treatment	Difference	t	P value	Summary
1d	1.283	4.635	P<0.001	***
2d	1.381	4.993	P<0.001	***
3d	1.544	5.579	P<0.001	***
4d	2.068	7.475	P<0.001	***
5d	4.014	14.51	P<0.001	***
6d	4.534	16.39	P<0.001	***
blank plasmid vs plasmid				
Treatment	blank plasmid	plasmid	Difference	95% CI of diff.
1d	0.8101	2.283	1.472	0.5838 to 2.361
2d	1.249	2.479	1.230	0.3417 to 2.119
3d	1.141	2.669	1.528	0.6391 to 2.416
4d	1.294	3.162	1.868	0.9794 to 2.757
5d	1.523	5.144	3.621	2.732 to 4.510
6d	1.461	5.501	4.040	3.151 to 4.929
Treatment	Difference	t	P value	Summary
1d	1.472	5.322	P<0.001	***
2d	1.230	4.447	P<0.001	***
3d	1.528	5.522	P<0.001	***
4d	1.868	6.752	P<0.001	***
5d	3.621	13.09	P<0.001	***
6d	4.040	14.60	P<0.001	***

Two way ANOVA test for RT-PCR data of *Plp*; siRNA treatment in DM (Figure 9)				
Source of Variation	% of total variation	P value		
Interaction	12.15	0.7458		
Time	10.34	0.3639		
Treatment	5.42	0.4434		
Subjects (matching)	17.3976	0.1843		
Source of Variation	P value summary	Significant?		

Source of Variation				
Interaction	ns	No		
Time	ns	No		
Treatment	ns	No		
Subjects (matching)	ns	No		
Source of Variation	**Df**	**Sum-of-squares**	**Mean square**	**F**
Interaction	10	0.4163	0.04163	0.6663
Time	5	0.3544	0.07088	1.134
Treatment	2	0.1856	0.09281	0.9341
Subjects (matching)	6	0.5962	0.09936	1.590
Residual	30	1.874	0.06248	
Number of missing values	0			

Bonferroni post hoc test				
wildtype vs control siRNA				
Treatment	wildtype	control siRNA	Difference	95% CI of diff.
1d	1.000	0.8027	-0.1973	-0.8843 to 0.4897
2d	1.097	1.089	-0.008462	-0.6954 to 0.6785
3d	1.125	1.289	0.1639	-0.5231 to 0.8509
4d	1.093	1.371	0.2778	-0.4092 to 0.9648
5d	1.130	1.311	0.1814	-0.5056 to 0.8684
6d	0.9670	1.184	0.2171	-0.4698 to 0.9041
Treatment	Difference	t	P value	Summary
1d	-0.1973	0.9225	P > 0.05	ns
2d	-0.008462	0.03956	P > 0.05	ns
3d	0.1639	0.7662	P > 0.05	ns
4d	0.2778	1.299	P > 0.05	ns
5d	0.1814	0.8482	P > 0.05	ns
6d	0.2171	1.015	P > 0.05	ns
wildtype vs siRNA				
Treatment	wildtype	siRNA	Difference	95% CI of diff.
1d	1.000	1.165	0.1652	-0.5218 to 0.8522
2d	1.097	1.240	0.1423	-0.5447 to 0.8293
3d	1.125	1.297	0.1717	-0.5153 to 0.8587
4d	1.093	1.144	0.05057	-0.6364 to 0.7375
5d	1.130	1.161	0.03158	-0.6554 to 0.7186
6d	0.9670	1.228	0.2608	-0.4262 to 0.9478
Treatment	Difference	t	P value	Summary

1d	0.1652	0.7724	P > 0.05	ns
2d	0.1423	0.6653	P > 0.05	ns
3d	0.1717	0.8028	P > 0.05	ns
4d	0.05057	0.2364	P > 0.05	ns
5d	0.03158	0.1476	P > 0.05	ns
6d	0.2608	1.219	P > 0.05	ns
control siRNA vs siRNA				
Treatment	control siRNA	siRNA	Difference	95% CI of diff.
1d	0.8027	1.165	0.3625	-0.3244 to 1.050
2d	1.089	1.240	0.1508	-0.5362 to 0.8377
3d	1.289	1.297	0.007843	-0.6791 to 0.6948
4d	1.371	1.144	-0.2272	-0.9142 to 0.4597
5d	1.311	1.161	-0.1498	-0.8368 to 0.5371
6d	1.184	1.228	0.04365	-0.6433 to 0.7306
Treatment	Difference	t	P value	Summary
1d	0.3625	1.695	P > 0.05	ns
2d	0.1508	0.7049	P > 0.05	ns
3d	0.007843	0.03667	P > 0.05	ns
4d	-0.2272	1.062	P > 0.05	ns
5d	-0.1498	0.7006	P > 0.05	ns
6d	0.04365	0.2041	P > 0.05	ns

TWO WAY ANOVA TEST FOR RT-PCR DATA OF SIRT2 IN DM (Figure 8)				
Source of Variation	**% of total variation**	**P value**		
Interaction	31.67	< 0.0001		
Time	20.51	< 0.0001		
Treatment	42.72	0.0003		
Subjects (matching)	3.0652	< 0.0001		
Source of Variation	**P value summary**	**Significant?**		
Interaction	***	Yes		
Time	***	Yes		
Treatment	***	Yes		
Subjects (matching)	***	Yes		
Source of Variation	**Df**	**Sum-of-squares**	**Mean square**	**F**
Interaction	10	38.81	3.881	46.67
Time	5	25.14	5.029	60.47
Treatment	2	52.36	26.18	41.81
Subjects (matching)	6	3.757	0.6262	7.530
Residual	30	2.495	0.08316	
Number of missing values	0			

Bonferroni post hoc test				
wildtype vs blank plasmid				
Treatment	wildtype	blank plasmid	Difference	95% CI of diff.
1d	1.000	1.089	0.08899	-1.004 to 1.182
2d	1.103	0.9616	-0.1412	-1.234 to 0.9516
3d	0.9746	1.314	0.3393	-0.7535 to 1.432
4d	1.377	1.310	-0.06739	-1.160 to 1.025
5d	1.219	1.421	0.2024	-0.8904 to 1.295
6d	1.162	1.191	0.02943	-1.063 to 1.122
Treatment	Difference	t	P value	Summary
1d	0.08899	0.2615	P > 0.05	ns
2d	-0.1412	0.4150	P > 0.05	ns
3d	0.3393	0.9973	P > 0.05	ns
4d	-0.06739	0.1981	P > 0.05	ns
5d	0.2024	0.5949	P > 0.05	ns
6d	0.02943	0.08648	P > 0.05	ns

wildtype vs plasmid				
Treatment	wildtype	plasmid	Difference	95% CI of diff.
1d	1.000	1.318	0.3175	-0.7753 to 1.410
2d	1.103	1.652	0.5489	-0.5439 to 1.642
3d	0.9746	1.862	0.8875	-0.2053 to 1.980
4d	1.377	3.225	1.848	0.7555 to 2.941
5d	1.219	6.077	4.859	3.766 to 5.951
6d	1.162	5.454	4.292	3.200 to 5.385
Treatment	Difference	t	P value	Summary
1d	0.3175	0.9332	P > 0.05	ns
2d	0.5489	1.613	P > 0.05	ns
3d	0.8875	2.608	P > 0.05	ns
4d	1.848	5.432	P<0.001	***
5d	4.859	14.28	P<0.001	***
6d	4.292	12.61	P<0.001	***
blank plasmid vs plasmid				
Treatment	blank plasmid	plasmid	Difference	95% CI of diff.
1d	1.089	1.318	0.2285	-0.8643 to 1.321
2d	0.9616	1.652	0.6901	-0.4027 to 1.783
3d	1.314	1.862	0.5482	-0.5447 to 1.641
4d	1.310	3.225	1.916	0.8229 to 3.009
5d	1.421	6.077	4.656	3.563 to 5.749
6d	1.191	5.454	4.263	3.170 to 5.356
Treatment	Difference	t	P value	Summary
1d	0.2285	0.6716	P > 0.05	ns
2d	0.6901	2.028	P > 0.05	ns
3d	0.5482	1.611	P > 0.05	ns
4d	1.916	5.630	P<0.001	***
5d	4.656	13.68	P<0.001	***
6d	4.263	12.53	P<0.001	***

TWO WAY ANOVA TEST FOR RT-PCR DATA OF SIRT2; SIRNA TREATMENT IN DM (Figure 9)				
Source of Variation	% of total variation	P value		
Interaction	9.21	0.6779		
Time	21.25	0.0142		
Treatment	3.64	0.6998		
Subjects (matching)	28.7990	0.0055		
Source of Variation	P value summary	Significant?		

Interaction	ns	No		
Time	*	Yes		
Treatment	ns	No		
Subjects (matching)	**	Yes		
Source of Variation	**Df**	**Sum-of-squares**	**Mean square**	**F**
Interaction	10	0.06048	0.006048	0.7447
Time	5	0.1395	0.02790	3.436
Treatment	2	0.02389	0.01195	0.3791
Subjects (matching)	6	0.1891	0.03152	3.881
Residual	30	0.2436	0.008121	
Number of missing values	0			

Bonferroni post hoc test				
wildtype vs control siRNA				
Treatment	wildtype	control siRNA	Difference	95% CI of diff.
1d	1.033	1.053	0.01993	-0.2676 to 0.3074
2d	0.9925	1.176	0.1834	-0.1041 to 0.4709
3d	1.023	1.060	0.03712	-0.2504 to 0.3246
4d	1.171	1.125	-0.04609	-0.3336 to 0.2414
5d	1.138	1.146	0.008346	-0.2792 to 0.2959
6d	1.100	1.157	0.05633	-0.2312 to 0.3438
Treatment	Difference	t	P value	Summary
1d	0.01993	0.2226	P > 0.05	ns
2d	0.1834	2.049	P > 0.05	ns
3d	0.03712	0.4147	P > 0.05	ns
4d	-0.04609	0.5149	P > 0.05	ns
5d	0.008346	0.09323	P > 0.05	ns
6d	0.05633	0.6292	P > 0.05	ns
wildtype vs siRNA				
Treatment	wildtype	siRNA	Difference	95% CI of diff.
1d	1.033	1.020	-0.01350	-0.3010 to 0.2740
2d	0.9925	1.076	0.08309	-0.2044 to 0.3706
3d	1.023	0.9569	-0.06632	-0.3538 to 0.2212
4d	1.171	1.140	-0.03067	-0.3182 to 0.2568
5d	1.138	1.089	-0.04833	-0.3358 to 0.2392
6d	1.100	1.160	0.05912	-0.2284 to 0.3466
Treatment	Difference	t	P value	Summary

1d	-0.01350	0.1508	P > 0.05	ns
2d	0.08309	0.9282	P > 0.05	ns
3d	-0.06632	0.7408	P > 0.05	ns
4d	-0.03067	0.3426	P > 0.05	ns
5d	-0.04833	0.5399	P > 0.05	ns
6d	0.05912	0.6604	P > 0.05	ns
control siRNA vs siRNA				
Treatment	control siRNA	siRNA	Difference	95% CI of diff.
1d	1.053	1.020	-0.03343	-0.3209 to 0.2541
2d	1.176	1.076	-0.1003	-0.3878 to 0.1872
3d	1.060	0.9569	-0.1034	-0.3909 to 0.1841
4d	1.125	1.140	0.01542	-0.2721 to 0.3029
5d	1.146	1.089	-0.05668	-0.3442 to 0.2308
6d	1.157	1.160	0.002790	-0.2847 to 0.2903
Treatment	Difference	t	P value	Summary
1d	-0.03343	0.3735	P > 0.05	ns
2d	-0.1003	1.121	P > 0.05	ns
3d	-0.1034	1.156	P > 0.05	ns
4d	0.01542	0.1723	P > 0.05	ns
5d	-0.05668	0.6331	P > 0.05	ns
6d	0.002790	0.03117	P > 0.05	ns

Two way ANOVA test for Western Blot data of QKI-5 in DM (Figure 10)				
Source of Variation	**% of total variation**	**P value**		
Interaction	8.68	< 0.0001		
Time	10.09	< 0.0001		
Treatment	76.04	< 0.0001		
Subjects (matching)	1.3070	0.1594		
Source of Variation	**P value summary**	**Significant?**		
Interaction	***	Yes		
Time	***	Yes		
Treatment	***	Yes		
Subjects (matching)	ns	No		
Source of Variation	**Df**	**Sum-of-squares**	**Mean square**	**F**
Interaction	10	2.788	0.2788	6.710
Time	5	3.242	0.6485	15.61
Treatment	2	24.43	12.21	174.5
Subjects (matching)	6	0.4198	0.06997	1.684
Residual	30	1.247	0.04155	
Number of missing values	0			

Bonferroni post hoc test				
wildtype vs blank plasmid				
Treatment	wildtype	blank plasmid	Difference	95% CI of diff.
1d	1.000	0.9262	-0.07383	-0.6380 to 0.4904
2d	0.9759	1.005	0.02868	-0.5355 to 0.5929
3d	1.058	1.212	0.1543	-0.4099 to 0.7185
4d	0.9553	1.316	0.3608	-0.2034 to 0.9250
5d	1.168	1.134	-0.03378	-0.5980 to 0.5304
6d	1.344	1.131	-0.2137	-0.7779 to 0.3505
Treatment	Difference	t	P value	Summary
1d	-0.07383	0.4203	P > 0.05	ns
2d	0.02868	0.1633	P > 0.05	ns
3d	0.1543	0.8784	P > 0.05	ns
4d	0.3608	2.054	P > 0.05	ns
5d	-0.03378	0.1923	P > 0.05	ns
6d	-0.2137	1.217	P > 0.05	ns

wildtype vs plasmid				
Treatment	wildtype	plasmid	Difference	95% CI of diff.
1d	1.000	1.667	0.6671	0.1029 to 1.231
2d	0.9759	2.034	1.058	0.4934 to 1.622
3d	1.058	2.604	1.546	0.9817 to 2.110
4d	0.9553	2.571	1.616	1.052 to 2.180
5d	1.168	3.006	1.838	1.273 to 2.402
6d	1.344	3.289	1.945	1.381 to 2.509

Treatment	Difference	t	P value	Summary
1d	0.6671	3.797	P<0.01	**
2d	1.058	6.020	P<0.001	***
3d	1.546	8.800	P<0.001	***
4d	1.616	9.199	P<0.001	***
5d	1.838	10.46	P<0.001	***
6d	1.945	11.07	P<0.001	***

blank plasmid vs plasmid				
Treatment	blank plasmid	plasmid	Difference	95% CI of diff.
1d	0.9262	1.667	0.7409	0.1767 to 1.305
2d	1.005	2.034	1.029	0.4647 to 1.593
3d	1.212	2.604	1.392	0.8274 to 1.956
4d	1.316	2.571	1.255	0.6909 to 1.819
5d	1.134	3.006	1.871	1.307 to 2.436
6d	1.131	3.289	2.159	1.595 to 2.723

Treatment	Difference	t	P value	Summary
1d	0.7409	4.218	P<0.001	***
2d	1.029	5.857	P<0.001	***
3d	1.392	7.921	P<0.001	***
4d	1.255	7.145	P<0.001	***
5d	1.871	10.65	P<0.001	***
6d	2.159	12.29	P<0.001	***

Two way ANOVA test for Western Blot data of QKI-5; siRNA treatment in DM (Figure 11)				
Source of Variation	**% of total variation**	**P value**		
Interaction	2.69	0.4281		
Time	1.66	0.2915		
Treatment	82.52	0.0002		
Subjects (matching)	5.4421	0.0091		

Source of Variation	P value summary	Significant?		
Interaction	ns	No		
Time	ns	No		
Treatment	***	Yes		
Subjects (matching)	**	Yes		
Source of Variation	Df	Sum-of-squares	Mean square	F
Interaction	10	0.1360	0.01360	1.050
Time	5	0.08398	0.01680	1.297
Treatment	2	4.170	2.085	45.49
Subjects (matching)	6	0.2750	0.04584	3.539
Residual	30	0.3885	0.01295	
Number of missing values	0			

Bonferroni post hoc test				
wildtype vs control siRNA				
Treatment	wildtype	control siRNA	Difference	95% CI of diff.
1d	1.067	1.174	0.1069	-0.2492 to 0.4629
2d	1.073	1.194	0.1210	-0.2351 to 0.4770
3d	1.158	1.112	-0.04627	-0.4023 to 0.3098
4d	1.022	1.135	0.1127	-0.2433 to 0.4688
5d	1.101	1.205	0.1039	-0.2522 to 0.4599
6d	1.278	1.270	-0.007775	-0.3638 to 0.3483
Treatment	Difference	t	P value	Summary
1d	0.1069	0.9640	P > 0.05	ns
2d	0.1210	1.091	P > 0.05	ns
3d	-0.04627	0.4174	P > 0.05	ns
4d	0.1127	1.017	P > 0.05	ns
5d	0.1039	0.9371	P > 0.05	ns
6d	-0.007775	0.07013	P > 0.05	ns
wildtype vs siRNA				
Treatment	wildtype	siRNA	Difference	95% CI of diff.
1d	1.067	0.5677	-0.4990	-0.8550 to -0.1429
2d	1.073	0.5551	-0.5175	-0.8735 to -0.1614
3d	1.158	0.6611	-0.4968	-0.8529 to -0.1408
4d	1.022	0.5087	-0.5133	-0.8693 to -0.1572
5d	1.101	0.5769	-0.5246	-0.8806 to -0.1685
6d	1.278	0.5031	-0.7745	-1.131 to -0.4185

Treatment	Difference	t	P value	Summary
1d	-0.4990	4.501	P<0.001	***
2d	-0.5175	4.668	P<0.001	***
3d	-0.4968	4.482	P<0.001	***
4d	-0.5133	4.630	P<0.001	***
5d	-0.5246	4.732	P<0.001	***
6d	-0.7745	6.987	P<0.001	***
control siRNA vs siRNA				
Treatment	control siRNA	siRNA	Difference	95% CI of diff.
1d	1.174	0.5677	-0.6058	-0.9619 to -0.2498
2d	1.194	0.5551	-0.6385	-0.9945 to -0.2824
3d	1.112	0.6611	-0.4506	-0.8066 to -0.09452
4d	1.135	0.5087	-0.6260	-0.9820 to -0.2700
5d	1.205	0.5769	-0.6285	-0.9845 to -0.2724
6d	1.270	0.5031	-0.7668	-1.123 to -0.4107
Treatment	Difference	t	P value	Summary
1d	-0.6058	5.465	P<0.001	***
2d	-0.6385	5.759	P<0.001	***
3d	-0.4506	4.064	P<0.01	**
4d	-0.6260	5.647	P<0.001	***
5d	-0.6285	5.669	P<0.001	***
6d	-0.7668	6.917	P<0.001	***

Two way ANOVA test for Western Blot data of QKI-6 in DM (Figure 10)				
Source of Variation	**% of total variation**	**P value**		
Interaction	8.22	0.8981		
Time	26.61	0.0251		
Treatment	1.87	0.6119		
Subjects (matching)	10.4860	0.4480		
Source of Variation	**P value summary**	**Significant?**		
Interaction	ns	No		
Time	*	Yes		
Treatment	ns	No		
Subjects (matching)	ns	No		
Source of Variation	**Df**	**Sum-of-squares**	**Mean square**	**F**
Interaction	10	0.1837	0.01837	0.4670
Time	5	0.5945	0.1189	3.024
Treatment	2	0.04168	0.02084	0.5338
Subjects (matching)	6	0.2342	0.03904	0.9928
Residual	30	1.180	0.03933	
Number of missing values	0			

Bonferroni post hoc test				
wildtype vs blank plasmid				
Treatment	wildtype	blank plasmid	Difference	95% CI of diff.
1d	0.9822	0.9262	-0.05604	-0.5758 to 0.4637
2d	0.9759	0.9879	0.01201	-0.5077 to 0.5317
3d	1.025	1.212	0.1876	-0.3321 to 0.7074
4d	0.9886	1.116	0.1275	-0.3922 to 0.6472
5d	1.135	1.158	0.02289	-0.4968 to 0.5426
6d	1.311	1.164	-0.1471	-0.6668 to 0.3727
Treatment	Difference	t	P value	Summary
1d	-0.05604	0.3463	P > 0.05	ns
2d	0.01201	0.07423	P > 0.05	ns
3d	0.1876	1.160	P > 0.05	ns
4d	0.1275	0.7879	P > 0.05	ns
5d	0.02289	0.1415	P > 0.05	ns
6d	-0.1471	0.9088	P > 0.05	ns

wildtype vs plasmid				
Treatment	wildtype	plasmid	Difference	95% CI of diff.
1d	0.9822	1.012	0.02938	-0.4904 to 0.5491
2d	0.9759	0.9912	0.01529	-0.5044 to 0.5350
3d	1.025	1.048	0.02345	-0.4963 to 0.5432
4d	0.9886	1.217	0.2281	-0.2916 to 0.7479
5d	1.135	1.179	0.04445	-0.4753 to 0.5642
6d	1.311	1.374	0.06268	-0.4570 to 0.5824

Treatment	Difference	t	P value	Summary
1d	0.02938	0.1815	P > 0.05	ns
2d	0.01529	0.09450	P > 0.05	ns
3d	0.02345	0.1449	P > 0.05	ns
4d	0.2281	1.410	P > 0.05	ns
5d	0.04445	0.2747	P > 0.05	ns
6d	0.06268	0.3873	P > 0.05	ns

blank plasmid vs plasmid				
Treatment	blank plasmid	plasmid	Difference	95% CI of diff.
1d	0.9262	1.012	0.08542	-0.4343 to 0.6051
2d	0.9879	0.9912	0.003280	-0.5164 to 0.5230
3d	1.212	1.048	-0.1642	-0.6839 to 0.3555
4d	1.116	1.217	0.1006	-0.4191 to 0.6204
5d	1.158	1.179	0.02156	-0.4982 to 0.5413
6d	1.164	1.374	0.2097	-0.3100 to 0.7295

Treatment	Difference	t	P value	Summary
1d	0.08542	0.5279	P > 0.05	ns
2d	0.003280	0.02027	P > 0.05	ns
3d	-0.1642	1.015	P > 0.05	ns
4d	0.1006	0.6219	P > 0.05	ns
5d	0.02156	0.1333	P > 0.05	ns
6d	0.2097	1.296	P > 0.05	ns

Two way ANOVA test for Western Blot data of QKI-6; siRNA treatment in DM (Figure 11)				
Source of Variation	**% of total variation**	**P value**		
Interaction	3.65	0.9971		
Time	18.87	0.1476		
Treatment	4.30	0.3274		
Subjects (matching)	9.5280	0.6155		

Source of Variation	P value summary	Significant?		
Interaction	ns	No		
Time	ns	No		
Treatment	ns	No		
Subjects (matching)	ns	No		
Source of Variation	Df	Sum-of-squares	Mean square	F
Interaction	10	0.07050	0.007050	0.1718
Time	5	0.3647	0.07294	1.778
Treatment	2	0.08307	0.04153	1.353
Subjects (matching)	6	0.1842	0.03070	0.7483
Residual	30	1.231	0.04102	
Number of missing values	0			

Bonferroni post hoc test				
wildtype vs control siRNA				
Treatment	wildtype	control siRNA	Difference	95% CI of diff.
1d	1.000	1.074	0.07352	-0.4464 to 0.5934
2d	1.043	1.194	0.1510	-0.3689 to 0.6709
3d	1.058	1.145	0.08707	-0.4328 to 0.6070
4d	1.155	1.235	0.07939	-0.4405 to 0.5993
5d	1.168	1.139	-0.02945	-0.5493 to 0.4904
6d	1.344	1.337	-0.007775	-0.5277 to 0.5121
Treatment	Difference	t	P value	Summary
1d	0.07352	0.4542	P > 0.05	ns
2d	0.1510	0.9327	P > 0.05	ns
3d	0.08707	0.5379	P > 0.05	ns
4d	0.07939	0.4905	P > 0.05	ns
5d	-0.02945	0.1819	P > 0.05	ns
6d	-0.007775	0.04803	P > 0.05	ns
wildtype vs siRNA				
Treatment	wildtype	siRNA	Difference	95% CI of diff.
1d	1.000	1.168	0.1677	-0.3522 to 0.6876
2d	1.043	1.155	0.1125	-0.4074 to 0.6324
3d	1.058	1.161	0.1032	-0.4167 to 0.6231
4d	1.155	1.309	0.1534	-0.3665 to 0.6733
5d	1.168	1.244	0.07543	-0.4445 to 0.5953
6d	1.344	1.303	-0.04121	-0.5611 to 0.4787

Treatment	Difference	t	P value	Summary
1d	0.1677	1.036	P > 0.05	ns
2d	0.1125	0.6951	P > 0.05	ns
3d	0.1032	0.6374	P > 0.05	ns
4d	0.1534	0.9476	P > 0.05	ns
5d	0.07543	0.4660	P > 0.05	ns
6d	-0.04121	0.2546	P > 0.05	ns

control siRNA vs siRNA				
Treatment	control siRNA	siRNA	Difference	95% CI of diff.
1d	1.074	1.168	0.09418	-0.4257 to 0.6141
2d	1.194	1.155	-0.03845	-0.5583 to 0.4814
3d	1.145	1.161	0.01612	-0.5038 to 0.5360
4d	1.235	1.309	0.07400	-0.4459 to 0.5939
5d	1.139	1.244	0.1049	-0.4150 to 0.6248
6d	1.337	1.303	-0.03344	-0.5533 to 0.4865

Treatment	Difference	t	P value	Summary
1d	0.09418	0.5818	P > 0.05	ns
2d	-0.03845	0.2375	P > 0.05	ns
3d	0.01612	0.09956	P > 0.05	ns
4d	0.07400	0.4571	P > 0.05	ns
5d	0.1049	0.6479	P > 0.05	ns
6d	-0.03344	0.2066	P > 0.05	ns

Two way ANOVA test for Western Blot data of *Plp* in DM (Figure 12)				
Source of Variation	**% of total variation**	**P value**		
Interaction	1.91	0.6809		
Time	88.55	< 0.0001		
Treatment	0.38	0.4981		
Subjects (matching)	1.4479	0.4826		
Source of Variation	**P value summary**	**Significant?**		
Interaction	ns	No		
Time	***	Yes		
Treatment	ns	No		
Subjects (matching)	ns	No		
Source of Variation	**Df**	**Sum-of-squares**	**Mean square**	**F**
Interaction	10	0.2292	0.02292	0.7413
Time	5	10.65	2.129	68.85
Treatment	2	0.04553	0.02277	0.7847
Subjects (matching)	6	0.1741	0.02901	0.9382
Residual	30	0.9278	0.03093	
Number of missing values	0			

Bonferroni post hoc test				
wildtype vs blank plasmid				
Treatment	wildtype	blank plasmid	Difference	95% CI of diff.
1d	1.000	0.8355	-0.1645	-0.6233 to 0.2943
2d	0.9010	1.117	0.2156	-0.2432 to 0.6744
3d	0.9518	0.9639	0.01212	-0.4467 to 0.4709
4d	1.444	1.436	-0.007621	-0.4664 to 0.4512
5d	1.750	1.865	0.1153	-0.3435 to 0.5741
6d	1.998	2.169	0.1712	-0.2876 to 0.6300
Treatment	Difference	t	P value	Summary
1d	-0.1645	1.152	P > 0.05	ns
2d	0.2156	1.509	P > 0.05	ns
3d	0.01212	0.08485	P > 0.05	ns
4d	-0.007621	0.05335	P > 0.05	ns
5d	0.1153	0.8072	P > 0.05	ns
6d	0.1712	1.198	P > 0.05	ns

wildtype vs plasmid				
Treatment	wildtype	plasmid	Difference	95% CI of diff.
1d	1.000	0.9453	-0.05472	-0.5135 to 0.4041
2d	0.9010	1.007	0.1062	-0.3526 to 0.5650
3d	0.9518	1.152	0.2001	-0.2587 to 0.6589
4d	1.444	1.389	-0.05483	-0.5136 to 0.4040
5d	1.750	1.771	0.02138	-0.4374 to 0.4802
6d	1.998	2.172	0.1740	-0.2848 to 0.6328
Treatment	Difference	t	P value	Summary
1d	-0.05472	0.3830	P > 0.05	ns
2d	0.1062	0.7435	P > 0.05	ns
3d	0.2001	1.401	P > 0.05	ns
4d	-0.05483	0.3838	P > 0.05	ns
5d	0.02138	0.1497	P > 0.05	ns
6d	0.1740	1.218	P > 0.05	ns
blank plasmid vs plasmid				
Treatment	blank plasmid	plasmid	Difference	95% CI of diff.
1d	0.8355	0.9453	0.1098	-0.3490 to 0.5686
2d	1.117	1.007	-0.1094	-0.5682 to 0.3494
3d	0.9639	1.152	0.1879	-0.2708 to 0.6467
4d	1.436	1.389	-0.04721	-0.5060 to 0.4116
5d	1.865	1.771	-0.09392	-0.5527 to 0.3649
6d	2.169	2.172	0.002796	-0.4560 to 0.4616
Treatment	Difference	t	P value	Summary
1d	0.1098	0.7688	P > 0.05	ns
2d	-0.1094	0.7657	P > 0.05	ns
3d	0.1879	1.316	P > 0.05	ns
4d	-0.04721	0.3305	P > 0.05	ns
5d	-0.09392	0.6575	P > 0.05	ns
6d	0.002796	0.01957	P > 0.05	ns

Two way ANOVA test for Western Blot data of *Plp*; siRNA treatment in DM (Figure 13)				
Source of Variation	% of total variation	P value		
Interaction	0.67	0.9646		
Time	92.19	< 0.0001		
Treatment	0.35	0.3054		
Subjects (matching)	0.7282	0.7270		
Source of Variation	P value summary	Significant?		

Interaction	ns	No		
Time	***	Yes		
Treatment	ns	No		
Subjects (matching)	ns	No		
Source of Variation	**Df**	**Sum-of-squares**	**Mean square**	**F**
Interaction	10	0.1053	0.01053	0.3339
Time	5	14.40	2.880	91.36
Treatment	2	0.05517	0.02759	1.455
Subjects (matching)	6	0.1138	0.01896	0.6013
Residual	30	0.9458	0.03153	
Number of missing values	0			

Bonferroni post hoc test				
wildtype vs control siRNA				
Treatment	wildtype	control siRNA	Difference	95% CI of diff.
1d	1.000	0.8449	-0.1551	-0.6050 to 0.2948
2d	1.100	1.157	0.05776	-0.3921 to 0.5077
3d	1.230	1.314	0.08404	-0.3659 to 0.5339
4d	1.550	1.681	0.1309	-0.3190 to 0.5808
5d	2.091	2.165	0.07383	-0.3761 to 0.5237
6d	2.274	2.398	0.1245	-0.3254 to 0.5744
Treatment	Difference	t	P value	Summary
1d	-0.1551	1.107	P > 0.05	ns
2d	0.05776	0.4123	P > 0.05	ns
3d	0.08404	0.6000	P > 0.05	ns
4d	0.1309	0.9342	P > 0.05	ns
5d	0.07383	0.5270	P > 0.05	ns
6d	0.1245	0.8886	P > 0.05	ns
wildtype vs siRNA				
Treatment	wildtype	siRNA	Difference	95% CI of diff.
1d	1.000	0.9968	-0.003229	-0.4531 to 0.4467
2d	1.100	1.172	0.07289	-0.3770 to 0.5228
3d	1.230	1.351	0.1213	-0.3286 to 0.5712
4d	1.550	1.610	0.05991	-0.3900 to 0.5098
5d	2.091	2.127	0.03623	-0.4137 to 0.4861
6d	2.274	2.446	0.1720	-0.2779 to 0.6219

Treatment	Difference	t	P value	Summary
1d	-0.003229	0.02305	P > 0.05	ns
2d	0.07289	0.5204	P > 0.05	ns
3d	0.1213	0.8658	P > 0.05	ns
4d	0.05991	0.4277	P > 0.05	ns
5d	0.03623	0.2587	P > 0.05	ns
6d	0.1720	1.228	P > 0.05	ns
control siRNA vs siRNA				
Treatment	control siRNA	siRNA	Difference	95% CI of diff.
1d	0.8449	0.9968	0.1519	-0.2980 to 0.6018
2d	1.157	1.172	0.01514	-0.4348 to 0.4650
3d	1.314	1.351	0.03724	-0.4127 to 0.4871
4d	1.681	1.610	-0.07096	-0.5209 to 0.3789
5d	2.165	2.127	-0.03760	-0.4875 to 0.4123
6d	2.398	2.446	0.04751	-0.4024 to 0.4974
Treatment	Difference	t	P value	Summary
1d	0.1519	1.084	P > 0.05	ns
2d	0.01514	0.1081	P > 0.05	ns
3d	0.03724	0.2658	P > 0.05	ns
4d	-0.07096	0.5065	P > 0.05	ns
5d	-0.03760	0.2684	P > 0.05	ns
6d	0.04751	0.3392	P > 0.05	ns

Two way ANOVA test for Western Blot data of Sirt2 in DM (Figure 12)				
Source of Variation	**% of total variation**	**P value**		
Interaction	1.26	0.9590		
Time	85.21	< 0.0001		
Treatment	0.37	0.6345		
Subjects (matching)	2.2783	0.4151		
Source of Variation	**P value summary**	**Significant?**		
Interaction	ns	No		
Time	***	Yes		
Treatment	ns	No		
Subjects (matching)	ns	No		
Source of Variation	**Df**	**Sum-of-squares**	**Mean square**	**F**
Interaction	10	0.1976	0.01976	0.3487
Time	5	13.32	2.665	47.01
Treatment	2	0.05834	0.02917	0.4913
Subjects (matching)	6	0.3562	0.05937	1.048
Residual	30	1.700	0.05668	
Number of missing values	0			

Bonferroni post hoc test				
wildtype vs blank plasmid				
Treatment	wildtype	blank plasmid	Difference	95% CI of diff.
1d	1.000	0.8053	-0.1947	-0.8215 to 0.4321
2d	0.9996	0.8921	-0.1075	-0.7343 to 0.5192
3d	1.469	1.556	0.08741	-0.5394 to 0.7142
4d	1.419	1.411	-0.008455	-0.6353 to 0.6183
5d	1.941	2.069	0.1279	-0.4989 to 0.7547
6d	2.156	2.346	0.1899	-0.4369 to 0.8167
Treatment	Difference	t	P value	Summary
1d	-0.1947	0.9978	P > 0.05	ns
2d	-0.1075	0.5511	P > 0.05	ns
3d	0.08741	0.4479	P > 0.05	ns
4d	-0.008455	0.04333	P > 0.05	ns
5d	0.1279	0.6555	P > 0.05	ns
6d	0.1899	0.9731	P > 0.05	ns

wildtype vs plasmid				
Treatment	wildtype	plasmid	Difference	95% CI of diff.
1d	1.000	0.9806	-0.01941	-0.6462 to 0.6074
2d	0.9996	1.013	0.01302	-0.6138 to 0.6398
3d	1.469	1.595	0.1266	-0.5001 to 0.7534
4d	1.419	1.451	0.03153	-0.5953 to 0.6583
5d	1.941	2.169	0.2276	-0.3992 to 0.8544
6d	2.156	2.234	0.07811	-0.5487 to 0.7049
Treatment	Difference	t	P value	Summary
1d	-0.01941	0.09943	P > 0.05	ns
2d	0.01302	0.06671	P > 0.05	ns
3d	0.1266	0.6490	P > 0.05	ns
4d	0.03153	0.1615	P > 0.05	ns
5d	0.2276	1.166	P > 0.05	ns
6d	0.07811	0.4002	P > 0.05	ns
blank plasmid vs plasmid				
Treatment	blank plasmid	plasmid	Difference	95% CI of diff.
1d	0.8053	0.9806	0.1753	-0.4515 to 0.8021
2d	0.8921	1.013	0.1206	-0.5062 to 0.7474
3d	1.556	1.595	0.03924	-0.5876 to 0.6660
4d	1.411	1.451	0.03998	-0.5868 to 0.6668
5d	2.069	2.169	0.09970	-0.5271 to 0.7265
6d	2.346	2.234	-0.1118	-0.7386 to 0.5150
Treatment	Difference	t	P value	Summary
1d	0.1753	0.8983	P > 0.05	ns
2d	0.1206	0.6178	P > 0.05	ns
3d	0.03924	0.2010	P > 0.05	ns
4d	0.03998	0.2049	P > 0.05	ns
5d	0.09970	0.5109	P > 0.05	ns
6d	-0.1118	0.5729	P > 0.05	ns

Two way ANOVA test for Western Blot data of Sirt2; siRNA treatment in DM (Figure 13)				
Source of Variation	% of total variation	P value		
Interaction	1.07	0.9693		
Time	85.30	< 0.0001		
Treatment	1.27	0.2781		
Subjects (matching)	2.3870	0.3350		
Source of Variation	P value summary	Significant?		

Interaction	ns	No		
Time	***	Yes		
Treatment	ns	No		
Subjects (matching)	ns	No		
Source of Variation	**Df**	**Sum-of-squares**	**Mean square**	**F**
Interaction	10	0.2237	0.02237	0.3204
Time	5	17.91	3.582	51.31
Treatment	2	0.2667	0.1333	1.596
Subjects (matching)	6	0.5012	0.08354	1.197
Residual	30	2.095	0.06982	
Number of missing values	0			

Bonferroni post hoc test				
wildtype vs control siRNA				
Treatment	wildtype	control siRNA	Difference	95% CI of diff.
1d	1.000	0.9166	-0.08337	-0.7875 to 0.6208
2d	1.243	1.229	-0.01399	-0.7182 to 0.6902
3d	1.388	1.219	-0.1696	-0.8738 to 0.5346
4d	1.593	1.824	0.2309	-0.4733 to 0.9350
5d	2.296	2.247	-0.04935	-0.7535 to 0.6548
6d	2.447	2.614	0.1671	-0.5371 to 0.8713
Treatment	Difference	t	P value	Summary
1d	-0.08337	0.3803	P > 0.05	ns
2d	-0.01399	0.06381	P > 0.05	ns
3d	-0.1696	0.7736	P > 0.05	ns
4d	0.2309	1.053	P > 0.05	ns
5d	-0.04935	0.2251	P > 0.05	ns
6d	0.1671	0.7621	P > 0.05	ns
wildtype vs siRNA				
Treatment	wildtype	siRNA	Difference	95% CI of diff.
1d	1.000	1.154	0.1543	-0.5499 to 0.8584
2d	1.243	1.264	0.02138	-0.6828 to 0.7255
3d	1.388	1.411	0.02244	-0.6817 to 0.7266
4d	1.593	1.907	0.3141	-0.3901 to 1.018
5d	2.296	2.448	0.1524	-0.5518 to 0.8565
6d	2.447	2.715	0.2680	-0.4362 to 0.9721

Treatment	Difference	t	P value	Summary
1d	0.1543	0.7036	P > 0.05	ns
2d	0.02138	0.09752	P > 0.05	ns
3d	0.02244	0.1024	P > 0.05	ns
4d	0.3141	1.433	P > 0.05	ns
5d	0.1524	0.6949	P > 0.05	ns
6d	0.2680	1.222	P > 0.05	ns
control siRNA vs siRNA				
Treatment	control siRNA	siRNA	Difference	95% CI of diff.
1d	0.9166	1.154	0.2376	-0.4665 to 0.9418
2d	1.229	1.264	0.03537	-0.6688 to 0.7395
3d	1.219	1.411	0.1921	-0.5121 to 0.8962
4d	1.824	1.907	0.08323	-0.6209 to 0.7874
5d	2.247	2.448	0.2017	-0.5025 to 0.9059
6d	2.614	2.715	0.1009	-0.6033 to 0.8050
Treatment	Difference	t	P value	Summary
1d	0.2376	1.084	P > 0.05	ns
2d	0.03537	0.1613	P > 0.05	ns
3d	0.1921	0.8760	P > 0.05	ns
4d	0.08323	0.3796	P > 0.05	ns
5d	0.2017	0.9200	P > 0.05	ns
6d	0.1009	0.4601	P > 0.05	ns

Two way ANOVA test of A2B5+ve% in DM (Figure 14)				
Source of Variation	% of total variation	P value		
Interaction	6.90	0.0014		
Time	75.68	< 0.0001		
Treatment	11.31	0.0005		
Subjects (matching)	0.9994	0.4572		
Source of Variation	P value summary	Significant?		
Interaction	**	Yes		
Time	***	Yes		
Treatment	***	Yes		
Subjects (matching)	ns	No		
Source of Variation	Df	Sum-of-squares	Mean square	F
Interaction	10	1428	142.8	4.050
Time	5	15660	3132	88.86
Treatment	2	2341	1170	33.96
Subjects (matching)	6	206.8	34.47	0.9779
Residual	30	1057	35.25	
Number of missing values	0			

Bonferroni post hoc test				
wildtype vs blank plasmid				
Treatment	wildtype	blank plasmid	Difference	95% CI of diff.
1d	80.67	81.66	0.9967	-14.54 to 16.54
2d	69.92	67.59	-2.337	-17.88 to 13.20
3d	48.01	47.68	-0.3267	-15.87 to 15.21
4d	35.83	35.53	-0.3067	-15.85 to 15.23
5d	29.50	26.65	-2.847	-18.39 to 12.69
6d	29.17	26.38	-2.790	-18.33 to 12.75
Treatment	Difference	t	P value	Summary
1d	0.9967	0.2060	P > 0.05	ns
2d	-2.337	0.4829	P > 0.05	ns
3d	-0.3267	0.06751	P > 0.05	ns
4d	-0.3067	0.06338	P > 0.05	ns
5d	-2.847	0.5883	P > 0.05	ns
6d	-2.790	0.5766	P > 0.05	ns

wildtype vs plasmid				
Treatment	wildtype	plasmid	Difference	95% CI of diff.
1d	80.67	77.76	-2.907	-18.45 to 12.63
2d	69.92	71.41	1.490	-14.05 to 17.03
3d	48.01	64.67	16.66	1.120 to 32.20
4d	35.83	60.37	24.54	8.997 to 40.08
5d	29.50	54.00	24.50	8.963 to 40.04
6d	29.17	44.62	15.45	-0.08658 to 30.99
Treatment	Difference	t	P value	Summary
1d	-2.907	0.6007	P > 0.05	ns
2d	1.490	0.3080	P > 0.05	ns
3d	16.66	3.443	P<0.01	**
4d	24.54	5.071	P<0.001	***
5d	24.50	5.064	P<0.001	***
6d	15.45	3.194	P < 0.05	*
blank plasmid vs plasmid				
Treatment	blank plasmid	plasmid	Difference	95% CI of diff.
1d	81.66	77.76	-3.903	-19.44 to 11.64
2d	67.59	71.41	3.827	-11.71 to 19.37
3d	47.68	64.67	16.99	1.447 to 32.53
4d	35.53	60.37	24.84	9.303 to 40.38
5d	26.65	54.00	27.35	11.81 to 42.89
6d	26.38	44.62	18.24	2.703 to 33.78
Treatment	Difference	t	P value	Summary
1d	-3.903	0.8067	P > 0.05	ns
2d	3.827	0.7909	P > 0.05	ns
3d	16.99	3.511	P<0.01	**
4d	24.84	5.135	P<0.001	***
5d	27.35	5.653	P<0.001	***
6d	18.24	3.771	P<0.01	**

Two way ANOVA test of A2B5+ve%; siRNA treatment in DM (Figure 14)				
Source of Variation	% of total variation	P value		
Interaction	2.01	0.3551		
Time	91.14	< 0.0001		
Treatment	0.12	0.7971		
Subjects (matching)	1.5218	0.2251		
Source of Variation	P value summary	Significant?		

Interaction	ns	No		
Time	***	Yes		
Treatment	ns	No		
Subjects (matching)	ns	No		
Source of Variation	**Df**	**Sum-of-squares**	**Mean square**	**F**
Interaction	10	460.9	46.09	1.159
Time	5	20879	4176	105.0
Treatment	2	27.38	13.69	0.2356
Subjects (matching)	6	348.6	58.11	1.461
Residual	30	1193	39.77	
Number of missing values	0			

Bonferroni post hoc test				
wildtype vs control siRNA				
Treatment	wildtype	control siRNA	Difference	95% CI of diff.
1d	81.01	78.21	-2.797	-19.96 to 14.36
2d	70.34	73.33	2.993	-14.17 to 20.15
3d	51.51	58.05	6.547	-10.61 to 23.71
4d	35.47	35.46	-0.01334	-17.17 to 17.15
5d	29.52	26.69	-2.830	-19.99 to 14.33
6d	28.95	23.99	-4.960	-22.12 to 12.20
Treatment	Difference	t	P value	Summary
1d	-2.797	0.5234	P > 0.05	ns
2d	2.993	0.5602	P > 0.05	ns
3d	6.547	1.225	P > 0.05	ns
4d	-0.01334	0.002496	P > 0.05	ns
5d	-2.830	0.5296	P > 0.05	ns
6d	-4.960	0.9283	P > 0.05	ns
wildtype vs siRNA				
Treatment	wildtype	siRNA	Difference	95% CI of diff.
1d	81.01	67.09	-13.92	-31.08 to 3.245
2d	70.34	69.84	-0.4933	-17.65 to 16.67
3d	51.51	56.97	5.463	-11.70 to 22.62
4d	35.47	36.33	0.8567	-16.30 to 18.02
5d	29.52	31.02	1.500	-15.66 to 18.66
6d	28.95	26.00	-2.957	-20.12 to 14.20

Treatment	Difference	t	P value	Summary
1d	-13.92	2.604	P > 0.05	ns
2d	-0.4933	0.09233	P > 0.05	ns
3d	5.463	1.022	P > 0.05	ns
4d	0.8567	0.1603	P > 0.05	ns
5d	1.500	0.2807	P > 0.05	ns
6d	-2.957	0.5533	P > 0.05	ns
control siRNA vs siRNA				
Treatment	control siRNA	siRNA	Difference	95% CI of diff.
1d	78.21	67.09	-11.12	-28.28 to 6.042
2d	73.33	69.84	-3.487	-20.65 to 13.67
3d	58.05	56.97	-1.083	-18.24 to 16.08
4d	35.46	36.33	0.8700	-16.29 to 18.03
5d	26.69	31.02	4.330	-12.83 to 21.49
6d	23.99	26.00	2.003	-15.16 to 19.16
Treatment	Difference	t	P value	Summary
1d	-11.12	2.081	P > 0.05	ns
2d	-3.487	0.6525	P > 0.05	ns
3d	-1.083	0.2027	P > 0.05	ns
4d	0.8700	0.1628	P > 0.05	ns
5d	4.330	0.8104	P > 0.05	ns
6d	2.003	0.3749	P > 0.05	ns

APPENDIX XII RESULTS OF TWO WAY ANOVA TEST FOR CELL COUNT DATA OF GALC+ CELLS

Two way ANOVA test of GalC+ve% in DM (Figure 15)				
Source of Variation	% of total variation	P value		
Interaction	2.84	0.0076		
Time	87.04	< 0.0001		
Treatment	6.31	0.0031		
Subjects (matching)	1.0718	0.1029		
Source of Variation	P value summary	Significant?		
Interaction	**	Yes		
Time	***	Yes		
Treatment	**	Yes		
Subjects (matching)	ns	No		
Source of Variation	Df	Sum-of-squares	Mean square	F
Interaction	10	585.7	58.57	3.121
Time	5	17943	3589	191.2
Treatment	2	1301	650.6	17.67
Subjects (matching)	6	220.9	36.82	1.962
Residual	30	562.9	18.76	
Number of missing values	0			

Bonferroni post hoc test				
wildtype vs blank plasmid				
Treatment	wildtype	blank plasmid	Difference	95% CI of diff.
1d	3.477	4.510	1.033	-11.20 to 13.27
2d	6.340	8.027	1.687	-10.55 to 13.92
3d	27.17	25.21	-1.960	-14.20 to 10.28
4d	32.43	34.45	2.023	-10.21 to 14.26
5d	49.46	48.44	-1.023	-13.26 to 11.21
6d	60.74	58.54	-2.203	-14.44 to 10.03
Treatment	Difference	t	P value	Summary
1d	1.033	0.2712	P > 0.05	ns
2d	1.687	0.4427	P > 0.05	ns
3d	-1.960	0.5144	P > 0.05	ns
4d	2.023	0.5311	P > 0.05	ns
5d	-1.023	0.2686	P > 0.05	ns
6d	-2.203	0.5783	P > 0.05	ns

wildtype vs plasmid				
Treatment	wildtype	plasmid	Difference	95% CI of diff.
1d	3.477	5.087	1.610	-10.63 to 13.85
2d	6.340	4.090	-2.250	-14.49 to 9.987
3d	27.17	11.92	-15.24	-27.48 to -3.006
4d	32.43	19.65	-12.78	-25.01 to -0.5398
5d	49.46	32.96	-16.50	-28.74 to -4.263
6d	60.74	43.20	-17.54	-29.78 to -5.303
Treatment	Difference	t	P value	Summary
1d	1.610	0.4226	$P > 0.05$	ns
2d	-2.250	0.5905	$P > 0.05$	ns
3d	-15.24	4.001	$P < 0.01$	**
4d	-12.78	3.353	$P < 0.05$	*
5d	-16.50	4.331	$P < 0.001$	***
6d	-17.54	4.604	$P < 0.001$	***
blank plasmid vs plasmid				
Treatment	blank plasmid	plasmid	Difference	95% CI of diff.
1d	4.510	5.087	0.5767	-11.66 to 12.81
2d	8.027	4.090	-3.937	-16.17 to 8.300
3d	25.21	11.92	-13.28	-25.52 to -1.046
4d	34.45	19.65	-14.80	-27.04 to -2.563
5d	48.44	32.96	-15.48	-27.71 to -3.240
6d	58.54	43.20	-15.34	-27.57 to -3.100
Treatment	Difference	t	P value	Summary
1d	0.5767	0.1514	$P > 0.05$	ns
2d	-3.937	1.033	$P > 0.05$	ns
3d	-13.28	3.486	$P < 0.01$	**
4d	-14.80	3.885	$P < 0.01$	**
5d	-15.48	4.062	$P < 0.01$	**
6d	-15.34	4.025	$P < 0.01$	**

Two way ANOVA test of GalC+ve%; siRNA treatment in DM (Figure 15)				
Source of Variation	% of total variation	P value		
Interaction	1.89	0.0652		
Time	91.74	< 0.0001		
Treatment	3.19	0.0013		
Subjects (matching)	0.3872	0.6567		
Source of Variation	P value summary	Significant?		

Interaction	ns	No		
Time	***	Yes		
Treatment	**	Yes		
Subjects (matching)	ns	No		
Source of Variation	**Df**	**Sum-of-squares**	**Mean square**	**F**
Interaction	10	404.5	40.45	2.032
Time	5	19620	3924	197.1
Treatment	2	682.8	341.4	24.74
Subjects (matching)	6	82.81	13.80	0.6934
Residual	30	597.1	19.90	
Number of missing values	0			

Bonferroni post hoc test				
wildtype vs control siRNA				
Treatment	wildtype	control siRNA	Difference	95% CI of diff.
1d	3.383	2.860	-0.5233	-11.92 to 10.87
2d	6.447	9.783	3.337	-8.060 to 14.73
3d	27.28	20.44	-6.847	-18.24 to 4.550
4d	29.01	27.68	-1.330	-12.73 to 10.07
5d	40.72	37.49	-3.230	-14.63 to 8.167
6d	54.10	55.06	0.9567	-10.44 to 12.35
Treatment	Difference	t	P value	Summary
1d	-0.5233	0.1475	P > 0.05	ns
2d	3.337	0.9403	P > 0.05	ns
3d	-6.847	1.930	P > 0.05	ns
4d	-1.330	0.3748	P > 0.05	ns
5d	-3.230	0.9103	P > 0.05	ns
6d	0.9567	0.2696	P > 0.05	ns
wildtype vs siRNA				
Treatment	wildtype	siRNA	Difference	95% CI of diff.
1d	3.383	3.087	-0.2967	-11.69 to 11.10
2d	6.447	11.59	5.147	-6.250 to 16.54
3d	27.28	28.07	0.7833	-10.61 to 12.18
4d	29.01	40.43	11.42	0.02669 to 22.82
5d	40.72	51.00	10.27	-1.123 to 21.67
6d	54.10	67.73	13.63	2.230 to 25.02

Treatment	Difference	t	P value	Summary
1d	-0.2967	0.08361	P > 0.05	ns
2d	5.147	1.450	P > 0.05	ns
3d	0.7833	0.2208	P > 0.05	ns
4d	11.42	3.219	P < 0.05	*
5d	10.27	2.895	P < 0.05	*
6d	13.63	3.840	P<0.01	**
control siRNA vs siRNA				
Treatment	control siRNA	siRNA	Difference	95% CI of diff.
1d	2.860	3.087	0.2267	-11.17 to 11.62
2d	9.783	11.59	1.810	-9.587 to 13.21
3d	20.44	28.07	7.630	-3.767 to 19.03
4d	27.68	40.43	12.75	1.357 to 24.15
5d	37.49	51.00	13.50	2.107 to 24.90
6d	55.06	67.73	12.67	1.273 to 24.07
Treatment	Difference	t	P value	Summary
1d	0.2267	0.06388	P > 0.05	ns
2d	1.810	0.5101	P > 0.05	ns
3d	7.630	2.150	P > 0.05	ns
4d	12.75	3.594	P<0.01	**
5d	13.50	3.805	P<0.01	**
6d	12.67	3.571	P<0.01	**